



Controlling of Reproductive Organs Maturation in Shrimp

Kunwadee Palasin

**A Thesis Submitted in Partial Fulfillment of the Requirements for the
Degree of Doctor of Philosophy in Molecular Biology and Bioinformatics
Prince of Songkla University
2018**

Copyright of Prince of Songkla University



Controlling of Reproductive Organs Maturation in Shrimp

Kunwadee Palasin

**A Thesis Submitted in Partial Fulfillment of the Requirements for the
Degree of Doctor of Philosophy in Molecular Biology and Bioinformatics
Prince of Songkla University
2018**

Copyright of Prince of Songkla University

Thesis Title Controlling of Reproductive Organs Maturation in Shrimp
Author Miss Kunwadee Palasin
Major Program Molecular Biology and Bioinformatics

Major Advisor

.....
 (Assoc. Prof. Dr. Wilaiwan Chotigeat)

Examining Committee:

.....Chairperson
 (Prof. Dr. Amornrat Phongdara)

.....Committee
 (Prof. Dr. Naoya Kenmochi)

.....Committee
 (Assoc. Prof. Dr. Wilaiwan Chotigeat)

The Graduate School, Prince of Songkla University, has approved this thesis as partial fulfillment of the requirements for the Doctor of Philosophy Degree in Molecular Biology and Bioinformatics

.....
 (Prof. Dr. Damrongsak Faroongsarng)
 Dean of Graduate School

This is to certify that the work here submitted is the result of the candidate's own investigations. Due acknowledgement has been made of any assistance received.

.....Signature
(Assoc. Prof. Dr. Wilaiwan Chotigeat)
Major Advisor

.....Signature
(Miss Kunwadee Palasin)
Candidate

I hereby certify that this work has not accepted in substance for any degree, and is not being currently submitted in candidature for any degree.

.....Signature

(Miss Kunwadee Palasin)

Candidate

ชื่อวิทยานิพนธ์ การควบคุมการพัฒนาอวัยวะสืบพันธุ์ในกุ้ง
 ผู้เขียน นางสาวกุลวดี พลาสิน
 สาขาวิชา ชีววิทยาโมเลกุลและชีวสารสนเทศ
 ปีการศึกษา 2561

บทคัดย่อ

โดยทั่วไปแล้วในสิ่งมีชีวิตทุกชนิด Ribosomal proteins ทำหน้าที่ช่วยในการสังเคราะห์โปรตีน ต่อมาได้มีรายงานเกี่ยวกับการทำหน้าที่อย่างอื่นของ Ribosomal proteins เป็นจำนวนมาก ได้แก่การซ่อมแซม DNA กระบวนการตายของเซลล์ การควบคุมการแปลรหัสโปรตีน และการควบคุมการพัฒนาของเม็ดเลือดแดง หนึ่งในโปรตีนดังกล่าวคือ ribosomal protein L10a หรือ Rpl10a protein ซึ่งแปลรหัสจากยีน *rpl10a* ก่อนหน้านี้ได้มีรายงานเกี่ยวกับหน้าที่อื่นได้แก่ ช่วยการการเจริญเติบโตของเอ็มบริโอ การพัฒนาอวัยวะ และการพัฒนารังไข่ เป็นต้น ในงานวิจัยนี้ได้ทำการศึกษาหน้าที่ของโปรตีน Rpl10a ต่อการพัฒนาอวัยวะสืบพันธุ์ และพบว่าโปรตีนลูกผสม His-Rpl10a ช่วยในการกระตุ้นการพัฒนารังไข่ในระยะแรก ปริมาณที่ให้ผลดีที่สุดในการกระตุ้นคือ 180 ไมโครกรัมต่อตัวกุ้ง ซึ่งสามารถกระตุ้นการพัฒนารังไข่ภายใน 7 วันเข้าสู่ระยะที่ 1 และ 2 หลังจากฉีดโปรตีน His-Rpl10a นอกจากนี้โปรตีนลูกผสม His-Rpl10a ช่วยในการกระตุ้นการพัฒนาเซลล์สืบพันธุ์เพศผู้ได้ในกุ้งกุลาดำ และหนูถีบจักร ได้ทำการยืนยันผลด้วยวิธีทางเนื้อเยื่อวิทยาและการแสดงออกของยีนที่เป็นตัวบ่งชี้ที่มีการแสดงออกในระยะแรกและระยะหลังของการพัฒนา ได้แก่ ยีน *Dmrt1* และ *Rhau* ซึ่งแสดงออกสูงในระยะแรกและมีการแสดงออกที่ลดลงเมื่อมีการบ่มกับโปรตีนลูกผสม His-Rpl10a ในขณะที่ยีน *Prm2* ซึ่งแสดงออกสูงในระยะที่มีการพัฒนาเพิ่มขึ้นในหนู และได้ทำการยืนยันการพัฒนาโดยการตรวจสอบการเพิ่มการสังเคราะห์ดีเอ็นเอเพื่อเป็นการยืนยันผลอีกด้วย นอกจากนี้ได้ทำการศึกษาหน้าที่ของยีน *rpl10a* ในการเกิดภาวะโลหิตจางโดยใช้ปลาหมึกที่มีการกลายพันธุ์ของยีน *rpl10a* ในการศึกษา และพบว่าเอ็มบริโอของปลาหมึกลายที่มียีน *rpl10a* บกพร่องมีการพัฒนาผิดปกติ ในเวลา 25 ชั่วโมงหลังจากการผสมพันธุ์ ตัวอ่อนมีความยาวของไข่แดงลดลง ตาเล็ก ลำตัวสั้นและมีหางอ นอกจากนี้ลักษณะดังกล่าวชัดเจนเมื่อ 50 ชั่วโมงหลังจากการผสมพันธุ์ พบว่ามีถุงไข่แดงใหญ่ขึ้น เกิดภาวะบวมน้ำที่หัวใจ ตาเล็กลง เม็ดสีจางลงและหางโค้งงอชัดเจน และพบว่าลักษณะที่ผิดปกติดังกล่าวนั้นสามารถที่จะทำให้คืนสู่สภาวะเดิมได้โดยการช่วยเหลือด้วย mRNA ของ *rpl10a* จากผลการทดลองดังกล่าวแสดงให้เห็นว่าโปรตีน Rpl10a มีความจำเป็นต่อการพัฒนาระยะแรกของเอ็มบริโอ ทำให้เกิดการชะลอการเจริญเติบโตและเกิดการตายภายใน 3-7 วัน นอกจากนั้นเกิดภาวะโลหิตจางและจำนวนของเม็ดเลือดแดงลดลง เมื่อยีน *rpl10a* เกิดความผิดปกติ ผลการทดลอง

ดังกล่าวได้ทำการยืนยันทางชีววิทยาโมเลกุลโดยการศึกษาการแสดงออกของยีนที่เป็นตัวบ่งชี้ในการสังเคราะห์ฮีโมโกลบิน ได้แก่ *gata1*, *hbae3* และ *hbbe1* ซึ่งยีนดังกล่าวมีการแสดงออกลดลง ในขณะที่ยีน *tp53* ซึ่งเป็นยีนที่เกิดการตายของเซลล์มีการแสดงออกสูงขึ้น จากการศึกษาดังกล่าวสนับสนุนว่าโปรตีน Rpl10a ทำหน้าที่ในการควบคุมการเกิดสภาวะโลหิตจาง และยังพบว่าเมื่อเกิดการบกพร่องของยีน *rpl10a* ส่งผลต่อการแสดงออกที่ลดลงของยีน *nanos1* และ *vasa* ที่เป็นตัวบ่งชี้ primordial germ cell (PGC) ซึ่งเป็นเซลล์ที่ทำหน้าที่ในการสร้างเซลล์สืบพันธุ์อย่างมีนัยสำคัญ จากผลการศึกษาทั้งหมดนี้เป็นที่น่าสนใจว่าโปรตีน Rpl10a ทำหน้าที่ในการกระตุ้นการพัฒนาอวัยวะสืบพันธุ์ การพัฒนาการสร้างเซลล์สืบพันธุ์ การเจริญเติบโตของอีมบริโอ และการสร้างฮีโมโกลบินอีกด้วย

Thesis Title	Controlling of Reproductive Organs Maturation in Shrimp
Author	Miss Kunwadee Palasin
Major Program	Molecular Biology and Bioinformatics
Academic Year	2018

ABSTRACT

Ribosomal protein was known to play a function in protein synthesis. Recently, many studies reported the extraribosomal activity including DNA repair, apoptosis, regulation of translation, controlling of development and red blood cell development. Ribosomal protein L10a (Rpl10a) encoded by the *rpl10a* gene has been reported the secondary function during embryogenesis, organogenesis and ovarian development. In this study, the activity of Rpl10a protein on reproductive organs development was investigated. The recombinant His-Rpl10a protein (rRpl10a) was injected into shrimps to promote the ovarian development in shrimps. The concentration at 180 µg of His-rRpl10a per shrimp was the effective dose to stimulate ovaries to reach to stages I and II of ovarian maturation within 7 days post injection. In addition, the spermatogenesis in shrimp and mouse were stimulated by His-rRpl10a protein *in vitro*. The early stage marker gene expressions (*Dmrt1* in shrimp or *Rhau* in mouse) were decreased, while *Prm2*, late-stage marker gene was upregulated. The cell proliferation was also confirmed in rRpl10a treated testis.

Furthermore, the other functions of *rpl10a* on anemia using *rpl10a* mutant zebrafish (*Danio rerio*) as a model were also studied. The *rpl10a*-deficient embryos displayed the abnormality phenotypes including thinner yolk extension, smaller eyes, shorter body length and bent tail at 25 hpf (hour-post fertilization). Besides, *rpl10a* gene deficiency showed the phenotypes as a bigger yolk sac, edema, smaller eyes, melanophore pigment reduction, and a curved tail at 50 hpf. These morphological abnormalities were recovered by *rpl10a* full-length mRNA. This result indicated that *rpl10a* gene is essential for early embryogenic development. Moreover, loss activity of *rpl10a* affected growth retardation and embryonic lethality within 3-7 dpf. Anemic phenotype and hemoglobin activity were observed both knockdown and

knockout model. The hemoglobin marker genes including *gata1*, *hbae3*, and *hbbe1* have declined expression, whereas *tp53* transcript was increased. These findings supported that Rpl10a protein might play an extra-function in anemia. Knockdown of *rpl10a* gene also affected the low expression of primordial germ cell (PGC) marker genes (*nanos1* and *vasa*) significantly. Interestingly, these findings suggested that Rpl10a protein is necessary on the early stage of reproductive organs development, primordial germ cells development, embryogenesis, and hemoglobin synthesis.

ACKNOWLEDGEMENTS

I would like to express my sincere gratitude to my supervisor, Assoc. Prof. Dr. Wilaiwan Chotigeat, for giving me the opportunity, supporting, bright advice and valuable guidance throughout the during of my degree.

I am extremely grateful for Prof. Dr. Naoya Kenmochi, Frontier Science Research Center, University of Miyazaki, Miyazaki, Japan for providing me laboratory space during a year and 3 months to perform special experiment in zebrafish model, valuable suggestion and helpful discussions during my work in aboard. A special thanks goes to Kenmochi lab's members who give me a warm welcome, taking good care of me, kind assistance, helpful suggestion and interesting point on my work, especially Assist. Prof. Tamayo Uechi, Assist. Prof. Maki Yoshihama, Dr. Saya Okui and Ms. Yukari Nakajima. I also appreciate Prof. Yoshitaka Hishikawa and his lab members for providing the histology facility and discussion.

I am thankful to the examining committee: Prof Dr. Naoya Kenmochi and Prof. Dr. Amornrat Phongdara, Faculty of Medical Technology for valuable advice and taking time to review my thesis.

In my journey towards my degree, I have found many teachers, friends support me. I truly appreciate to all my friends in BSc. 1007 and Chotigeat's lab members for all valuable assistance, warm atmosphere, encouragement and taking care of me like family. I am also thankful to the Department of Molecular Biotechnology and Bioinformatics for providing me the facilities to carry out my research.

Many thanks to my scholarship. This work was supported by the Royal Golden Jubilee Graduate Program from the Thailand Research Fund (TRF) for Kunwadee Palasin (4.J.PS/52/B.1) and Thailand Government Research Fund 2016.

Finally, none of my successful would have been possible without the truly love and moral support from my family.

Kunwadee Palasin

CONTENTS

	Page
Abstract	v
Acknowledgements	ix
Contents	x
List of Figures	xi
List of Tables	xiv
List of abbreviations and symbols	xv
Chapter	
1. Introduction	1
2. Literature Reviews	3
Objectives	21
3. Materials and Methods	22
4. Results	54
5. Discussion	99
6. Conclusions	104
References	107
Appendix	116
Appendix A	117
Appendix B	119
Vitae	131

LIST OF FIGURES

Figure	Page
1. Male reproductive system of marine shrimp	3
2. Ovary of female marine shrimp	4
3. Thelycum of female shrimp	4
4. Physical observation of shrimp ovary during ovarian development	6
5. Histological picture revealed oocyte of shrimp at a different stage of ovarian development	6
6. Histological picture presented stage of testicular development in <i>Panulirus argus</i> (Latr.)	7
7. Two types of morpholinos	14
8. Schematic representation of type II CRISPR-cas9 system in bacterial immunity system	15
9. A schematic representation of the heteroduplex mobility assay (HMA)	16
10. Camera lucida sketches of the zebrafish embryogenic stages	18
11. Phylogenetic tree of full-length <i>rpl10a</i> sequences	54
12. Multiple alignment of mouse, zebrafish, shrimp and fruit Rpl10a protein sequences	55
13. Expression and purification of recombinant protein His-Rpl10a and Western blotting	56
14. Histological section observation of different shrimp ovarian development stage under light and fluorescence microscope	58
15. Graph percentages of vitellogenic stages of shrimp ovarian development after 180 µg rRpl10a protein injection at 7 and 15 days	60
16. MF level in the hemolymph at different stages of ovarian development after injection with 180 µg Rpl10a protein 7 days	62
17. Histological picture presented stage of testicular development of shrimp testis	64
18. The percentages of testicular development of shrimp testis explants after incubation	65

LIST OF FIGURES (continued)

Figure	Page
19. Shrimp testes sections with hematoxylin and eosin staining in different concentration of rRpl10a protein	66
20. The fold change of <i>Dmrt1/EF1α</i> in treated testis in shrimp	67
21. Cross section of mice testis presented different cell of testicular development	68
22. Effect of the recombinant His-rRpl10a protein at the different dosage on testicular development in male mice	69
23. The picture presented mice testes sections with hematoxylin and eosin staining in different concentration of rRpl10a protein	70
24. WGA lectin histochemistry confirmed the spermatid cells in seminiferous tubules	72
25. Effect of the recombinant Rpl10a protein on the levels of <i>Rhau</i> and <i>Prm2</i> mRNA on mice's testis explants	74
26. Effect of rRpl10a protein on cell proliferation	75
27. Schematic presents zebrafish <i>rpl10a</i> gene structure and RT-PCR	77
28. Morphology of zebrafish embryos after <i>rpl10a</i> MO ^{aug} injection	78
29. Morphology of zebrafish embryos after <i>rpl10a</i> MO ^{spE515} injection	79
30. PCR product of morphants after MO ^{spE414} injection	80
31. The sequence of <i>rpl10a</i> gene which was deleted after exon 5 splice-modification embryos	80
32. Predicted amino acids after Rpl10a protein deficiency using <i>rpl10a</i> MO ^{spE515} injection	81
33. The morphology of rescued <i>rpl10a</i> MO ^{aug} morphants with the synthetic full length of <i>rpl10a</i> mRNA at 24 and 48 hpf	82
34. The zebrafish embryo morphology of morphants which rescued with the synthetic full length of <i>rpl10a</i> mRNA	82

LIST OF FIGURES (continued)

Figure	Page
35. Hemoglobin staining after <i>rpl10a</i> MO ^{spE515} recovery with <i>rpl10a</i> mRNA	83
36. Fold change expression of <i>nanos1</i> and <i>vasa</i> gene in <i>rpl10a</i> knockdown embryos	84
37. Fold change expression level of PGCs marker genes after <i>rpl10a</i> MO ^{sp} injection and rescue experiment	85
38. qRT-PCR results presented fold change expression of <i>gata1</i> and <i>tp53</i> gene in <i>rpl10a</i> knockdown embryos	86
39. Fold change expression of <i>hbae3</i> and <i>hbbe1</i> mRNA in Rpl10a-deficient Embryos	87
40. The expression of <i>vasa</i> , <i>nanos1</i> , <i>myoD</i> and gene in zebrafish using WISH assay after MO injection	88
41. Whole-mount <i>in situ</i> hybridization presented the expression of PGCs marker genes	89
42. The percentage of expression intensity of PGCs marker genes	90
43. The morphology of zebrafish embryos after CRISPR injection and HMA	91
44. Insertion/deletion mutation patterns after <i>rpl10a</i> exon5 CRISPR injection (F0 embryos)	92
45. HMA patterns of each F1 embryo mutation	94
46. Mutation patterns and amino acid changing in F1 embryos	95
47. Heteroduplex pattern was observed after CRISPR-Cas9 injection	96
48. Abnormality phenotype and morphology of homozygous 5-bp deletion embryos	97
49. Hemoglobin staining of 5 bp deletion	98

LIST OF TABLES

Table	Page
1. Primer sequences were used in zebrafish experiments	23
2. Reagents for cDNA synthesis	40
3. PCR reaction reagents	41
4. Thermal cycling for PCR analysis	41
5. Sequencing PCR reaction composition	42
6. Thermal cycling for sequencing sample PCR analysis	43
7. The reagents for rpl10a mRNA synthesis	45
8. Reaction component for DIG RNA probe synthesis	47
9. Reaction component for CRISPR-Cas9 injection buffer	50
10. PCR reaction reagents for HMA assay	51
11. Thermal cycling for PCR analysis for HMA assay	51
12. Percentages of vitellogenic stages of shrimp ovarian development after 180 µg rRpl10a protein injection at 7 and 15 days	59
13. Rpl10a protein levels in a different stage of shrimp ovarian development after 180 µg rRpl10a protein injection at 7 days	61
14. Composition of 12% SDS-polyacrylamide gel	118

LIST OF ABBREVIATIONS AND SYMBOLS

AMV	=	Avian myeloblastosis virus
AP	=	Alkaline phosphatase
APS	=	Ammonium persulphate
BCIP	=	Bromochloro indolyl phosphate
BSA	=	Bovine serum albumin
Cas9	=	CRISPR associated protein 9
cDNA	=	complementary DNA
CR	=	Cortical rod
CRISPR	=	clustered regularly interspaced short palindromic repeats
crRNA	=	CRISPR RNA
DBS	=	Double-strand break
DMEM	=	Dulbecco's Modified Eagle's Medium
Dmrt1	=	Doublesex and Mab-3-related transcription factor 1
dNTP	=	Deoxyribonucleotide triphosphate
dpf	=	days post fertilization
DTT	=	1, 4-Dithio-DL-threitol
EDTA	=	Ethylenediaminetetraacetic acid
EF1 α	=	Elongation factor-1-alpha
ELISA	=	Enzyme-linked immunosorbent assay
FC	=	Follicle cell
g	=	gram
gata1	=	GATA-binding factor 1
h	=	hour (s)
hbae3	=	embryonic globin alpha e3
hbbe1	=	embryonic globin beta e1
HEPES	=	4-(2-hydroxyethyl)-1-piperazineethanesulfonic acid
HMA	=	Heteroduplex mobility assay
His	=	Histidine
hpf	=	hours post fertilization

LIST OF ABBREVIATIONS AND SYMBOLS (continued)

HSP70	=	Heat shock protein 70
IPTG	=	Isopropylthiogalactose
kDa	=	Kilodalton (s)
L-15	=	Leibovitz's L-15 Medium
LB	=	Luria-Bertani (medium)
mA	=	milliampere
MF	=	Methyl farnesoate
mg	=	milligram
min	=	minute (s)
mL	=	milliliter
mM	=	millimolar
mm	=	millimeter
mRNA	=	Messenger ribonucleic acid
μg	=	microgram
μL	=	microliter
μM	=	micromolar
μm	=	micrometer
mpi	=	month-post injection
MO	=	Morpholino Oligonucleotides
N	=	Nucleus
NBT	=	Nitroblue tetrazolium salt
μg	=	microgram
ng	=	nanogram
nm	=	nanometer
nt	=	nucleotide (s)
PAGE	=	Polyacrylamide gel electrophoresis
PAM	=	Protospacer adjacent motif
PBS	=	Phosphate buffer saline
PBST	=	Phosphate buffer saline Tween-20
PCR	=	Polymerase chain reaction

LIST OF ABBREVIATIONS AND SYMBOLS (continued)

PFA	=	Paraformaldehyde
pg	=	picogram
PGCs	=	Primordial germ cells
Prm2	=	Protamine 2
Rhau	=	RNA helicase associated with AU-rich element
RNA	=	Ribonucleic acid
RNase	=	Ribonuclease
RPs	=	Ribosomal proteins
Rpl10a	=	Ribosomal protein L10a
rpl38	=	Ribosomal protein L38
rps19	=	Ribosomal protein S19
RT	=	Reverse transcription
s	=	second
SDS	=	Sodium dodecyl sulfate
sec	=	second
SOP	=	Shrimp ovarian peritrophin
SSC	=	saline-sodium citratesaline-sodium citrate
SSCT	=	saline-sodium citratesaline-sodium citrate tween20
TBS	=	Tris-Buffered Saline
TCTP	=	Translationally controlled tumor protein
TEMED	=	N,N,N',N' –tetramethyl-ethylenediamine
tp53	=	Tumor protein p53
tracrRNA	=	trans-activating crRNA
Tris	=	Tris (hydroxymethyl) aminethane
Tris-HCl	=	Tris (hydroxymethyl) aminoethane hydrochloric acid
U	=	unit (s)
V	=	volt
v/v	=	volume per volume
W	=	Watt (s)
WGA	=	Wheat germ agglutinin

LIST OF ABBREVIATIONS AND SYMBOLS (continued)

WISH	=	Whole mount in situ hybridization
WT	=	wild-type
w/v	=	weight per volume

CHAPTER 1

INTRODUCTION

Ribosomal protein was known to play a role in protein synthesis. Many studies reported the secondary function including DNA repair, apoptosis, translation control, development regulation and red blood cell development (Wool, 1996). Extra-ribosomal functions in the organism development regulation were widely studied. Ribosomal protein S2 (RPS2) in mosquito controlled diapause of adult female by knocking down the *rps2* gene, then ovarian maturation was interrupted (Kim and Denlinger, 2010). Similarly, the *rpl24* gene mutation, the protein synthesis and proliferation were disturbed (Oliver et al., 2004). Also, RPL24 protein in ovary of marine shrimp was highly expressed and it played a role in oogenesis maturation (Zhang et al., 2007). Moreover, several ribosomal protein mutations relate to Diamond-Blackfan anemia (DBA) patients especially *RPS19* (25%) (Draptchinskaia et al., 1999). The other ribosomal proteins have also been identified including *RPL5*, *RPS10*, *RPS7*, *RPL11*, *RPS17*, *RPS26*, *RPS24*, *RPL26* and *RPL35A* (Gadav et al., 2006; Cmejla et al., 2007; Farrar et al., 2008; Gadav et al., 2008; Doherty et al., 2010).

Rpl10a is a component of the 60s subunit and encoded by the *rpl10a* gene. In the previous study, there are few studies of other ribosomal functions of Rpl10a. The previous study, Rpl10a protein plays a function during organogenesis and embryogenesis (Fiscaro et al., 1995). The recombinant Rpl10a protein was also known to involve in shrimp ovarian maturation *in vitro* (Wonglapsuwan et al., 2010). It was also found that the expression pattern of the transcripts was the highest at early ovarian developmental stages in the fruit fly or *Drosophila melanogaster* (Wonglapsuwan et al., 2011). Furthermore, the study function of Rpl10a in fruit fly revealed that the appropriate expression level of Rpl10a is required for controlling oogenesis. Therefore, several roles of the Rpl10a were checked out as follows:

The function of rRpl10a protein on ovarian maturation of banana shrimp (*F. merguensis*) was investigated by *in vivo* to pave the way for industrial aquaculture in the future.

In addition, there is no report of the Rpl10a function associated with spermatogenesis in shrimp and mammalian, so the function of Rpl10a was investigated in the testicular development of shrimp and mouse.

Moreover, other functions of *rpl10a* on anemia using zebrafish (*Danio rerio*) as a model were also studied. Zebrafish is one of the most common animal models because of its many advantages including small size, easy to maintain and produce the progeny, high resolution genetic and conserved sequences with mice and human. One of them, the transparent embryo is useful to study the organogenesis and red blood cell development (Amatruda et al., 2002). The Morpholinos are very useful for function analysis or loss-of-function of responsive genes. Moreover, clustered regularly interspaced short palindromic repeats (CRISPR)/CRISPR-associated protein 9 (Cas9) is a tool for genome modification that has highly efficient and specific to target. Therefore, in this research, we investigated the activity of the secondary function of *rpl10a* gene using knockdown and knockout zebrafish model by Morpholinos and CRISPR-Cas9 technique, respectively. Furthermore, the *rpl10a* gene-deficient embryo was rescued to determine the recovery of the embryo development and anemia. Also, we observed the effect of *rpl10a* deficiency on primordial germ cells (PGCs) marker gene expression. Our findings will indicate the effect of the loss function of Rpl10a on secondary function especially embryo development and anemia.

Overall these studies will enrich the understanding the secondary function of the *rpl10a* that play an essential role in embryogenesis development, reproduction and anemia.

CHAPTER 2

LITERATURE REVIEWS

1. Reproductive organs of shrimp

1.1 Male reproductive system

The male reproductive system consists of paired testes, paired vasa deferens, and a petasma (Figure. 1). The testis is an unpigmented and translucent organ. The position of testes is in the body. Each testis includes cavity anterior and five lateral lobes located under the carapace. The lobes are connected to the vas deferens. The vas deferens occurs from the posterior edges of the main axis of the testes and opens to the exterior through genital pores located on the coxae of the 5th pereopods (Motoh, 1981). Each vas deferens comprises of four regions including a short and narrow (proximal vas deferens); a thickened middle section (medial vas deferens); a long narrow tube which tapers to form (distal vas deferens); a muscular region or terminal ampoule. The terminal ampoule is a distal region that is formed the spermatophore. The spermatophore is the structure in which the sperm cells are transported from male to female (King, 1948).

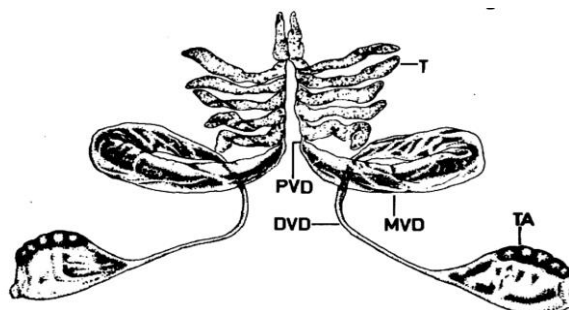


Figure 1. The figure showed male reproductive system of marine shrimp (T, testis; PVD, proximal vas deferens; MVD, medial vas deferens; DVD, distal vas deferens; TA, terminal ampoule (Motoh, 1981).

1.2 Female reproductive system

Shrimp female reproductive system composes of oviducts and paired ovaries (Figure 2) and a thelycum (Figure 3). The ovaries are fused in the body cavity covering the region from the stomach to the telson (Motoh, 1981). The mature ovaries extend from the oesophageal region to the sixth abdominal somite and the mature ovaries consist of two posterior lobes and anterior lobes (6-8 short lateral lobes). The oviducts lead from the sixth lateral lobe to the genital openings (Dall, 1990). The thelycum which is an organ for spermatophore attachment during mating is located between a pair of the 5th pleopods (King, 1948).

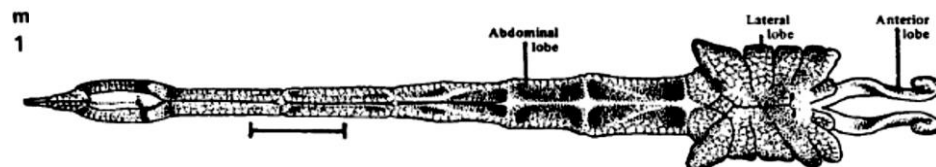


Figure 2. Ovary of female marine shrimp (Motoh, 1981)



Figure 3. Thelycum of female shrimp (Motoh, 1981)

2. Gonadal development in male and female shrimp

2.1 Ovarian development in female shrimp

The stage of ovarian development in shrimp could be distinguished based on the observation of external physiology of ovaries (Figure 4) and the histology of ovarian tissues (Figure 5).

Undeveloped ovary is a translucent ovary, therefore, it is difficult to divide it through the carapace. At this point, the ovary is comprised of a connective tissue capsule call oogonia, and follicle or nurse cells. Previtellogenic oocytes developed from oogonia were observed.

Stage I (developing) filling some of the abdominal cavity, the ovary is better developed when compared to stage I. The thin band of ovary can be observed through the carapace. The developing eggs are increasing in size; they are yolkless oocytes. Also, the ovarian follicle cells were observed surrounding the oocyte.

Stage II (Nearly ripe ovary) is yellow ovary and thicker in diameter than the adjacent gut. The most of yolky oocytes or vitellogenic oocytes were observed.

Stage III (Fully ripe or mature ovary) represented by the thick band, dark green which filling most of the abdominal cavity. The ovary covers part of the stomach in the cephalothorax region. The ovary is easy seen by naked eyes. The cortical rods in the mature oocyte were presented (Ikhwanuddin et al., 2012).

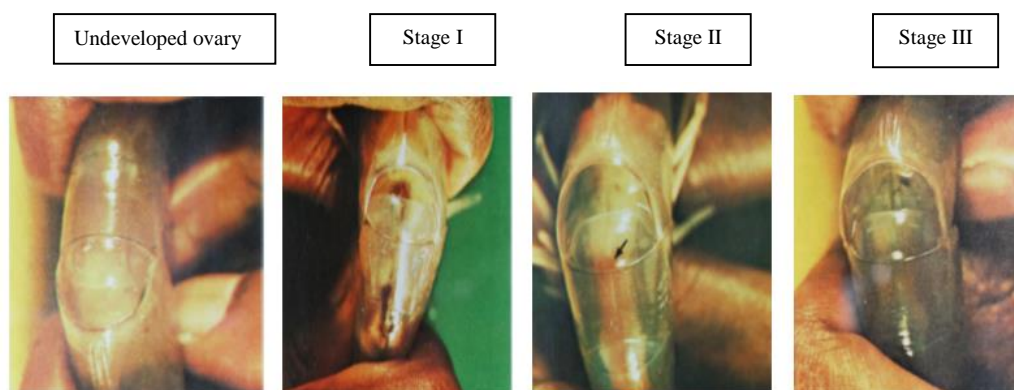


Figure 4. Physical observation of shrimp ovary during ovarian maturation (Brown. and Daniel, 1974).

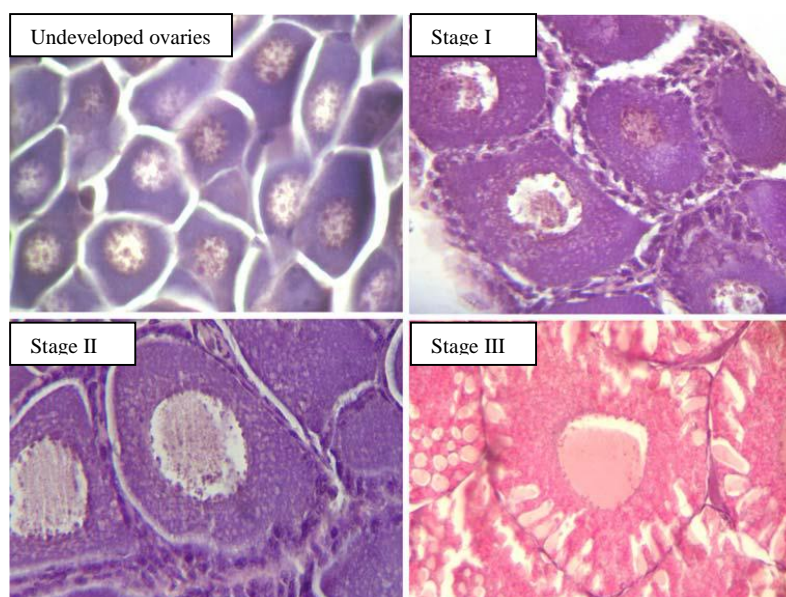


Figure 5. Histological picture revealed oocyte of shrimp at a different stage of ovarian development (Wonglapsuwan et al., 2010).

2.2 Testicular development in male shrimp

Stage I spermatogonia cells located in seminiferous tubule's periphery, contact with the basal membrane. Most spermatogonia cells divide into primary spermatocytes.

Stage II presented spermatogonia cells are formed more division clearly than stage I. Many of spermatocytes I also in the division was observed.

Stage III presented by the appearance of the spermatids and spermatozoa. In this stage, cut of seminiferous tubule which are stratified spermatogonia and spermatocytes were found (Mota and Tome, 1956) (Figure 6).

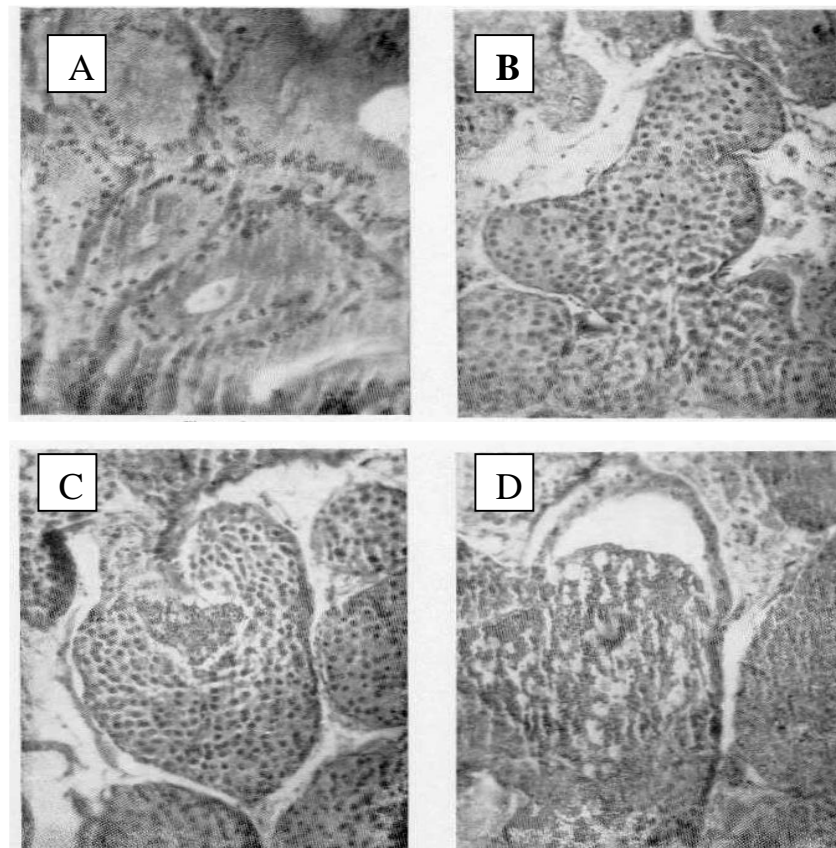


Figure 6. Histological picture presented stage of testicular development in *Panulirus argus* (Latr.). A: spermatogonia, B: spermatocyte I, C: spermatocyte II, D: spermatid (Mota and Tome, 1965).

3. Spermatogenesis in mouse

Spermatogenesis is the process of spermatozoa in which the mature gametes are produced. This process is divided into three phases which included mitosis, meiosis and spermiogenesis. Mitosis is a process when spermatogonia type A is proliferated and differentiated to type B. Then type B spermatogonia cells are meiotically divided into primary spermatocytes. In meiosis, the secondary spermatocytes are produced from primary spermatocytes which are then divided again to form round spermatid. Spermiogenesis is the transformation process of the round spermatid forming into spermatozoa (Gartner and Hiatt, 2012). Spermatogenesis efficiency relies on the activity of spermatogonia cell proliferation and the extinction of sperm production (Johnson et al., 1992). Regulating of spermatogenesis occurs via controlling hormones in the hypothalamus. The hypothalamus secretes gonadotropins including luteinizing hormone (LH) and follicle-stimulating hormone (FSH). LH stimulates the Leydig cells which support production of sperm by stimulating the testosterone hormone production. The FSH is necessary for the spermatogonia proliferation and development of spermatogenesis by stimulating the Sertoli cells (Sharma and Agarwal, 2011). O'Shaughnessary et al. (2010) reported that FSH enriches the number of spermatogonia and spermatocytes cells in the hypogonadal mice.

4. Detection of spermatozoa using lectin

Lectins are useful for spermatozoa detection because of their complex form and cross-link with carbohydrate and glycoconjugate on the surface of the membrane. Then the sperm membrane can change morphology and induce acrosome forming. In Babirusa, (*Babirusa babyrussa*), WGA stained acrosome with low intensity, and the binding in acrosome that has an affinity for N-acetyl-d-glucosamine sugar was observed in the acrosome of Golgi complex and cap phase spermatid. WGA was also

observed in the cytoplasm of spermatid. Moreover, spermatocytes, spermatogonia, and Sertoli cells were stained with WGA (Agungpriyono et al., 2007).

Similarly, WGA was stained both in the acrosome and cytoplasm of spermatid in the lesser mouse deer because of the represented of N-acetyl-d-glucosamine and sialic acid sugar residues. WGA staining was observed in acrosomal spermatid and spermatocytes; while WGA was detected only spermatid acrosome (Agungpriyono et al., 2009). Moreover, the binding of WGA to testis was detected a weak signal in early spermatids, whereas the acrosomal staining of late spermatids showed high intensity. WGA receptor is synthesized during spermiogenesis (Söderström et al., 1984).

5. Ribosomal protein L10a (Rpl10a)

Rpl10a is a component of the 60s subunit and encoded by the *rpl10a* gene. The *rpl10a* gene expression in the thymus is decreased by cyclosporin-A (CsA) which is an immunosuppressive drug. In mouse study, the decreasing of *rpl10a* gene expression is regulated in neural precursor cells during development. Previously, *rpl10a* gene was also referred to NEDD6 (neural precursor cell expressed, developmentally downregulated 6). Moreover, Rpl10a might has a function in organogenesis and embryogenesis (Fiscaro et al., 1995). Also, an interaction between Rpl10a and trichosanthin (TCS) was indicated that the specific cytotoxicity of TCS seemed to be relevant to the distribution of Rpl10a (Xia et al., 2005). Rpl10a protein comprised of 669 bp and formed to polypeptide that contained 217 amino acids. The calculated molecular mass and pI of shrimp Rpl10a protein were 25.7 and 10.06, respectively. The localization of the Rpl10a protein was confirmed with anti-Rpl10a antibody by an immunohistochemical technique. This protein was in the cytoplasm and nucleus of developing oocytes and follicle cells. The intranuclear localization signal was demonstrated by translocation of synthesized Rpl10a protein from the cytoplasm into the nucleus (Wonglapsuwan et al., 2010). Wonglapsuwan et al. (2009) reported differentially genes that expressed in the ovaries of banana shrimp (*F. merguensis*) during ovarian maturation. They reported that the *rpl10a* mRNA

expression level was highly expressed in an early stage of vitellogenesis (stage I). Also, the *rpl10a* transcript expression in lymphoid of shrimp was highly expressed during vitellogenesis when compared with undeveloped ovary while its level in heart and hepatopancreas was a low and down-regulated expression in brain and intestine. The effects of His-Rpl10a protein on shrimp ovarian development by incubating undeveloped ovary with rRpl10a protein showed that His-Rpl10a protein could stimulate early vitellogenesis. Wonglapsuwan et al. (2010) indicated that after rRpl10a protein and ovary incubation, the levels of early vitellogenesis gene such as *TCTP*, *SOP*, and *HSP70* gene was observed maximum level at 4 h. Moreover, they confirmed the specificity of His-Rpl10a as ovarian stimulator by treated muscle tissue with His-Rpl10a. The result showed that there was very little change in those genes.

In *D. melanogaster*, Wonglapsuwan et al. (2011) found that shrimp Rpl10a over-expression in wild-type flies caused cell death in germline, follicle cell and eyes of *Drosophila*. Over-expression of Rpl10a in eyes showed increase roughness and loss of color due to pigment cell death. This result suggested that the excess of Rpl10a may toxic to cells, so the optimal level of Rpl10a is important. Furthermore, Rpl10Ab gene in *D. melanogaster* may be involved in the insulin signaling pathway.

In addition, a recent study in rainbow trout (*Oncorhynchus mykiss*), Makkapan et al. (2014) characterized the expression profile of Rpl10a during gonadal development. The result showed that Rpl10a transcript and protein expressed in spermatogonia type A and the Sertoli cells surrounding spermatogonia of the immature testis and expressed both spermatogonia type A and B of mature testis but rarely detected in spermatocytes and not detected in spermatids and spermatozoa. They also reported that Rpl10a mRNA expression levels were significantly reduced in ovarian tissue after treated with 17β -estradiol when compared with control, whereas Rpl10a transcripts within testicular tissue were up-regulated considerably after incubation with 11-ketotestosterone at 100 and 1,000 ng/mL.

6. Early stage related gene in shrimp spermatogenesis (Doublesex and Mab-3-related transcription factor 1 or *Dmrt1*)

Dmrt1 gene contains *Doublesex/Mab-3* DNA-binding motif (DM domain) which is transcription factor for regulating the alteration of early stage Sertoli cell in testis. This gene has conserved region from invertebrate to human. Many reports studied the expression of this gene. Marchand et al. (2000) reported that the expression of *Dmrt1* was changed only in the testis in rainbow trout (*Oncorhynchus mykiss*). The expression was found thought of the spermatogenesis. In contrast, the expression of *Dmrt1* gene in the mouse was found only in the Sertoli cell and germ cell, and was not found in spermatid and spermatozoa (Raymond et al., 1999). Thus, the *Dmrt1* gene was a high expression in Sertoli cell and decreased in the late stage of spermatogenesis. Yamaguchi et al. (2006) studied the function of *Dmrt* in *Takifugu rubripes* in the early stage of gonadal development using RT-PCR. *Dmrt1* was upregulated in testis, but no expression was observed in ovary.

Moreover, they found that *Dmrt3* and *Dmrt1* gene expression involved the gonad development. From the *in situ* hybridization indicated that *Dmrt1* was transcription factor to control the Sertoli cell differentiation. *Dmrt1* was upregulated in Sertoli cell and spermatogonia, but not expressed in the spermatocyte and spermatid. Herpin et al. (2011) investigated the expression of *Dmrt1* gene in various fish; the result showed that it was expressed in a Sertoli cell, spermatogonia and spermatocytes except for *Danio rerio*. In addition, a *Dmrt1* gene in crab (*Eriocheir sinensis*) was expressed in immature testis higher than mature testis. Therefore, *Dmrt1* gene is necessary for early stage of spermatogenesis (Zhang and Qiu, 2010).

7. Early and late stage marker gene of spermatogenesis in mouse

7.1 RNA helicase associated with AU-rich element (*Rhau*) gene

RNA helicase associated with AU-rich element (*Rhau*) gene was reported that required for spermatogonia differentiation. The previous study indicated that the maleless gene (*mle*) which is belonging of DEAD/H box proteins in *Drosophila* is involved in spermatogenesis (Rastelli et al., 1998). The characterization of human DDX36 and mouse Ddx36 genes, which belong to the DEAD/H box was studied and showed highly homologous to *mle* gene in *Drosophila*. Therefore, the DDX36 and Ddx36 genes might be associated with spermatogenesis and male reproduction (Fu et al., 2002). Gao et al. (2015) reported that *Rhau* gene was upregulated in mouse testis higher than in other tissues. They also found that *Rhau* was expressed at high levels in spermatogonia stem cells and primary spermatocytes, but expressed at low levels in spermatid cells. In mice *Rhau* knockout testes, the percentage of primary spermatocytes was decreased, resulting in abnormal cell proliferation during spermatogonia differentiation. Therefore, *Rhau* plays an important role in spermatogonia differentiation.

7.2 Protamine 2 (*Prm2*)

Protamines are the major proteins in the nucleus of sperm that are involved with late chromatin condensation. There are 2 types of protamine in mice which is protamine 1 (PMR1) and protamine 2 (PRM2). Both protamine transcripts are detected in round spermatid stage and then they are translated during elongating spermatid stage (Bower et al. 1987). The change in expression of PRM1:PRM2 ratio within the spermatozoa cause infertility in human (Torregrosa et al., 2006). Deficiency of protamine affected the decrease in number, motility and spermatozoa morphology. Moreover, *Prm2* caused male infertility and a reduction of the number of child production (Akmal et al., 2016). In mice, found that knockout mice for only and of the *Prm1* or *Prm2* alleles lead to infertility. The *Prm2*-deficient sperm is immotile

because of chromatin deterioration (Cho et al., 2001). From these reports indicated that *Prm2* gene is an essential gene in the late stage of spermatogenesis.

8. Morpholino Oligonucleotides (MOs)

Morpholinos are one of gene knockdown tools that widely used in the zebrafish. They are very useful for function analysis or loss-of-function of interested genes. There are 2 types of MO including translation blocking and transcript defect. To target protein translation inhibition, the 25 bases are bind with the 5' untranslated region (5' UTR) near the start site. The expression of target protein degradation is detected by the disappearance of western blot or immunohistochemistry. While splicing MO is designed to modify pre-mRNA splicing. This activity is easily identified using RT-PCR. The quantity of interested gene expression and PCR product band is changed (Bill et al., 2009). To understand these MOs function, the illustration was shown in Figure 7.

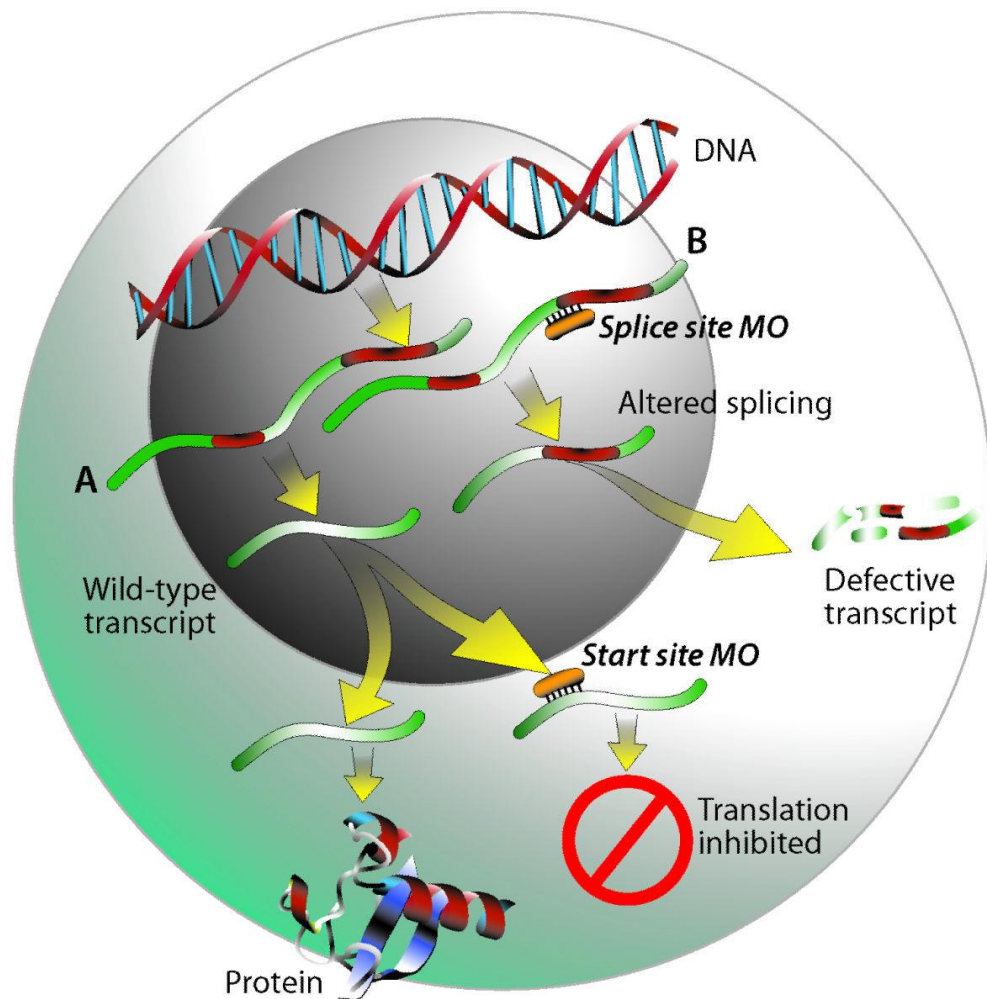


Figure 7. A schematic representation of two types of morpholinos including (A) start site MO and (B) splice site MO which target to translation blocking and mRNA deficiency, respectively. For wild-type, the pre-mRNA is transcribed from DNA and splicing is altered to be mature RNA. Then mature mRNA is exported to the cytoplasm for translation. To inhibit protein translation, a start site MO is bind to complement nucleotides near the start codon (AUG). Splice site MO is designed to alter splicing by binding to intron-exon junctions and degrade transcript (Timme-Laragy et al., 2012).

9. CRISPR-Cas9 system

The clustered regularly interspaced short palindromic repeats (CRISPR)-CRISPR-associated protein 9 (Cas9) system is a useful tool for genome editing. It is an essential bacterial immunity that responds to pathogens. CRISPR systems have been identified according to CRISPR-Cas loci and Cas protein for crRNA binding into 6 types (Jiang and Doudna, 2017). Type II CRISPR mechanism is the most used for study. This system requires endonuclease Cas9 protein for double-stranded DNA substrate recognition and cleavage. A short protospacer adjacent motif (PAM) preises required to recognize the target sequences for editing. The trans-activating crRNA (tracrRNA) is a small non-coding RNA. The combination between 2 components including crRNA and tracrRNA are called guide RNA or gRNA for guiding target sequence specifically. The cleavage dsDNA at specific site results in the double-strand break (DSB) and genome modification. This technique is useful to study loss-of-function of interested genes by establishing frameshift mutations via induction insertion/deletions (indels) (Figure 8).

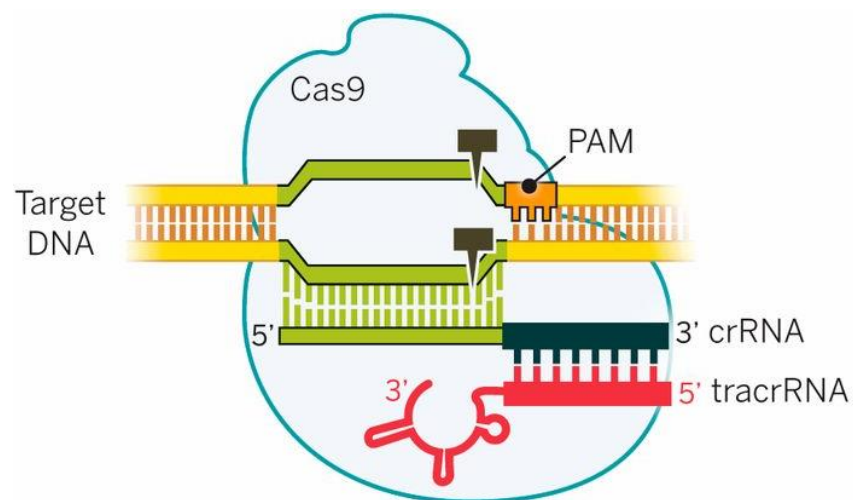


Figure 8. Schematic representation of type II CRISPR- cas9 system in bacterial immunity system. CrRNA and tracrRNA are combined into guide RNA. The crRNA contains 20 nucleotides complementary DNA target sequences. The PAM sequence is strictly recognized, and the target sequence is edited by Cas9 protein (Doudna and Charpentier, 2014).

10. Heteroduplex mobility assay (HMA)

Ota et al. (2013) recently found the simple and multipurpose method for detection of insertion or deletion mutation after genomic modification is heteroduplex mobility assay or HMA assay. The genomic DNA that contains a wild-type allele is found in homoduplexes pattern. While, a mutant allele is found heteroduplexes. These patterns are formed when PCR amplification are performed using specific primers. During polyacrylamide gel electrophoresis, heteroduplexes migrate more slowly than homoduplexes because of their mismatched structure.

HMA assay is useful for the knockout generating processes including the assessment activity of CRISPR/Cas9 editing in F0 embryos, the potential F0 founders with mutant alleles producing, and the genotyping of the mutant F1 generation.

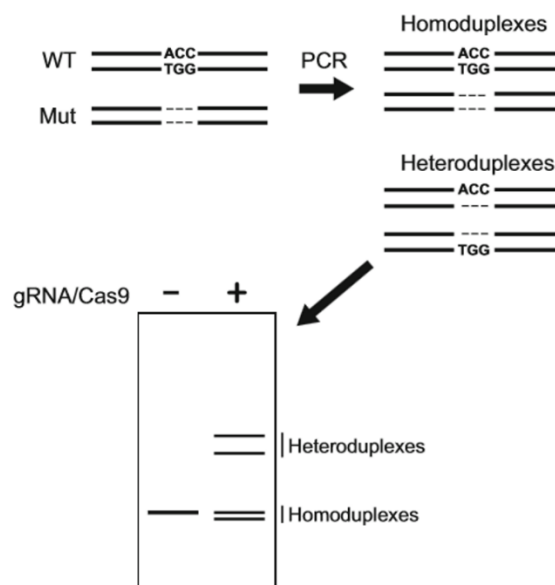


Figure 9. A schematic represented the heteroduplex mobility assay (HMA). The PCR is performed using genomic DNA as a template. The sequences that contained a mutant allele and a wild-type allele are amplified, the PCR product presents both homoduplexes and heteroduplexes. Migration of heteroduplexes under polyacrylamide gel electrophoresis is slower than homoduplexes due to the configuration at the mutation site (Ota and Kawahara, 2016).

11. Stages of zebrafish embryogenic development

The embryogenesis stage of zebrafish (*Danio rerio*) was clarified into 7 periods of development including zygote, cleavage, blastula, gastrula, segmentation, pharyngula, and hatching periods. The morphology and major events that occurred in that period was briefly explained during the first 3-day post fertilization (dpf) in below (Kimmel et al., 1995).

1. The zygote period one-cell stage (0 h). They are newly fertilized eggs that easily appearance within 10 minutes. The egg is a 500 to the 600 pm sphere and the chorion swells and lifts away from the zygote's membrane (Kane, 1994). This stage appears blastodisc forming. During early cell division stages, this segregation is continued.

2. The cleavage period (2-cell to 64-cell: 2 h). After the first cell division of zygote. Cells in this stage called blastomeres, the cell cleavage occurs every 15-minute interval. The cytoplasmic division in early cleavage is incomplete.

3. Blastula period (2.25 h to 5.25 h). This period defines that the blastodisc stats from ball-like shape at the 128-cell stage until the gastrulation period is occurred. This processes, the yolk syncytial layer (YSL), the midblastula transition (MBT) forms, and epiboly is formed.

4. Gastrula period (5.5 h to 10 h). This period starts with the 50%-epiboly and begins to form germ layers.

5. Segmentation period (10 h to 24 h). The various morphogenetic differentiations occur including somite development, primary organs rudiments, tail bud, and the embryo elongation.

6. Pharyngula period (24 h to 48 h). The primordia of the liver make their present along the gut tract. Some organs begin development and differentiation such as head, notocod, fins, pigment cells, circulatory system

7. Hatching period (48 h to 72 h). At 48 hpf, yolk ball depletes, and the head grows. The bilateral of ventral melanophore rows join in the middle line of the developing swim bladder over the yolk ball. Xanthophore differentiation shows the

very pale yellow head cast but still distinct. The beat of the heart easily shows in the stage. The segmental vessels are along the trunk and tail show strong circulation. The hatched larva contains completed morphogenesis and it grow rapidly within 3 dpf. At 72 hpf, the melanin accumulation is placed on the swim bladder rudiment and it caused this region is very dark.

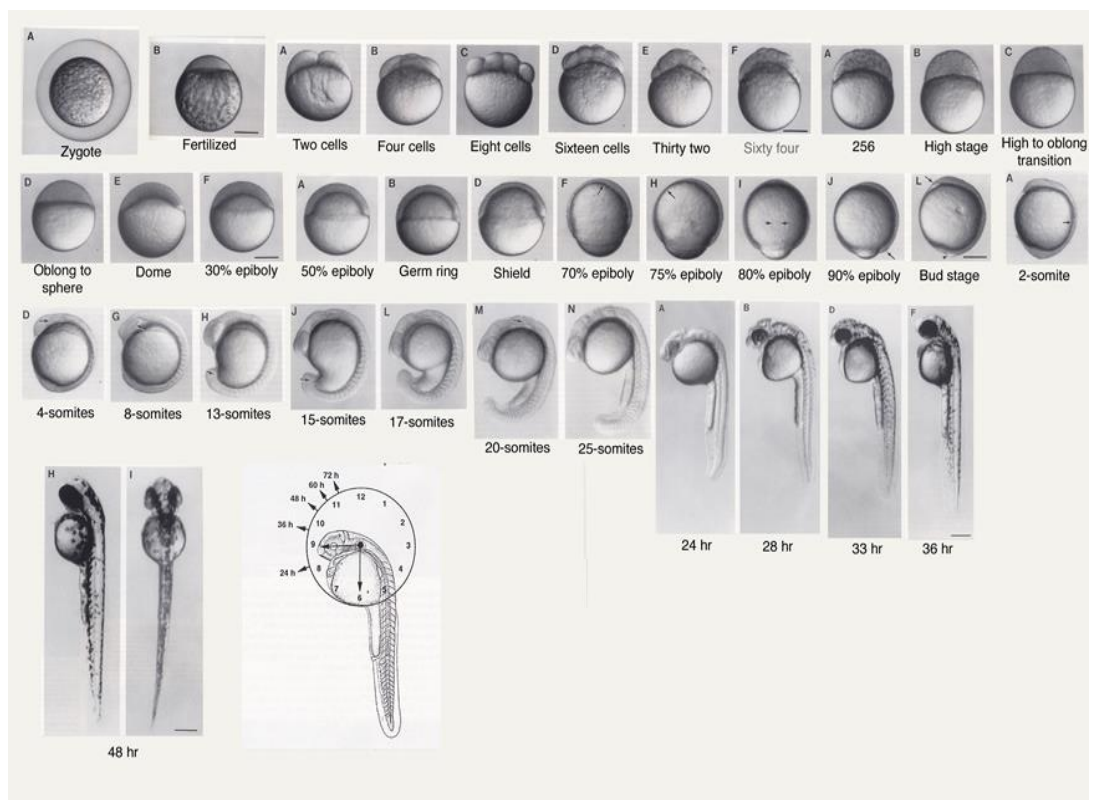


Figure 10. Picture presented the zebrafish embryogenic stages. Scale bar = 250 pm. (Kimmel et al., 1995).

12. Zebrafish erythropoiesis in embryos

Hematopoietic cells in zebrafish arise within the region which named intermediate cell mass (ICM) of embryo. This region is in the middle of the notochord and endoderm of the tail. Hemoglobin of zebrafish is generated in very early stage. Red blood cells or erythrocytes are initially produced about 15 hours post fertilization (hpf). Then, the hemoglobin is displayed in blood circulation during 24–48 hpf (Brownlie et al., 2003). Hemoglobin is synthesized from erythrocytes. It contains two β -globin subunits and two α -globin subunits to form the hemoglobin tetramer (Goodman et al., 1975). Zebrafish α - and β -globin genes are located on the same chromosome. The embryonic genes included hemoglobin beta embryonic-1.1 (*hbbe1.1*) and hemoglobin alpha embryonic-1 (*hbae1*). The expression of globin genes in zebrafish embryo was analyzed by mass spectrometric analysis and found that *hbae1*, *hbae3* and *hbbe1* at 50-60 hpf. In addition, RNA in situ hybridization analysis at 48 hpf indicated that *hbae1/ hbae2*, *hbae3* and *hbbe1* globin gene was higher upregulated than *hbbe2* and *hbbe3* (Brownlie et al., 2003). GATA-binding factor 1 or GATA1 is also named Erythroid transcription factor. The *gata1* transcript was high expressed in early erythroid cells. The expression level of *gata1* associated with severely anemic and also affected to the pigmentation (Ransom et al., 1996).

13. Primordium germ cells (PGCs) marker genes

13.1 *vasa* or a DEAD-box RNA helicase

The *vasa* is a gene which was identified as a marker for PGCs in zebrafish. The localization of *vasa* transcripts is in the cytoplasm, moreover, the position and number of *vasa* expressing cells were observed during somitogenesis and PGCs. (Yoon et al., 1997). The Vasa-positive PGCs migrate to the position of the future gonad and form two bilateral rows of cells during gastrulation and somitogenesis stages (Weidinger et al. 1999). Loss function of *vasa* gene caused reduction of germ cells in almost all organism such as, *Drosophila* species (Lasko et al., 1990); *Caenorhabditis elegans* (Gruidl et al., 1996); *Polyandrocampa misakiensis* (Sunanaga et al., 2007); *Neobenedeniagirellae* (Ohashi et al., 2007). In zebrafish, knockdown of Vasa protein using a *vasa* morpholino showed the normal PGC number and normal fertility because the maternal Vasa protein is not affected by antisense MO. This result revealed that the *vasa* transcript is essential for the zebrafish germline maintenance (Braat et al., 2001).

13.2 *nanos1*

Nanos was discovered and studied in *Drosophila melanogaster* (Irish et al., 1989). Nanos-encoding genes in zebrafish contain *nanos1*, *nanos2*, and *nanos3* (Köprunner et al., 2001). The knockdown of zebrafish *nanos1* by morpholino injection showed a reduced number of PGCs and migration defects. Nanos1 is required for migration and maintenance of PGCs. This demonstrated that *nanos1* plays an important role in germ cell development (Köprunner et al., 2001). In zebrafish, *nanos1* is expressed in germ cell during embryogenesis and adult ovaries. This gene is also required for maintaining the oocyte production, but it is not necessary for oocyte development (Draper et al., 2007).

OBJECTIVES

This research focused on the secondary function of ribosomal protein L10a (Rp110a) on ovarian development and spermatogenesis in shrimp. The mammal model was also used for investigating the activity of Rp110a in testicular development. Also, the deficiency of *rpl10a* gene was studied using zebrafish as a model. The objectives of this study are as follows:

1. To study the effect of His-rRp110a protein on ovarian maturation in banana shrimp (*Fenneropenaeus merguensis*) using *in vivo* assay.
2. To investigate the stimulation of recombinant Rp110a protein on spermatogenesis in black tiger shrimp (*Penaeus monodon*) comparative with the mouse (*Mus musculus*) *in vitro*.
3. To study the effect of *rpl10a* gene knockdown on the early stage of embryogenic development, primordial germ cells (PGCs) marker genes, and anemia using Morpholinos antisense technique in zebrafish (*Danio rerio*).
4. To investigate the function of *rpl10a* gene on abnormal development and anemia after genomic modification by CRISPR-Cas9 using zebrafish as a model.

CHAPTER 3

MATERIALS AND METHODS

I. Materials

1. Plasmid vector

pGEM[®]-T Easy was purchased from Promega (WI, USA).

pCS2⁺ vector was provided by Dr. Kunio Inoue, Kobe university, Japan.

2. Bacterial strains

Escherichia coli DH5 α strain was provided from Prof. Dr. Naoya Kenmochi, University of Miyazaki, Miyazaki, Japan. *Escherichia coli* Top10 strain and BL21 (DE3) was provided from Chotigeat's lab.

3. Chemicals

All of chemicals and solvents (analytical grade) were purchased from Life Technologies, USA; Fluka, Switzerland; Sigma, USA; PIERCE, USA; Amersham, Biosciences; Roche, Germany; Clontech, USA and BIO-RAD, USA; TOYOBO, Japan.

4. Primers

The nucleotide primers for real-time PCR in shrimp and mice tissue were purchased from Invitrogen, Life Technologies (CA, USA) as shown in Table 1. The nucleotide primers for PCR, RT-PCR and real-time PCR in zebrafish were purchased from Hokkaido System Science Co., Ltd. (Tokyo, Japan) as shown in Table 1.

Table 1. Primer sequences were used in experiments

Primer name	Primer sequences (5' → 3')
Forward RT znanos1	GAGCAGCATGGCTTTTTCTC
Reward RT znanos1	ACACAACACCAGTGCACACA
Forward RT zvasa	CACTGGGAGAAGAGGCTTTG
Reward RT zvasa	CAGGTCCCGTATGCAAACCTT
Forward RT zpiwi	AAGCACCGGTATGACAGGAC
Reward RT zpiwi	GGGATGTTGAATGGGTCATC
Forward zrpl10a (full)	CGGGATCCGCCAAAATGAGCAAGGTCTC
Reward zrpl10a (full)	GGAATTCTTGTAGAAAACCTGAGGAACAGAGTC
Forward zfli1 (ISH)	AATATTGTCGGGCTCCACTG
Reward zfli1 (ISH)	CCATCTTCGAGTGCAGTTCA
Forward znanos1 (qPCR)	TGCGAGTTTGCATGCATGTG
Reward znanos1 (qPCR)	AACACAACACCAGTGCACAC
Forward zvasa (qPCR)	AAGGGCTGCAATGTTCTGTG
Reward zvasa (qPCR)	TGCGCATTTCTGGCTCAAAG

Table 1. Primer sequences were used in experiments (continued)

Primer name	Primer sequences (5' → 3')
Forward zgata1 (qPCR)	ATTATTCCACCAGCGTCCAG
Reward zgata1 (qPCR)	TGGGGTTGTAGGGAGAGTTTAG
Forward ztp53 (qPCR)	CCCATCCTCACAATCATCAC
Reward ztp53 (qPCR)	TTGCTCTCCTCAGTTTTCTG
Forward zrpl38	ATGCCACGTAAAATCGAAGAA
Reward zrpl38	ATCTACTTCAGCTCCTTCACAGC
Forward zrpl10a_ex5	ATGTGCTCAGTGCTGTAGCT
Reward zrpl10a_ex5	GTGGATTTACCTCATCCACCT
Forward zrpl10a_full	CGGGATCCGCCAAAATGAGCAAGGTCTC
Reward zrpl10a_full	GGAATTCTTGTAGAAAAGTGGGAACAGAGTC
Forward zrpl10a_HMA	ATGTGCTCAGTGCTGTAGCT
Reward zrpl10a_HMA	GTGGATTTACCTCATCCACCT
Forward zhbae3	GCAAAGGACAAAGCGAACGT
Reward zhbae3	AGGAGAGTTGGGGCTTAGGT
Forward zhbbe1	GCTCTGGCAAGGTGTCTCAT
Reward zhbbe1	TTCTTCACTGCCAGCTCCAG
Forward RHAU (mice)	ATGGATGAACGTCGAGAAGAGC
Reverse RHAU (mice)	ATACCCATGATCCTCAGGAGC
Forward PRM2 (mice)	TACCGAATGAGGAGCCCCA
Reverse PRM2 (mice)	TGCGGATGCCGCCTCCTGT
Forward β -actin (mice)	GCTACAGCTTCACCACCACCG
Reverse β -actin (mice)	GATGTCCTCGTCRCACTTCAT

Table 1. Primer sequences were used in experiments (continued)

Primer name	Primer sequences (5' → 3')
Forward EF1 α (shrimp)	GAACTGCTGACCAAGATCGACAGG
Reverse EF1 α (shrimp)	GAGCATACTGTTGGAAGGTCTCCA
Forward Dmrt1 (shrimp)	CACCTGGGCCCGCCATGACT
Reverse Dmrt1 (shrimp)	CCCAAGTGCTCCCGCTGC

II. Methods

Phylogenetic tree analysis of mouse, zebrafish and shrimp *rpl10a* gene

The nucleotide sequences were obtained from NCBI database and analyzed alignment using ClustalW program Phylogenetic tree was constructed using neighbor-joining method by MEGA7 and testes confidence of data by bootstrap value. The out group of this study was soil-living ameba (*Dictyostelium discoideum*). The amino acid alignment was also performed using ClustalX2 program.

Part I: The effect of rRpl10a protein on shrimp ovarian maturation

1. Expression and purification of rRpl10a protein

To produce the recombinant His-Rpl10a protein, BL21 (DE3) *Escherichia coli* cell with the recombinant pET-28a(+) plasmid containing *rpl10a* gene was cultured (Wonglapsuwan et al., 2010). The protein expression was induced using 1 mM IPTG. Then, His-Rpl10a protein purification was performed using a His-Trap FF column following to the AktaPrime manufacturer's instruction (Amersham, Thailand).

2. Western blot analysis of purified rRpl10a protein

Purified His-Rpl10a protein from the recombinant lysate was confirmed using anti-Rpl10a antibody by western blot analysis. Briefly, the recombinant protein was checked by 12% SDS-PAGE electrophoresis and was transferred on to nitrocellulose membrane by the electro blotter with current (2 mA per cm² of gel) for 2 h. The transferred membrane was removed from the gel and blocked with 5% skim milk in phosphate buffered saline, pH 7.4 (PBS; 137 mM NaCl, 27 mM KCl, 43 mM Na₂HPO₄, 14 mM KH₂PO₄) for 1 h. The membrane was washed three times for 10 min with PBST (PBS plus 0.05% Tween). Then, the membrane was incubated with the primary anti-Rpl10a antibody (at 1:3,000 dilution) (Abcam®, Cambridge, UK) at room temperature for 1 h. After three times of PBST washing for 10 min, the membrane was incubated with antimouse-alkaline phosphatase (at 1:5,000 dilution) (Thermo Fisher Scientific Inc., Rockford, IL, USA) at room temperature for 1 h. Following washed with PBST again, the bound antibodies membrane was detected with a substrate solution comprising 0.37 mM nitroblue tetrazolium (NBT; USB Corporation, OH, USA), 0.23 mM 5-bromo-4-chloro-3-indolyl phosphate (BCIP; USB Corporation, OH, USA) in alkaline phosphatase buffer, pH 9.5 (100 mM NaCl, 50 mM MgCl₂, 100 mM Tris-HCl). The membrane was incubated

in the dark until the protein on the membrane appeared. Then, the reaction was stopped with 1% acetic acid.

3. Shrimp broodstock culture

Body weight of adult female and male shrimp were 40-60 g and 20-30 g, respectively. Those banana shrimp were obtained from the Gulf of Thailand, Nakornsrihammarat province, Thailand and maintained at Satun coastal fisheries research and development center, Satun province, Thailand. Non-vitellogenic shrimps were used in this experiment. Shrimps were cultured in tanks containing 30 ppt seawater, pH 7-8, at 25-28 °C and fed with blood cockle at 3.5% of their body weights twice a day.

4. Stimulation ovarian development using rRpl10a protein by *in vivo* assay

To study the effect of the rRpl10a on shrimp ovarian maturation, the adult female shrimp which exhibited undeveloped ovaries were randomly separated into 2 groups (7 shrimps for each experimental group). The buffer was used as a control (dialysis buffer for protein; 300 mM NaCl, 50 mM NaH₂PO₄, pH 8.0). Another group, 180 µg per shrimp of His-rRpl10a was injected. Each group was reared in concrete tank with the ratio of 7 female shrimps to 2 male shrimp, and they were fed with the cockle throughout the experiment. All of ovarian tissues were dissected on the 7th and 15th day after the first injection to determine the ovarian maturation stages by histological technique. After that, the vitellogenic stages were counted and calculated into percentages under H&E staining observation and also observed under fluorescent microscopy.

5. Shrimp ovarian development histology

5.1 Histology perform

5.1.1 Tissue preparation

Ovarian tissue samples after injection were dissected into small pieces and fixed in fixative buffer (10% formalin, 33 mM NaH₂PO₄, 45 mM Na₂HPO₄). The samples were placed in formalin solution for 72 h at room temperature. Subsequently, the fixed tissues were dehydrated by immersing in 50% ethanol for 2 h, 70% ethanol for 2 h, 95% ethanol for 2 h twice, 100% ethanol for 2 h three times, respectively. Then, the samples were immersed in xylene for 2 h three times and paraffin for 2 h twice. The paraffin blocks were made by filling the tissues with paraffin into the mold, and then cooled. The paraffin blocks were cut with 5 µm of thickness using rotary microtome. The tissues were put into a clean slide before observation.

5.1.2 Hematoxylin and Eosin staining

Dried tissue slides were deparaffinized in xylene for 5 min, twice. Then the slides were hydrated in 100% ethanol for 5 min, twice, 95% ethanol for 5 min, twice and tap water for 5 min. The slides were immersed in Mayer's hematoxylin for 5 min, washed in tap water for 10 min and stained in Eosin working solution for 5 min. After that the dehydration step was performed by dipping in 95% ethanol, three times and immersing in 100% ethanol for 5 min, three times. The slides were then immersed in xylene for 5 min, twice. Finally, the slides were mounted with permount and covered by cover glass. The sections were observed under a microscope. The histological result was presented as a percentage of vitellogenic stages.

For fluorescent detection, the tissue slides were deparaffinized in xylene for 5 min twice, followed by mounting with permount and covered by cover glass. The sections were observed under fluorescence microscopy

6. Shrimp ovarian development assessment

Based on H&E staining, the stages of ovarian development were divided into four stages. Undeveloped stage showed oogonia cells in the center of the tissue sections and the previtellogenic oocytes were $<65\ \mu\text{m}$ in diameter. In stage I, many early developing oocytes with follicle cells surrounding were observed. They had a size between 75 and 125 μm . Stage II, the oocytes are developing, they had 100–200 μm in diameter. The enlarged nucleus and network were observed in this stage. Stage III, the mature oocytes, they contained eosinophilic cortical rods. The cells had a diameter size $>125\ \mu\text{m}$.

7. Determination level of Rpl10a protein in a different stage of shrimp ovary after Rpl10a injection using ELISA technique

The ovarian of the Rpl10a injected shrimp were collected in PBS buffer and kept at $-80\ ^\circ\text{C}$ until determination. Then standard curve was done using the purified Rpl10a protein. The protein (0-16 $\mu\text{g}/\text{ml}$) was fixed to each well by incubation with 100 μL of coating buffer (0.1 M Na_2CO_3 , 0.1M NaHCO_3 pH 9.6) at room temperature for 2 h. The coated plate was washed three times with 200 μL PBST (1x PBS, pH 7.4 containing 0.05% Tween 20; PBST). The remaining protein-binding sites were blocked by adding 200 μL blocking buffer (5% non-fat dry milk in PBST) per well and incubated at room temperature for 2 h. The coated plate was washed and incubated with 100 μL of anti-Rpl10a antibody (diluted 1:3,000 in blocking buffer) each well for overnight at $4\ ^\circ\text{C}$. Then the plate was washed and incubated with 100 μL of anti-mouse-AP antibody (diluted at

1:5000 in blocking buffer) for 2 h at room temperature. After washing again, 100 μ L of the substrate solution (pNPP: *p*-Nitrophenyl-phosphate) was added to each well. After color was developed, then 100 μ L of stop solution (1N NaOH) was added. The absorbance was read using an ELISA microplate reader at 405 nm.

Rp110a protein was extracted from hemolymph, hepatopancreas, and ovary by dissecting explants and homogenized in 100 μ L PBS (1x phosphate buffer, pH 7.4). The extracted solution was centrifuged at 10,000 rpm, 10 min and removed into a new tube. Rp110a protein concentrations in the hemolymph, hepatopancreas or ovary extract were calculated from a standard curve of the Rp110a.

8. Determination level of methyl farnesoate detected by HPLC analysis

The MF concentration in the shrimp hemolymph was detected by HPLC technique. Three hundred μ L of hemolymph of each sample was collected from Rp110a protein injected shrimp at 7 day-post injection and added into the mixture of 200 μ L of 4% NaCl and 300 μ L of acetonitrile. Then, the sample was extracted with 600 μ L of hexane and centrifuged at 10,000 rpm for 10 min. The extracted solution was analyzed by HPLC technique with an Apollo Silica column (150 \times 4.6 mm ID length; a 1200 Series HPLC auto sampler, Agilent Technology, CA, USA). The mobile phase that used as the mobile phase was 1.0% diethyl ether in hexane, and the detection of MF was performed at 218 nm. After that, the MF levels in each sample was determined by calculating from the peak area and compared with MF standard (Echelon Biosciences Inc., UT, USA) (Makkapan et al., 2011).

Part II: The effect of recombinant Rpl10a protein on spermatogenesis

1. Effect of Rpl10a protein on spermatogenesis in black tiger shrimp (*Penaeus monodon*)

1.1 Male shrimp

Immature male black tiger shrimp were obtained from the Satun Coastal Fisheries Research and Development Center, Satun province, Thailand. The shrimp that contained 60-80 g body weight (B.W.) was used for this experiment.

1.2 Incubation of shrimp testis explants with rRpl10a protein

Immature male shrimps (*P. monodon*) was knocked in iced bucket. The testes were carefully separated from the abdomen and the base of the fifth walking leg. That testes were pulled out with a pair of sterile forceps, cut into small pieces of approximately 0.3-0.5 cm in length and cultured in the culture medium. The pieces of testis explants were placed in a 48-well plate that containing 1 ml of 2x Leibovitz's L-15 culture medium (pH 7.4) dissolved in dialysis buffer (300 mM NaCl, 50 mM Na₂HPO₄, pH 7.4) with or without 0.5, 1.0, 1.5 or 2 μ M of purified rRpl10a protein under sterile condition. To prevent bacterial growth, two percent penicillin G-streptomycin was also added. The explants tissues were incubated at 28°C and harvested at 4 h after incubation. Then, those tissues were fixed into fixative buffer. The tissue paraffin blocks were prepared followed by the protocol in 2.5.1-2.5.2 histology perform of part I.

1.3 Shrimp testis histology evaluation

To evaluate the stage of spermatogenesis, the sections are classified into three stages. Stage I, almost cells are spermatogonial cells. They have a round vascular nucleus with diffused chromatin. Nurse cells are found dispersed in between and close to spermatogonial cells. The size of the cells is $> 6.25 \mu\text{m}$ in diameter. Stage II, spermatocytes have basophilic nucleus and cytoplasm with a thin eosinophilic edge. Spermatocytes are dividing cells. This stage composes with spermatocyte I and II. The cells are $3- 6.25 \mu\text{m}$ in diameter. Stage III, there are two types of cells, including spermatid and spermatozoa. Spermatids had condensed chromatin. They are smaller than spermatocytes. Spermatozoa develop from spermatids. They have a circular shape and basophilic condensed chromatin material. The cells are $< 3 \mu\text{m}$ in diameter.

1.4 Determination levels of *Dmrt1* gene expression in shrimp treated testis

To confirm the early stage of spermatogenesis cell, the expression of *Dmrt1*, early stage marker gene was determined. Isolation of total RNA from rRp110a treated testes were performed using Trizol reagent (Invitrogen, California, USA) according to the manufacturer's protocol. One microgram of total RNA was reverse transcribed to cDNA using AMV reverse transcriptase (Promega, USA).

The fold change expression levels of *Dmrt1* transcript was determined by qRT-PCR. 25 μL of the reaction of real-time PCR were composed of 12.5 μL of FastStart Universal SYBR Green Master (Rox) (Roche, Germany), 20 pM of each primer, and 300 ng of cDNA. Thermal cycling and fluorescence detection were performed using the Mx3000P™ (Stratagene, CA, USA). The initial of PCR program was started with a denaturing step at 94 °C for 5 min, followed by 40 cycles of 94 °C for 30 sec, 57 °C for 30 sec and 72 °C for 30 sec. The relative copy number of gene expression was normalized to that of the *Ef1 α* gene in each sample. The testis sample which treated with buffer was

used as a control group. Data was expressed as mean±SD. The primers of these genes were shown in Table 1.

1.5 Statistical analysis

The data was presented as a mean of percentage in each stage and statistically analyzed using the R program. One-Way Analysis of Variance followed by Tukey's multiple comparison tests was used to analyze with a significance level of $p < 0.05$. Two sample t-tests were performed for comparing two control groups and qRT-PCR experiment result (p -value < 0.05).

2. Effect of rRpl10a protein on spermatogenesis in mouse (*Mus musculus*)

2.1 Mouse sample

Adult ICR male mice (*Mus musculus*) at 5-7 weeks of age and weighing 20-30 g were obtained from Southern Laboratory Animal Facility (Thailand). All procedures were followed by the Institute of Animals for Scientific Purpose Development, National Research Council of Thailand guidelines.

2.2 Stimulation spermatogenesis in mouse testis by rRpl10a protein (*in vitro*)

Male ICR mouse was anesthetized by intraperitoneal injection with 40 mg/kg of thiopental sodium B.P., the testes were removed under sterilized condition. The testis explants were washed twice with cell culture medium before cutting into small pieces 3 mm. The testes were then placed in a 48-well plate containing 1 ml of Dulbecco's modified Eagle's medium (DMEM; GIBCO, New York, USA) pH 7.4 containing 10 % FBS with different dosage of rRpl10a protein at 0, 0.5, 1, 1.5 and 2 μ M. The treated seminiferous tubules were incubated at 37 °C under 5 % CO₂. The tubules were collected for histological observation, after 4 h incubation. Then the different cell types in mouse seminiferous tubules were counted and calculated into a percentage of each cell type in spermatogenesis under H&E staining, compared to the testes without rRpl10a treatment.

2.3 Evaluation of differential cell types in mouse spermatogenesis by histological observation

The rRpl10a treated testis explants was fixed in 10% neutral formalin solution (10% formalin, 33 mM NaH₂PO₄, 45 mM Na₂HPO₄) (Wonglapsuwan et al., 2010). Subsequently, the fixed tissues were performed in the tissue processor. Tissues were then embedded to make paraffin blocks. Finally, the samples were sliced into 5 μ m of thickness using rotary microtome (Leica Biosystems, Germany). The sections were stained with Hematoxylin and Eosin staining (Bio-Optica, Italy).

To evaluate the testis stage in mouse, three semeniferous tubules of section in different areas nearly in diameters of tubules were determined. Spermatogenic cells in the tubules were evaluate into four types according to cell morphology containing spermatogonia, spermatocytes, spermatids, and spermatozoa cells. Spermatogonia are the cells which located in the basal compartment. They are the early stage of spermatogenesis

which include type A and type B spermatogonia. Nucleolus of spermatogonia type A and B is located in the peripheral and center of nuclear, respectively. However, we counted both spermatogonia into spermatogonia cells. The spermatocytes consist of two types that are primary and secondary spermatocytes. The primary spermatocyte is larger and less chromatin condensation than the secondary spermatogonia. The secondary spermatocytes replicate immediately and have short life, so they are rarely detected. The spermatid cells have little cytoplasm and form the acrosome. They have two shapes which are round spermatid and elongated spermatid. The elongated spermatid is built into spermatozoa which is located in the lumen of the tubule. Then, the mature spermatozoa leave into the epididymis (Gartner & Hiatt, 2012; Treuting & Dintzis, 2011). The cells in the different pattern were counted and calculated in percentages of spermatogenesis as follows:

$$(\text{Average of number of cell in same type} / \text{Total of cell in the seminiferous tubules}) \times 100\%$$

Then, the average of percentages of spermatogenesis was calculated from 4 samples in each experiment and performed in triplicate.

2.4 WGA lectin histochemistry for spermatid cells evaluation

As the sugar (*N*-acetylglucosamine) on spermatid cell has the property specific binding with wheat germ agglutinin (WGA) so the spermatid cells of the experiment tissue were confirmed by WGA histology. The testes sections were dewaxed, rehydrated and immersed in HBSS buffer. Then, tissue sections were incubated with 1 mg/mL of Alexa Fluor 594 WGA solution and 1 mM Hoechst 33342 stain (Image-iT™ LIVE Plasma Membrane and Nuclear Labeling Kit, Invitrogen, UK) in HBSS buffer 10 min at room temperature. Tissue slides were washed with HBSS buffer for 5 min 3 times before dehydration and mounting. The reaction was detected under fluorescence microscope observation (Olympus DP73, Olympus Corporation, Japan). The number of spermatid cell was counted and calculated in percentages of spermatid cells as follows:

(Average of number of the cell which WGA stained / Total number of the cell which Hoechst stained) \times 100%

2.5 Expression of *Rhau* and *Prm2* gene

To confirm the stage of spermatogenesis cell, the expression of the gene marker of early stage and late stage were determined. The *Rhau* gene which highly expressed in spermatogonia stem cells, and primary spermatocytes was used as a marker for early stage of spermatogenesis. For late stage of spermatogenesis, sperm protamine 2 (*Prm2*) gene which expressed in spermatid was detected. Total RNA was isolated from rRp110a treated testes using Trizol reagent (Invitrogen, California, USA) according to the manufacturer's protocol. Then, cDNA was reverse transcribed from 1 μ g of total RNA using AMV reverse transcriptase (Promega, USA). The levels of *Rhau* and *Prm2* gene expression were determined by qRT-PCR. Twenty-five μ L of the reaction of real-time PCR were composed of 12.5 μ L of FastStart Universal SYBR Green Master (Rox) (Roche, Germany), 20 pM of each primer, and 300 ng of cDNA. Fluorescence detection and thermal cycling were performed using the Mx3000P™ machine (Stratagene, CA, USA). The initial of PCR program was a denaturing step at 94 °C for 5 min, followed by 40 cycles of 94 °C for 30 sec, 57 °C for 30 sec and 72 °C for 30 sec. The gene expression were shown in the relative copy number which normalized to that of the *β -actin* gene in each sample. Data was expressed as mean \pm SD. The primers of these genes were shown in Table 1.

2.6 Determination the proliferation of cell using EdU assay

To detect DNA synthesis in proliferating cells, the EdU label was detected in the testis tissue. The testes were incubated with different concentration of rRp110a protein for 1 h, and EdU (Thermo Fisher Science, Oregon, USA) was added. The testes were collected after 4 h incubation. The treated tissue was fixed in neutral formaldehyde fixative buffer, embedded in paraffin and sectioned. The paraffin in 5 μm thickness of tissue sections was removed by 2 times of soaking in xylene. The sample slides were then rehydrated by ethanol and removed to TBS buffer before staining. The staining protocol was performed as described by Salic and Mitchison (2008). Briefly, the sections were stained by incubating with 10 μM Alexa Fluor® 488 azide (Thermo Fisher Science, Oregon, USA) in 100 mM Tris, pH 8.5 containing 1 mM CuSO_4 and 100 mM ascorbic acid for 20 min. The slides were washed three times with TBS with 0.1% Triton X-100. Thereafter, the sections were mounted with DAPI staining medium (Vector Laboratories, California, USA) and observed under fluorescence microscopy (Olympus DP73, Japan).

2.7 Statistical analysis

The data in each stage was reported as a mean of percentage and statistically analyzed using the R program. One-Way Analysis of Variance followed by Tukey's multiple comparison tests was used to analyze with a significance level of $p < 0.05$. Two sample t- tests were performed for comparing two control groups and qRT- PCR experiment result ($p\text{-value} < 0.05$).

Part III: The effects of *rpl10a* gene knockdown and knockout using zebrafish *D. rerio* as a model

1. The effects of *rpl10a* gene knockdown using morpholino antisense oligonucleotide

1.1 Experimental animals

The wild-type of AB line zebrafish were maintained in the Bio-resource Division at the Frontier Science Research Center, University of Miyazaki, Japan. The embryos were grown in E3 embryos medium at 28.5 °C under lighting conditions (14 h light and 10 hr dark).

1.2 The effect of *rpl10a* morpholinos on zebrafish embryos morphology

1.2.1 Morpholino Antisense Oligonucleotides (MO) injections

Two types of MOs to knock down *rpl10a* gene were designed from Gene Tools, LLC (USA). The AUG MO (MO^{aug} 5'-GACCTTGCTCATTTTGGCGTGATAT-3') contained 13 bp of 5' UTR, translation start site, 2 bp of exon1 and 7 bp of exon2 to block Rpl10a protein translation. The splice MOs were designed to target pre-mRNA splicing at exon 4/intron4 (MO^{spE4I4} 5'-ATTTTCGGTTTTTAAACTC ACCCAGC-3') and exon5/intron5 (MO^{spE5I5} 5'-ATCACAAATATAGACATACCTTCTT-3'). The *rps19* MO^{aug} sequences that were used as a control for this experiment was 5'-CACTGTTACACCACCTGGCATCTTG-3' (Uechi et al., 2006). MOs at different concentrations (MO^{aug} at 0.5 and 5 µg/µL; MO^{spE4I4} at 20 and 40 µg/µL; MO^{spE5I5} at 5 and

10 $\mu\text{g}/\mu\text{L}$) were injected into one or two-cell-stage embryos using an IM-30 Electric Micro-injector (Narishige, Japan). The morphology was observed at 25 and 50 hpf.

1.3 RT-PCR amplification after MOs injection

1.3.1 Total RNA extraction

The embryos at 24 hpf were collected in the Trizol reagent for total RNA extraction and isolated from 15- 20 embryos using Trizol reagent (Invitrogen, USA) according to the manufacturer's protocol.

1.3.2 cDNA synthesis

The cDNA was synthesized by using High-Capacity cDNA Reverse Transcription Kit (ABI) following the reaction in Table 2. Then, the mixture was incubated at 25°C for 10 min, 37 °C for 120 min followed by incubated at 85°C for 5 min.

Table 2. Reagents for cDNA synthesis

Reagent	Volume per reaction (μL)
RNase-free water	3.2
10x RT buffer	2.0
10X RT Random Primers	2.0
25X dNTP Mix (100 mM)	0.8
MultiScribe™ Reverse Transcriptase	1.0
RNase inhibitor	1.0
Total RNA (500 ng)	10.0
Final volume	20.0

1.3.3 PCR amplification

After cDNA synthesis, the expression of *rpl10a* mRNA was detected using PCR amplification using Expand™ High Fidelity PCR System Kit (Roche, Mannheim, Germany). The reaction and condition for PCR was shown in table 3 and 4.

Table 3. PCR reaction reagents

Reagent	Volume per reaction (μL)
Sterile H ₂ O	14.7
10X buffer	2.0
10 mM dNTP mix	1.0
forward and reverse primer mix (20 μM each)	1.0
High Fidelity Taq DNA polymerase	0.3
cDNA template	1.0
Final volume	20.0

Table 4. Thermal cycling for PCR analysis

Temperature	Time	Cycles
94°C	2 min	1
94°C	30 s	35
58°C	30 s	
72°C	30 s	
72°C	7 min	1

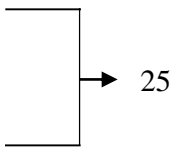
1.3.4 The sequencing performing

Sequencing samples were amplified using BigDye™ Terminator v3.1 Cycle Sequencing Kit (ABI) following the reaction composition and PCR condition in Table 5 and 6. The sequencing reaction was purified with ethanol/EDTA precipitation. The reaction was transferred into a new tube and added sterile water to make 20 μL total volume. Subsequently, 2 μL of 125 mM EDTA pH 8.0, 2 μL of 3 M NaOAc pH 5.2 and 100% ethanol were added in the reaction mixture. The mixture was centrifuged at 14,000 rpm, 4°C for 25 min after 15 min incubation at room temperature. The supernatant was removed followed by washing with 70 μL of 70% ethanol. Then, the pellet was dissolved in 18 μL of HiDi formamide and denatured at 96 °C for 3 min. The sequences were analyzed by the sequencer.

Table 5. Sequencing PCR reaction composition

Reagent	Volume per reaction (μL)
Sterile H ₂ O	4.9
5x BigDye buffer	2.0
1 μM of T7 or SP6 specific primer	1.6
BigDye enzyme	0.5
DNA template (50 ng)	1.0
Final volume	10.0

Table 6. Thermal cycling for sequencing sample PCR analysis

Temperature	Time	Cycles
96°C	1 min	1
96°C	15 s	
50°C	10 s	
60°C	2min	
25°C	5 min	1

1.4 *In vitro* mRNA synthesis for rescue experiments

1.4.1 Full-length *rpl10a*-pCS2⁺ construction

The *rpl10a* gene was amplified from the zebrafish full-length *rpl10a* cDNA sequence (GenBank accession number NM_199636.1). The PCR product and pCS2⁺ vector were digested with *Bam*HI and *Eco*RI restriction enzyme (NEB Inc., US) by incubation at 37 °C for 30 min. The digested fragments were purified using MagExtractor PCR clean-up kit (Toyobo, Japan) and checked by 1% agarose gel electrophoresis. The purified *rpl10a* gene and pCS2⁺ vector were then ligated and transformed into *E. coli* DH5α competent cells (Takara, Japan). One microliter of ligation mix was transferred into 50 μL of competent cells and placed on ice for 30 min. The reaction was heated shock for 45 sec at 42 °C before putting on ice for 2 min immediately. The 950 μL of SOC medium was added into the transformed bacteria and cultured at 37 °C for 1.5 h by shaking (180 rpm). The cultured bacteria were spread onto LB agar plate containing 100 μg/ml and IPTG/X-Gal and incubated overnight at 37 °C. The positive colony was purified using MagExtractor Plasmid kit (Toyobo, Japan) and confirmed by sequencing following protocol 1.3.4 in part III.

1.4.2 *In vitro* transcription

The recombinant *rpl10a*- pCS2⁺ plasmid was linearized using *NotI* restriction enzyme. The digestion reaction consisted of 2.5 µg of plasmid DNA, 10 µL of 10x NE buffer, 2 µL of *NotI* and adding sterilized water to 100 µL. After incubation for 30 min at 37 °C, the digested plasmid was purified using PCI (phenol/chloroform/isoamyl alcohol) solution. Briefly, 400 µL of PCI solution pH 7.4 was added into the digestion mixture, mixed and centrifuged at 14,000 rpm for 5 min. The aqueous phase was transferred to a new eppendorf, and then 400 µL of ether was added and centrifuged at 14,000 rpm for 5 min. The DNA precipitation was performed by adding 40 µL of 30 M NaOAc pH 5.2 and 1 mL of 100% ethanol before incubating at -80 °C for 15 min. The mixture was centrifuged and washed the pellet using 70% ethanol before dissolving in RNase-free water. After that, mRNA was transcribed using mMESSAGE mMACHINE SP6 Transcription kit (Ambion, CA, USA) (Table 7) and purified by ProbeQuant G-50 Micro Column (GE Healthcare). The *rpl10a* mRNA concentration was determined by 260 nm absorbance measurement, and the quality was checked by 1.5% MOPS agarose gel.

Table 7. The reagents for *rpl10a* mRNA synthesis

Reagent	Volume per reaction (μL)
RNase-free water	7.0
10x reaction buffer	2.0
2x NTP/CAP	25.0
Enzyme mix	3.0
Linear DNA template (300 ng)	1.0
Final volume	20.0

incubate for
2 h at 37 °C

1.4.3 The rescue experiments

To study the recovery *rpl10a* morphological defects, co-injection of *rpl10a*mRNA with *rpl10a* MO^{aug} (0.5 $\mu\text{g}/\mu\text{L}$) or MO^{spE515} (5 $\mu\text{g}/\mu\text{L}$) were performed. The concentration of *rpl10a* mRNA was varied at 100, 200 and 400 ng/ μL . The mixture was injected into 1-or 2-cell-stage embryos and observed the morphology at 25 and 50 hpf.

1.5 mRNA expression detected by in situ hybridization

1.5.1 DIG RNA probe preparation

The RNA probes were used including *vasa*, *nanos1*, *fli-1*, and *myoD*. Each PCR product was amplified from wild-type zebrafish cDNA using a specific primer as shown in Table 1. The PCR reagents (Expand High Fidelity PCR kit, Roche, Germany) and thermo cycling program were present in Table 3 and 4. The PCR fragments were purified using MagExtractor PCR & Gel clean up kit (Toyobo, Japan) before ligation into pGEM[®]-T Easy vector (Promega). Then, the ligation reaction was transformed into *E. coli* DH5 α competent cells. For the *myoD* gene, the DNA fragment was cloned into pBlueScript II vector. The positive colony was purified and confirmed the sequences by sequencing.

1.5.2 *In vitro* transcription

The recombinant DNA plasmids were digested to linear plasmid using specific restriction enzyme (*SacII*, *NcoI*, *SacII* and *EcoRI* for *vasa*, *nanos1*, *fli-1* and *myoD*, respectively). *In vitro* transcription was performed following the T7 or SP6 RNA polymerase kit (Roche, Germany) using linearized plasmid as a template. The components of the reaction were shown in the Table 8. The reaction mixture was incubated at 37°C for 2 h before RNase-free DNase I treatment at 37°C for 30 min. To purify the DIG-RNA labeled probe, the ProbeQuant G-50 Micro Column protocol was performed. Then, the concentration of RNA probe was measured using NanoDrop and the quality was detected by MOPS gel.

Table 8. Reaction component for DIG RNA probe synthesis

Reagent	Volume per reaction (μL)
RNase-free water	11.0
10x transcription buffer	2.0
0.1 M DTT	2.0
10x DIG-RNA labeling mix	2.0
RNase inhibitor	1.0
T7 or SP6 RNA polymerase	1.0
DNA template (150-300 ng)	1.0
Final volume	20.0

1.5.3 Detection of PGC gene expression using whole mount *in situ* hybridization (WISH)

The zebrafish embryos were collected after injection for 24 hpf and gently removed the chorions by forceps. The dechorionated embryos were fixed in 4% (w/v) paraformaldehyde (PFA) in 1x PBS overnight at 4°C. The next day, the embryos were dehydrated with 50% methanol in PBS and 100% methanol for 5 min each step at room temperature. The eggs were put in 100% methanol and placed at -20°C at least 4 h before use. Subsequently, the embryos were rehydrated in 75, 50, 25% (v/v) of methanol in PBS and washed with PBST (1x PBS pH 7.4+0.1% Tween20) for 5 min each. After that, the samples were permeabilized by incubating with 10 $\mu\text{g}/\text{mL}$ of proteinase K for 10 min at room temperature. The digestion embryos were inhibited by 4% PFA incubation for 20 min; the residual PFA was washed with PBST for 5 min 3 times. The embryos were soaked in hybridization buffer for 2 h at 56 °C for prehybridization, and the antisense DIG-labeled RNA probe (30-50 ng) was then replaced for 18 h. The second day, the solution was removed and then the embryos were rinsed with 2xSSCT in 50%

formaldehyde for 1 h at 56°C. To remove the endogenous RNA, RNase treatment (RNase A and RNase T1) step was carried out for 10 min. The solution was removed and incubated with 2xSSCT in 50% formaldehyde for 1 h at 56°C followed by adding with 2xSSCT, 0.2xSSCT and PBS. The nonspecific binding sites were saturated by soaking in blocking buffer at 4 °C for 2 h. Afterward, the embryos were incubated with the anti-DIG antibody (1:3,000) in blocking buffer overnight at 4°C with gentle shaking. Last day, the samples were washed with PBST and alkaline reaction buffer. To detect the alkaline phosphatase reaction, the NBT/BCIP staining was added until the color was developed and the reaction was stopped by rinsing with PBST, and then the embryos were kept in 4% PFA.

1.6 mRNA expression levels determined by quantitative RT-PCR

Quantitative PCR was conducted in 20 µL reaction containing 10 µL of 2x SYBR® Green PCR Master Mix (ABI, CA, USA), 300 nM of each primer and 5 ng of cDNA. Final volume of 20 µL was adjusted by adding deionized water. The primers used to amplify genes are shown in Table 1. The *rpl38* gene was used as an internal control gene. Fluorescence detection and thermal cycling and were conducted using the StepOne™ Real-Time PCR machine (ABI, CA, USA). The samples were run in triplicate. The thermal cycling was started with denaturation step of 10 min at 95 °C, followed by 40 cycles of 95 °C for 15 sec, annealing at 60 °C for 1 min and final cycle 95 °C for 15 sec, 60 °C for 1 min, and 95 °C for 15 sec. The sample was the 20-25 embryos pool cDNA after MO injection. The data was analyzed and calculated into fold change compared to control group using comparative $\Delta\Delta\text{CT}$ method. The wild-type group was used as calibrator data for the control group.

1.7 Hemoglobin staining

The embryos at 48 hpf were stained by the *o*-dianisidine staining to detect the active hemoglobin (Detrich et al., 1995). The dechorionated embryos were incubated with the staining buffer containing 0.6 mg/mL of *o*-dianisidine, 0.01 M sodium acetate pH 4.5, 0.65% H₂O₂ and 40% ethanol in the dark for 7 min.

2. The effects of *rpl10a* gene knockout using CRISPR-Cas9 genomic editing

2.1 crRNA design

The crRNA was designed using <http://crispr.dbcls.jp> website. Briefly, the accession number or genome location or nucleotide sequences were put for design. PAM sequence was selected in NGG, or NRG sequence depended on the bacterial strain which the Cas protein derived. Then, the design button was pressed. After getting results from the above website, the crRNA that located at exon 5 of zebrafish *rpl10a* was selected. The selected crRNA that targeted at interested sequences was produced from IDT (Integrated DNA Technology, IA, US).

2.2 crRNA preparation

After getting crRNA from the company, the crRNA was delivered by liophilized form and dissolved with RNase free water was added for dissolving. Then, the annealing step was performed. The 3 μ L of 250 ng/ μ L *rpl10a_ex5* crRNA and 3 μ L of 1,000 ng/ μ L tracrRNA was heated at 95 °C for 5 min and kept at -80 °C until use.

2.3 crRNA-tracrRNA-Cas9 complex injection

The crRNA-tracrRNA-Cas9 complex solution contained 25 pg of *rpl10a_ex5* crRNA, 100 pg of tracrRNA and 40 pg of Cas 9 protein in final concentration mixed in 2x fish injection buffer. The injection buffer composition was shown in table 9 and kept at -80 °C until use. The 1 nl of injection solution was injected into the 1-cell-stage of embryos and cultures in the E3 medium.

Table 9. Reaction component for CRISPR-Cas9 injection buffer

Reagent	Volume per reaction (μL)
RNase-free water	1.8
Annealing crRNA and tracrRNA	1.0
10 μg/μL of Cas 9 protein	0.2
2x fish injection buffer	2.0
Final volume	5.0

2.4 Checking genome editing using heteroduplex mobility assay

After injection with crRNA-tracrRNA-Cas9 complex, five dechorionated embryos were collected into 1.5 ml tube at 24 hpf and the medium was removed on ice. Then, 108 μL of 50 mM NaOH was added and incubated at 98 °C for 10 min for genomic extraction. The sample was mixed by pipetting before adding 12 μL of 1 M Tris-HCl pH 8.0. This solution contained a genomic DNA was used as template for PCR amplification with specific primer using Prime Taq kit (Table 10 and 11). The PCR result was checked using 15% acrylamide gel electrophoresis.

Table 10. PCR reaction reagents for HMA assay

Reagent	Volume per reaction (μL)
Sterile H ₂ O	14.5
10X buffer	2.0
10 mM dNTP mix	1.6
forward and reverse primer mix (20 μM each)	0.8
Prime Taq DNA polymerase	0.1
Template	1.0
Final volume	20.0

Table 11. Thermal cycling for PCR analysis for HMA assay

Temperature	Time	Cycles
94°C	2 min	1
94°C	30 s	35
58°C	30 s	
72°C	30 s	
72°C	7 min	1

2.5 Direct PCR sequencing

The PCR product from 2.4 was purified by treated with ExoSAP-IT PCR clean up (USB, OH, US) before sequencing. The mixture contained 0.15 μ L of 10x PCR buffer, 1.7 μ L of sterile water and 0.15 μ L of ExoSAP-IT was added into 2 μ L of PCR product. The reaction was incubated at 37 °C for 15 min and inactivated ExoSAP-IT by heating at 80 °C for 15 min.

2.6 crRNA efficiency

To evaluate the crRNA efficiency, 16 embryos of F0 mutant generation were extracted genomic DNA and sequenced for mutation prediction. The efficiency of crRNA was calculated from the below equation; (number of mutant/ number of total) x 100.

2.7 F1 and F2 founder generation

After getting F0 fish carried the interested mutation pattern, F0 mutant fish was grown to be adult about 3 month-post injection (mpi). Adult fish was mated with the opposite sex of wild-type fish for generating F1 heterozygous generation. The F1 heterozygous embryos were extracted genomic DNA and detected using HMA assay and sequenced to calculate germline transmission rate; germline transmission rate (indel mutations) = (number of mutant/number of total) x 100. The F1 heterozygous fish were grown up until 3 mpf. Subsequently, fin clip was performed and sequenced to confirm the mutation. Then, F1 heterozygous mutation in same pattern was fertilized for F2 generating. F2 generation was included wild-type (WT: +/+), heterozygous mutation (+/-) and homozygous mutation (-/-). In our study, we focused on 5 bp deletion mutation. The mutant fish from an F2 generation were used for further activity study.

2.8 Activity of *rpl10a* gene on embryonic development

To test the activity of *rpl10a* gene on embryonic development, the knockout zebrafish was used as a model. The F2 embryos were observed the morphology after 25 and 50 hpf. Moreover, the 3-dpf embryos were kept in 4% PFA in PBS to fix sample for 24 h, and the histological process was performed. Hematoxylin and Eosin were stained and the embryos were observed under light microscopy.

2.9 Function of *rpl10a* gene on anemia

To study the effect of *rpl10a* gene knockout on anemia, the active hemoglobin was stained with *o*-dianisidine staining (Detrich et al., 1995) followed by protocol 1.7 in part III.

CHAPTER 4

RESULTS

Determination of evolutionary relationships mouse, zebrafish and shrimp *rpl10a* gene using phylogenetic tree analysis

The result from phylogenetic tree showed that *rpl10a* gene of mouse (*Mus musculus*) and zebrafish (*Danio rerio*) were more closely to each other. The shrimp *rpl10a* gene (*Fenneropenaeus merguensis*) had a closer distance with fruit fly (*Drosophila melanogaster*). The phylogenetic tree was presented in figure 11.

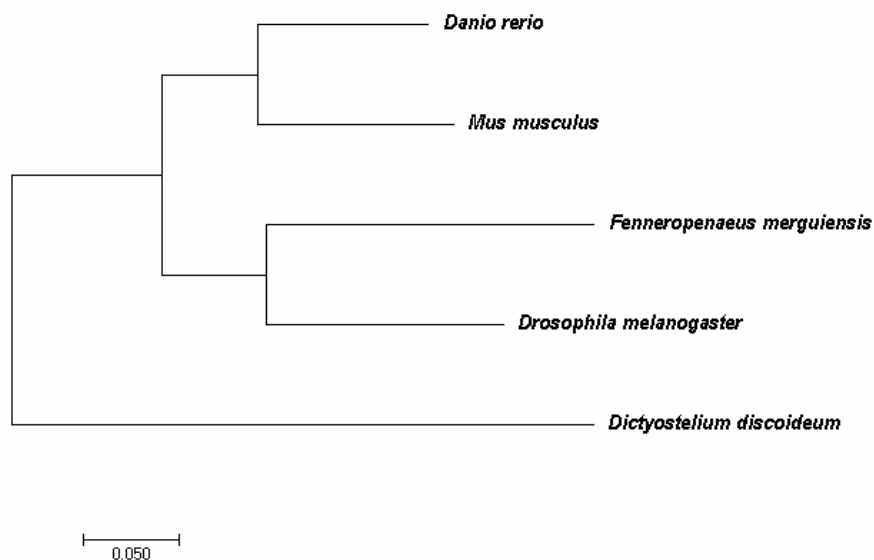


Figure 11. Phylogenetic tree of full-length *rpl10a* sequences in mouse (*Mus musculus*), zebrafish (*Danio rerio*), shrimp (*Fenneropenaeus merguensis*), and fruit fly (*Drosophila melanogaster*), compared to soil-living ameba (*Dictyostelium discoideum*) that was used as an out group by phylogenetic tree analysis.

Amino acid sequence alignment in mouse, zebrafish and shrimp

The Rpl10a protein alignment of mouse, zebrafish, fruit fly and shrimp are presented in Figure 12. The zebrafish and mouse protein sequences had 96% identity, whereas the predicted amino acid sequences are 86% and 84% identical to fruit fly and shrimp, respectively. While mouse and shrimp sequences are showed 86% identity.

```

          *           20           *           40           *           60           *           80           *           100
zebrafish : -MSKVSRDITLVEHNGVQASRKKRRFLETVELQISLKNYDPQDKRRFSGTVRLKTHPRPSESVCVLGDQHHDEARLAELEHMIELALKKLNKKNKLVKKLAKKYDA : 108
Drosophila : MASKVSRDITLVEHNGVQASRKKRRFLETVELQISLKNYDPQDKRRFSGTVRLKTHPRPSESVCVLGDQHHDEARLAELEHMIELALKKLNKKNKLVKKLAKKYDA : 109
mouse      : MASKVSRDITLVEHNGVQASRKKRRFLETVELQISLKNYDPQDKRRFSGTVRLKTHPRPSESVCVLGDQHHDEARLAELEHMIELALKKLNKKNKLVKKLAKKYDA : 109
shrimp     : MSKVTRDITLVEHNGVQASRKKRRFLETVELQISLKNYDPQDKRRFSGTVRLKTHPRPSESVCVLGDQHHDEARLAELEHMIELALKKLNKKNKLVKKLAKKYDA : 109
m SKV3RDTLYE 6 61 g K4R FLETVELQI LKNYDPQDKRRFSGTV4LK P4Pk 6C6LGDQqHcDEARa 6p Md eaLKKLNKIKKLVKKLAKKYDA

          *           120           *           140           *           160           *           180           *           200           *
zebrafish : FLASDSLIRKQIPRILGPNLRKGFPSLLTHNENISLTKVDEVKSTIKFQMKKVLCLDAVAVGHVRSSEELVYNIHLAVNFLVSLLRKMQQVRSLEIKSTMGPQRLY : 216
Drosophila : FLASDSLIRKQIPRILGPNLRKGFPSLLTHNENISLTKVDEVKSTIKFQMKKVLCLDAVAVGHVRSSEELVYNIHLAVNFLVSLLRKMQQVRSLEIKSTMGPQRLY : 217
mouse      : FLASDSLIRKQIPRILGPNLRKGFPSLLTHNENISLTKVDEVKSTIKFQMKKVLCLDAVAVGHVRSSEELVYNIHLAVNFLVSLLRKMQQVRSLEIKSTMGPQRLY : 217
shrimp     : FLASDSLIRKQIPRILGPNLRKGFPSLLTHNENISLTKVDEVKSTIKFQMKKVLCLDAVAVGHVRSSEELVYNIHLAVNFLVSLLRKMQQVRSLEIKSTMGPQRLY : 217
F6ASesLIRKQIPR6LGPGLNRKagKFP 613H E 6 K E6KsTIKFQMKKVLCL VA6GHV M dELv N6 La6NFLVSLLRKMQQVNR L 6KS3MG PQRLY

```

Figure 12. Multiple alignment of mouse (*Mus musculus*), zebrafish (*Danio rerio*), shrimp (*Fenneropenaeus merguensis*), and fruit fly (*Drosophila melanogaster*) Rpl10a protein sequences.

Part I: The effect of rRpl10a protein on shrimp ovarian maturation

1. Recombinant protein purification and confirmed by western blotting

After His- Rpl10a protein production and purification, the protein expression was checked by 12.5% SDS- acrylamide gel (Figure 13A) . The recombinant Rpl10a protein was expressed in soluble protein after induction with IPTG. The purified protein was detected purple band by western blotting (Figure 13B). The figure presented the recombinant protein size was 30 kDa.

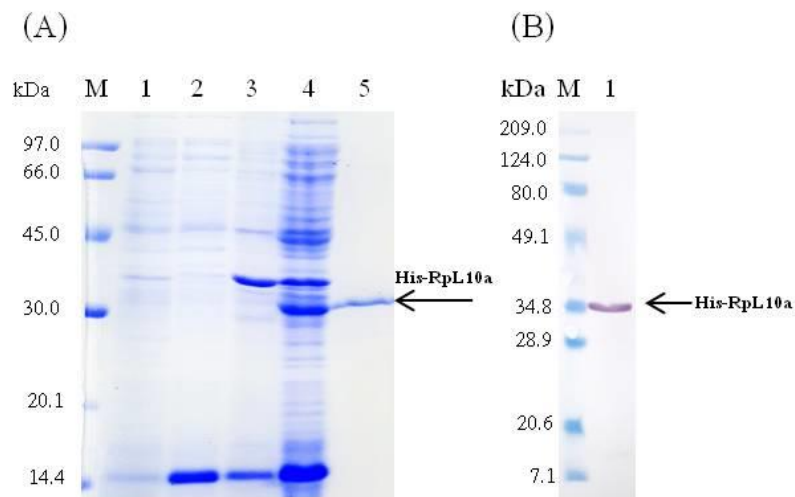


Figure 13. (A) Expression and purification of recombinant protein His-Rpl10a; lane1: non- induce insoluble protein, lane 2: non- induce soluble protein, lane 3: induce insoluble protein, lane 4: induce soluble protein, lane 5: purified His-Rpl10a. (B) Western blotting recombinant protein using a monoclonal anti- mouse Rpl10a antibody. The purple band was showed 30 kDa. The black arrow indicated the position of His-Rpl10a protein.

2. Shrimp ovarian development histology

Shrimp vitellogenic stages were evaluated after rRp110a protein injection at 7 and 15 days. The histology of the ovary was performed and evaluated based on H&E staining and fluorescence signal. The stages of ovarian development were divided into four stages follow as Wonglapsuwan et al. (2010). The undeveloped stage, the previtellogenic oocytes, and oogonia were found. The size of the cells was $<65\ \mu\text{m}$ in diameter. In stage I, the early developing oocytes $75\text{-}125\ \mu\text{m}$. in diameter which surrounded by follicle cells were observed. Stage II, the developing oocytes that had size $100\text{-}200\ \mu\text{m}$ were found. In this stage, the nucleus was enlarged. The mature oocytes with eosinophilic cortical rods and the size were $>125\ \mu\text{m}$ diameter. In this case, we also used the fluorescence signal to divide vitellogenic stages. This method was safe consuming time. The mature ovaries showed a strong fluorescence signal when compared to the early previtellogenic stage (Figure 14). In our results found that rRp110a protein induced vitellogenic stage into stage II.

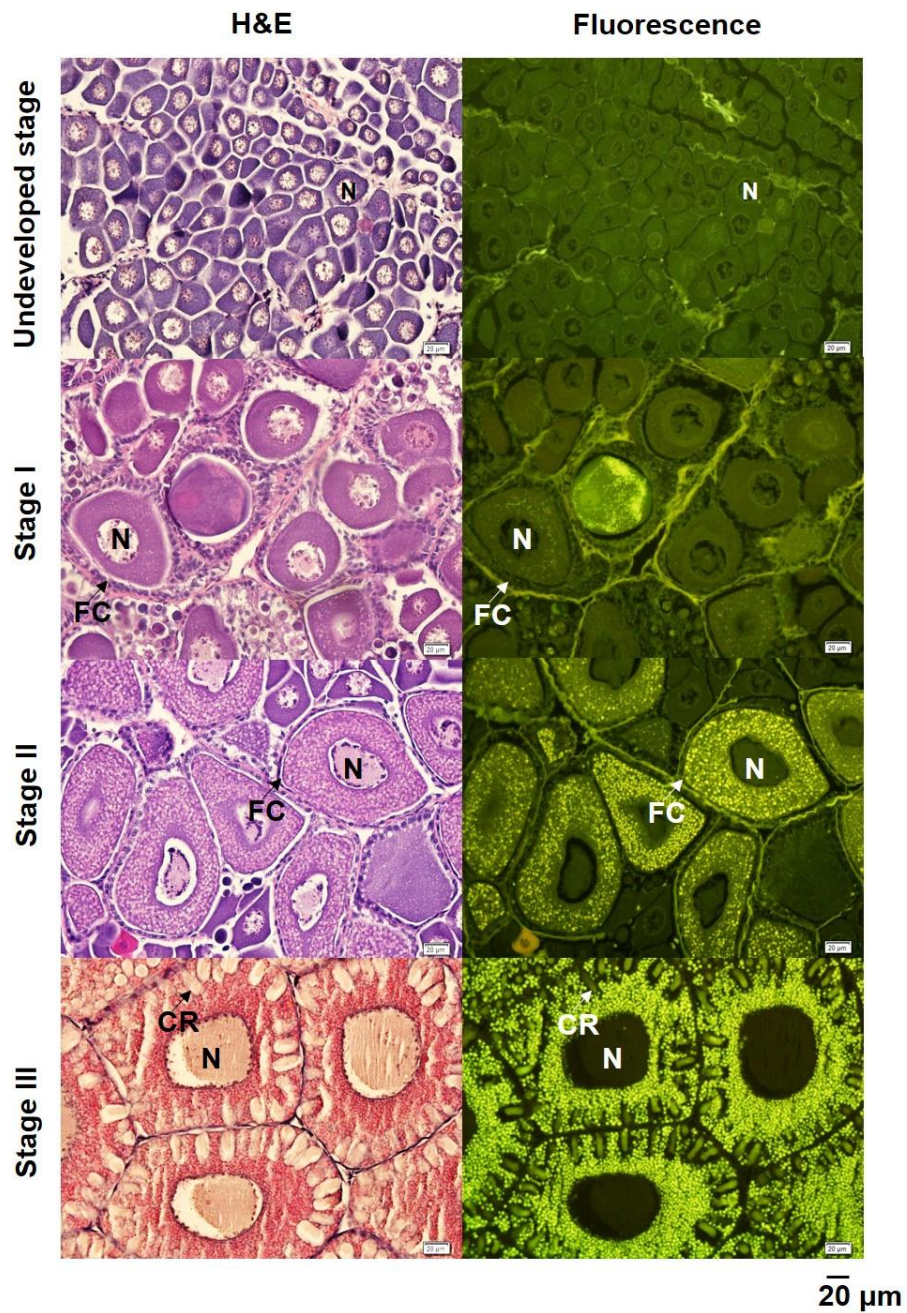


Figure 14. Histological section observation of different shrimp ovarian development stage under light and fluorescence microscope. The left panel showed hematoxylin, and eosin staining and right panel showed fluorescence view. FC: follicle cells, CR: cortical rods, N: nucleus. Original magnification x400, scale bar = 20 μm . (Palasin et al., 2014)

3. Effect of rRpl10a protein on ovarian maturation in shrimp

The ovarian development stages of shrimp were evaluated after the rRpl10a protein stimulation. The vitellogenic stages were evaluated and calculated into percentages of different stages. In this experiment, we found that 180 µg of rRpl10a protein induced ovarian development into stage II within 7 days (28.57%). Whereas, the undeveloped stage and stage I were evaluated as 42.86 and 28.57%, respectively. At day 15th, 28.57% of stage I and 71.43% of undeveloped ovaries were found. While both of dialysis buffer group after injection for 7 and 15 days were found 100% of the undeveloped (Table 12 and Figure 15).

Table 12. Percentages of vitellogenic stages of shrimp ovarian development after 180 µg rRpl10a protein injection at 7 and 15 days

Group	% of vitellogenic stage		
	undeveloped stage	stage I	stage II
dialysis buffer_7 days	100.00	0.00	0.00
180 µg rRpl10a_7 days	42.86	28.57	28.57
dialysis buffer_15 days	100.00	0.00	0.00
180 µg rRpl10a_15 days	71.43	28.57	0.00

Percentages of Vitellogenic stages

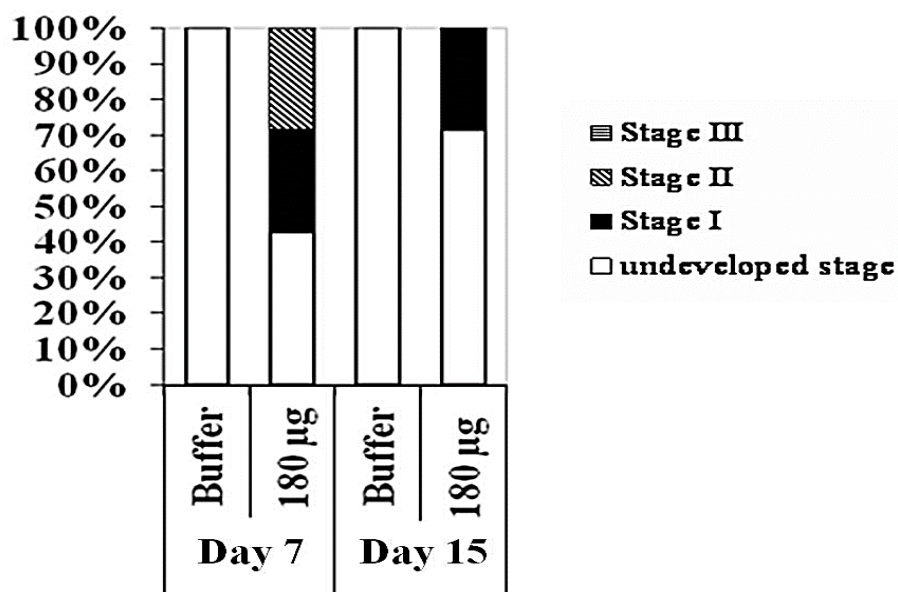


Figure 15. Graph percentages of vitellogenic stages of shrimp ovarian development after 180 µg rRpl10a protein injection at 7 and 15 days.

4. Determination level of Rpl10a protein in a different stage of shrimp ovary after 180 µg rRpl10a protein injection using ELISA technique

The level of Rpl10a protein was determined after 180 µg rRpl10a protein injection at 7 days. The result showed that the Rpl10a protein level was increased in stage I of ovarian development. The amount of Rpl10a protein detection at stage I was 4.45 ± 0.01 µg/g tissue in the ovary, 17.52 ± 0.09 µg/g tissue in hepatopancreas and 17.90 ± 0.29 µg/ml in hemolymph. The levels of Rpl10a protein were reduced in stage II (Table 13).

Table 13. Rp110a protein levels in a different stage of shrimp ovarian development after 180 µg rRp110a protein injection at 7 days

Organs of shrimp	Rp110a protein level in vitellogenic stages		
	Undeveloped stage	Stage I	Stage II
hepatopancreas (µg/g tissue)	15.84±0.76	17.52±0.09	5.35±2.54
ovary (µg/g tissue)	4.17±1.02	4.45±0.01	3.65±0.02
hemolymph (µg/ml)	17.76±0.86	17.90±0.29	15.17±0.11

5. MF level in hemolymph after rRp110a injection

The MF concentrations in the shrimp hemolymph after first injection of rRp110a protein for 7 days was determined by HPLC technique. MF levels was 0.18 ± 0.04 ng/ml at undeveloped stage and slightly increased to 0.27 ± 0.00 ng/ml at stage I. The MF levels was increased to 1.64 ± 0.63 ng/ml at stage II of ovarian development (Figure 16).

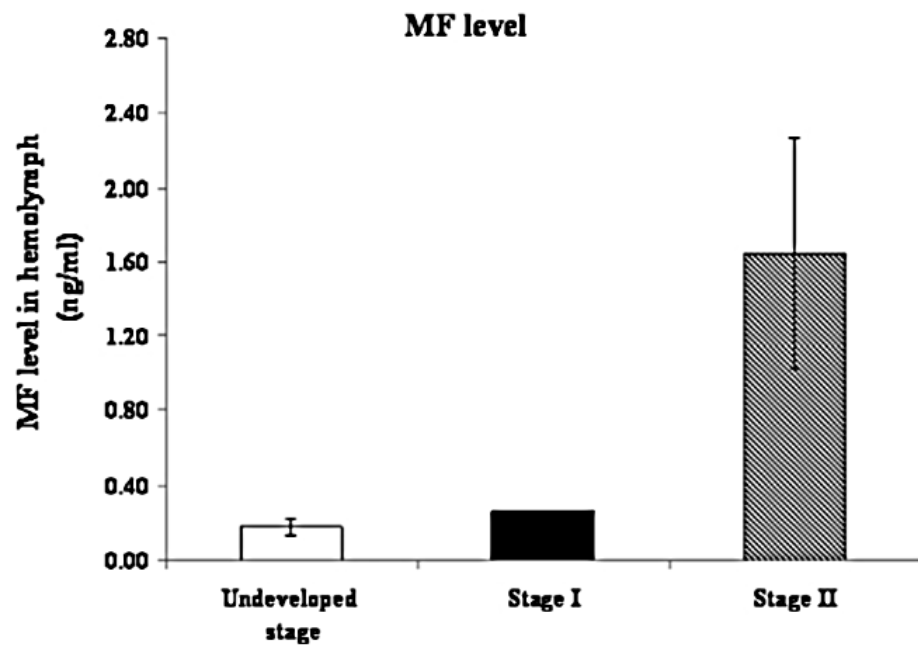


Figure 16. MF level in the hemolymph at different stages of shrimp ovarian development post 180 μ g rRpl10a protein injection for 7 days (each stage n=2).

Part II: The effect of recombinant Rpl10a protein on spermatogenesis

1. Effect of Rpl10a protein on testicular development in black tiger shrimp (*Penaeus monodon*)

1.1 Shrimp testis histology

In this study, shrimp spermatogenesis was divided into three stages based on cell diameter using histological observation under the microscope, accordingly stage I (spermatogonia cells, diameter $\geq 6.25 \mu\text{m}$), stage II (spermatocyte I and II, diameter = $3.00\text{-}6.25 \mu\text{m}$) and stage III (spermatid and spermatozoa, diameter $\leq 3.00 \mu\text{m}$). The cell characterization in different stages of spermatogenesis was observed under a microscope after H&E staining. Many spermatogonia cells were presented in stage I which located in seminiferous tubule's periphery of the basal membrane. The spermatogonia were a large oval shape and nucleus contained euchromatin (Figure 17A). Stage II presented spermatogonia form with more division clearly than stage I. The spermatocytes were divided into 2 types. These cells were unable to identify between spermatocyte I and II (Figure 17B). Stage III presented by the appearance of the spermatids and spermatozoa. The cells had a small round shape, and the nucleus had condensed chromatin. Mature sperm cells were strongly stained with hematoxylin staining (Figure 17C).

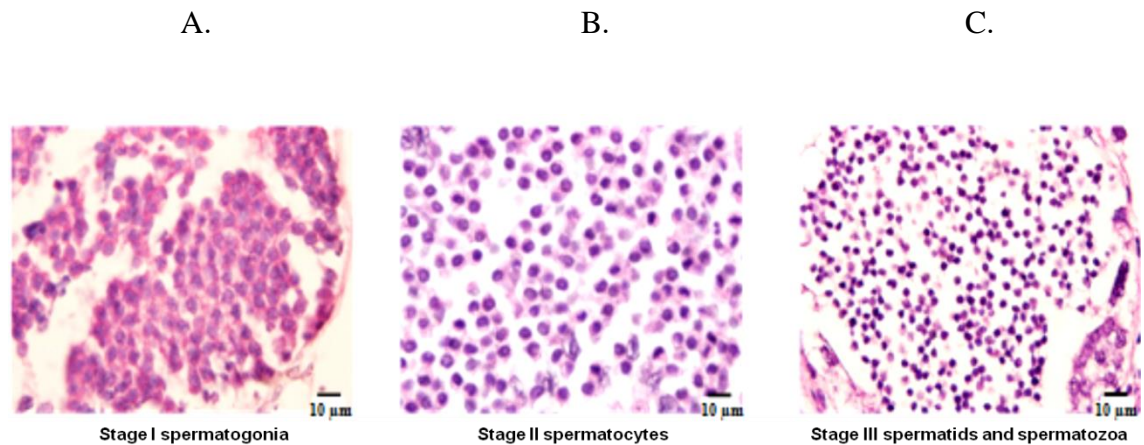


Figure 17. Histological picture showed stage of spermatogenesis of shrimp testis. Stage I: spermatogonia (A), Stage II: spermatocytes (B) and Stage III: spermatids and spermatozoa (C). Original magnification x1000, scale bars = 10 µm.

1.2 Effect of rRpl10a protein on shrimp spermatogenesis

The effect of rRpl10a protein on spermatogenesis was studied using black tiger shrimp as a model. All concentrations of rRpl10a protein (0.5, 1.0, 1.5 and 2.0 µM) induced development into stage III and the mature stage of sperm was calculated into 18.18%, 55.56%, 52.94 and 50.00%, respectively (Figure 18). The rRpl10a at 1.0 µM still contained stage I, although, this dose induced the highest percentage of stage III. While percentages of spermatogenesis stimulation of 1.5 µM rRpl10a was 52.94 % mature stage, 47.09 % stage II, and no observation of spermatogenesis in stage I. In contrast, mature stage was not detected in the control samples. This results suggested that after 4 h incubation, the effective concentration for shrimp spermatogenesis was 1.0 or 1.5 µM of rRpl10a. The overall of the shrimp testicular sections with H&E staining was individually shown in Figure 19.

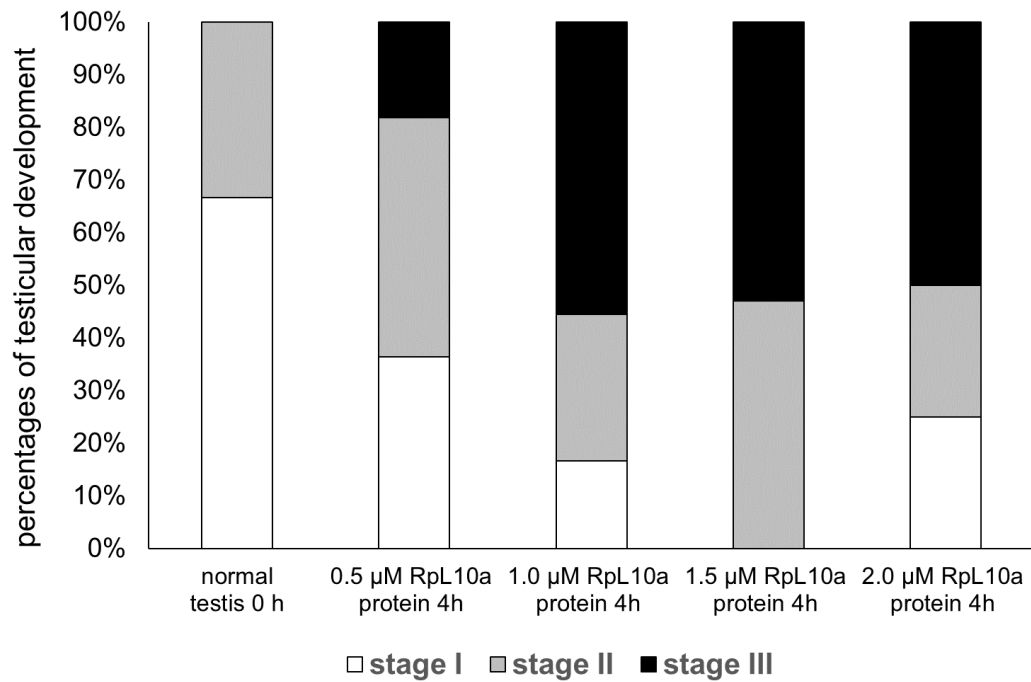


Figure 18. The percentages of spermatogenesis in shrimp testis explants after treatment with 0.5 μM , 1.0 μM , 1.5 μM and 2.0 μM of rRpL10a protein, compared to untreated testis at 4 hours in the 2x L-15 medium. (n=3, the data performed in the triplicate experiments)

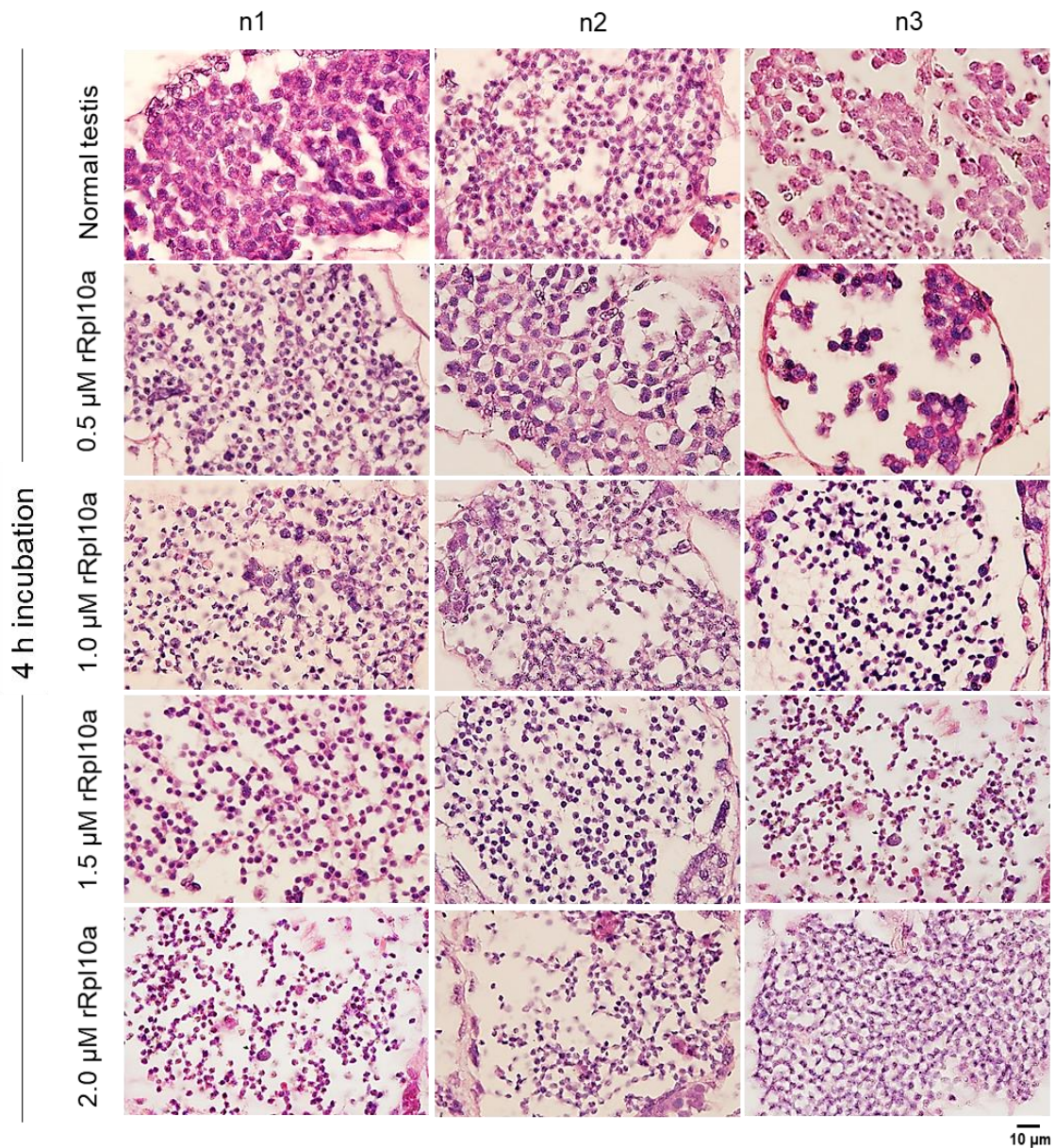


Figure 19. The picture presented shrimp testes sections with hematoxylin and eosin staining in different dosages of rRp110a protein (0.5, 1.0, 1.5 and 2.0 μM), compared to normal testes after 4h incubation in the 2x L-15 medium. Original magnification x1000, scale bar = 10 μm .

To confirm the rRp110a protein can promote cells in the early stage development into late stage, the *Dmrt1* gene expression in treated testis was performed. The *Dmrt1* gene was significantly decreased expression in the testes treated with 1 and 2 μM of rRp110a protein, compared to buffer (Figure 20).

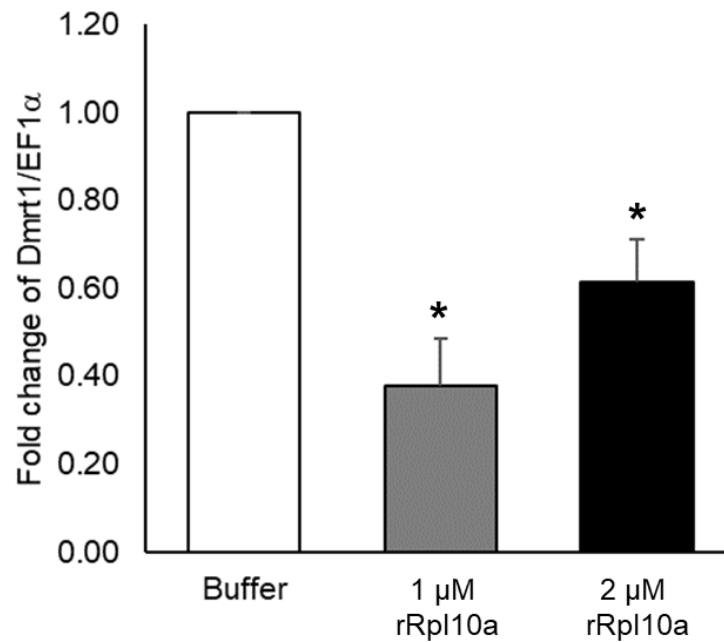


Figure 20. The fold change of *Dmrt1/EF1α* in treated testis in shrimp at 1.0 and 2.0 μM rRpl10a protein after incubating in 2x L-15 medium for 4h. The value of fold change was calculated using comparative CT method. The *EF1α* gene was used as an internal control and buffer group was used for normalize (number of shrimp = 3, replication = 3)

2. Effect of rRpl10a protein on spermatogenesis in mouse (*Mus musculus*)

2.1 Mouse testis histology

The result from mouse testis histology was shown in Figure 21. The cells in the seminiferous tubules with different kind was classified into 4 types including the spermatogonia, spermatocyte, and spermatid (round spermatid and elongated spermatid). All cell types in each seminiferous tubule were presented. We divided the cell type based on the cell shape. Spermatid cells had the small cytoplasm and located near the seminiferous tubule's membrane. These cells appeared round nucleus and differentiated into spermatocytes. During meiosis division, the spermatocyte cell was

divided. This cell had large and round nucleus and it was observed away from the membrane. Spermatid cells were located near the lumen, the cell shape changed following cell differentiation. Two types of spermatid cells included round spermatid and elongated spermatid cells. The cells in early of spermatid cells called round spermatids, these cells contained eosinophilic cytoplasm and round nucleus. Whereas, long rod spermatid cells called the elongated spermatid cells.

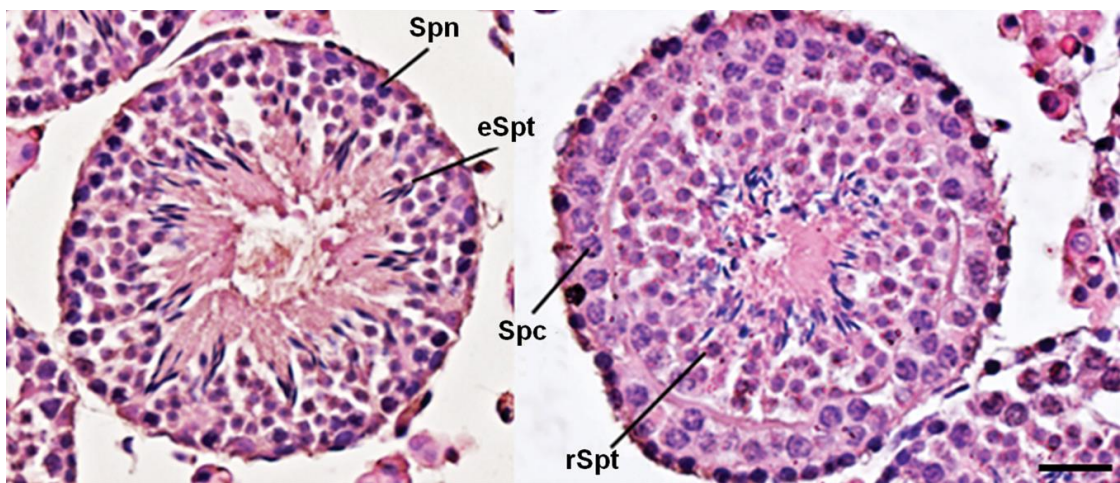


Figure 21. Cross section of mouse testis showed cell types in spermatogenesis. Different cells in the seminiferous tubules were included spermatogonia cells (Spn), spermatocytes (Spc), round spermatid (rSpt) and elongated spermatid (eSpt). Original magnification $\times 400$, scale bars = 20 μm .

2.2 Effect of rRpl10a protein on mouse spermatogenesis (*in vitro*)

To investigate the function of rRpl10a protein on spermatogenesis in the mammal, mouse testes were incubated with rRpl10a protein at different concentration (0, 0.5, 1.0, 1.5 and 2.0 μM of rRpl10a protein) for 4 h. Then, cells of testicular development were observed as shown in Figure 22. The rRpl10a protein treatment triggered mice spermatogenesis into spermatid cells, compared to control group. The

concentration of rRp110a at 0.5, 1.0, 1.5 and 2.0 μM promoted development into 40.78%, 49.65%, 45.03% and 45.33% of spermatid cell, respectively. The number of spermatid cells in the control group was 21.72%. The testes treated with rRp110a protein at 1 μM were induced differentiation of spermatid cells into elongated spermatid cells better than others. The percentages of spermatogonia cells and spermatocytes cells in all of rRp110a treatment were less than the control testis. This result found that a cell in seminiferous tubules developed from spermatogonia cells into a mature stage after rRp110a protein stimulation for 4 h. The overall of the shrimp testicular sections with H&E staining were shown in individual samples (Figure 23).

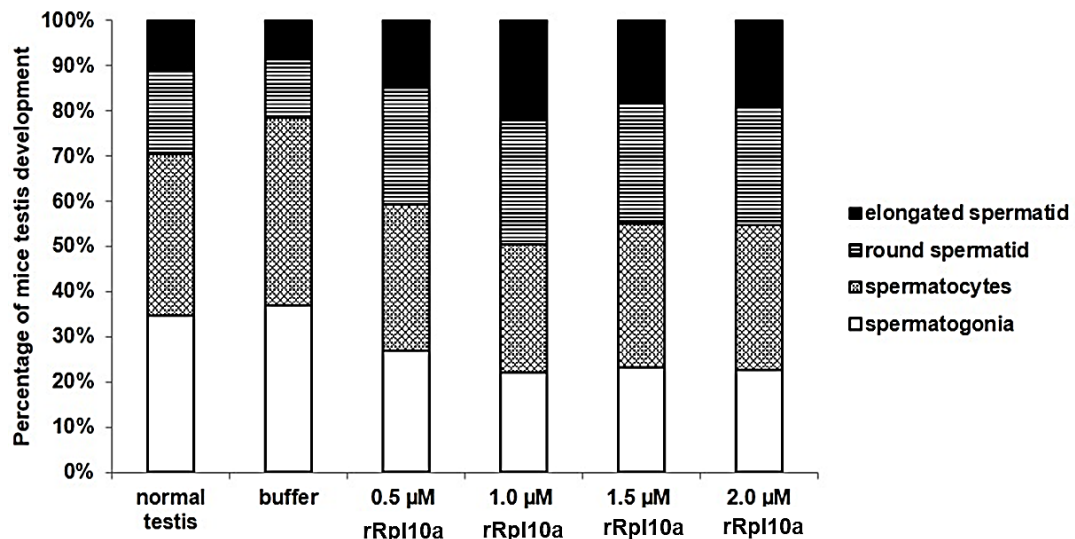


Figure 22. The graph showed the percentages of testicular development in mouse testis after His-rRp110a protein at the various concentrations (0.5, 1.0, 1.5 and 2.0 μM of rRp110a) treated for 4 h in DMEM medium (n=4, the data performed in the triplicate experiments).

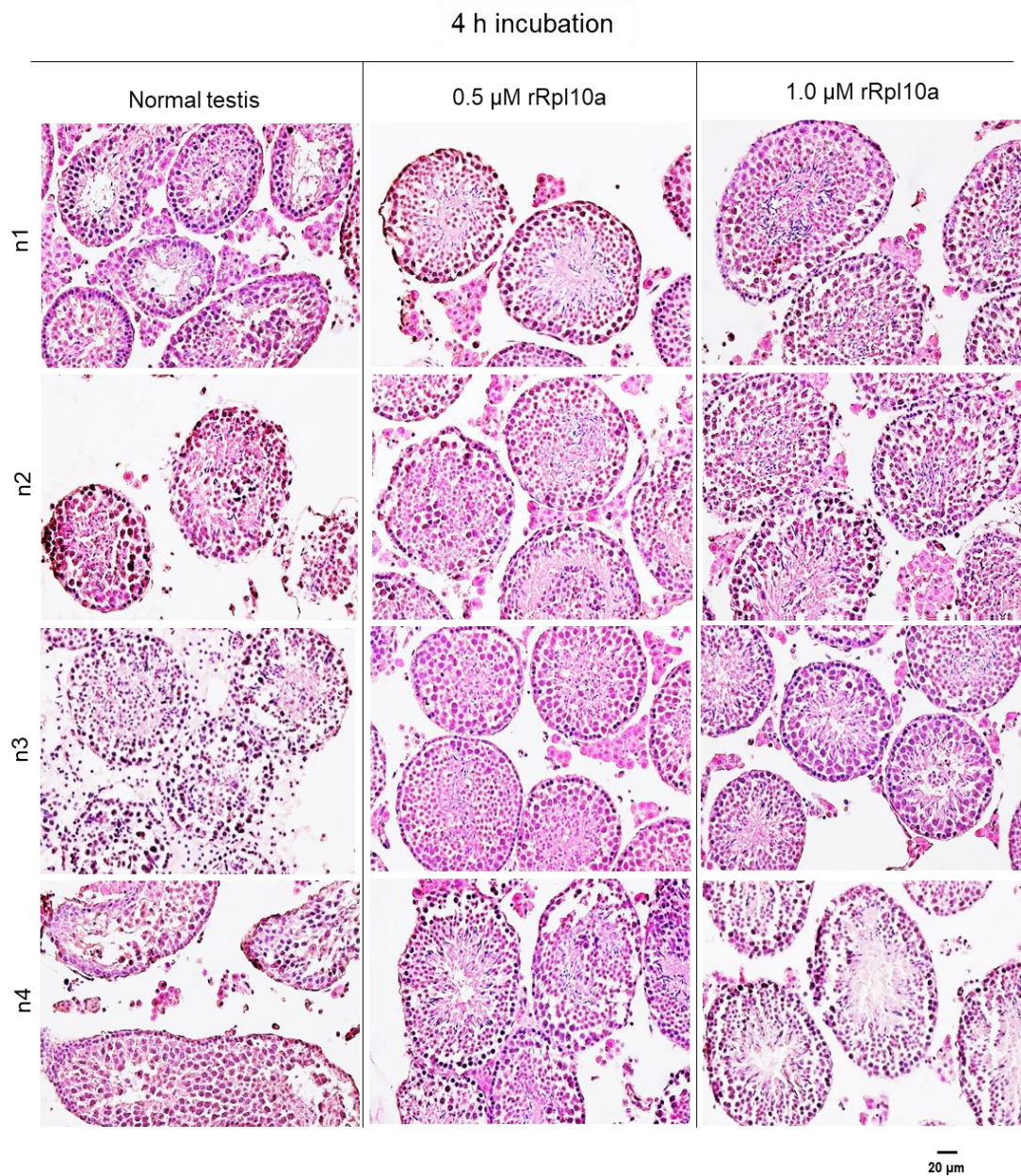


Figure 23. The picture presented mice testes sections with hematoxylin and eosin staining in different dosage of rRpl10a protein (0.5, 1.0, 1.5 and 2.0 μ M), compared to dialysis buffer and normal testes after 4 h incubation in DMEM medium (n=4). Original magnification x400, scale bars = 20 μ m.

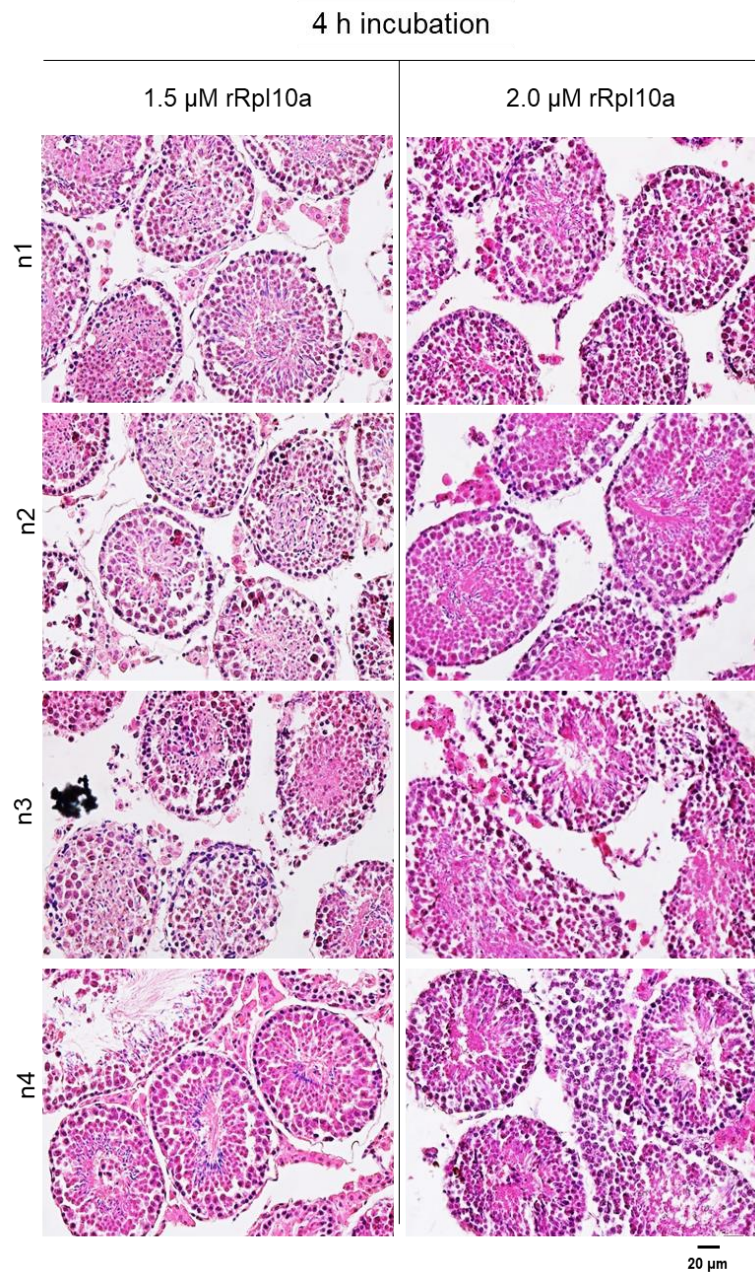


Figure 23 (continued). The picture presented mice testes sections with hematoxylin and eosin staining in different dosage of rRpl10a protein (0.5, 1.0, 1.5 and 2.0 μ M), compared to dialysis buffer and normal testes after 4 h incubation in DMEM medium (n=4). Original magnification x400, scale bars = 20 μ m.

2.3 Confirmation of the spermatid cells using WGA lectin histochemistry

The WGA staining was performed to confirm the spermatid cells. The Alexa Fluoro 594 WGA staining was detected for acrosome of spermatids (red fluorescent) and Hoechst 33342 staining stained chromatin in the nucleus (blue) (Figure 24A). The percentage of spermatid cells under WGA staining detection in 0.5, 1.0, 1.5 and 2.0 μM of rRpl10a protein treated group were 11.36%, 36.24%, 20.02% and 16.64%, respectively. The testes treated with 1 μM of rRpl10a protein showed the highest percentage of spermatid cell as compared with the other doses and the buffer group (Figure 24B). Although the percentage of spermatid evaluated by WGA detection was not equal to H&E assessment, the result showed the percentage of spermatid cell counted by WGA staining had a similar to counting under histology method.

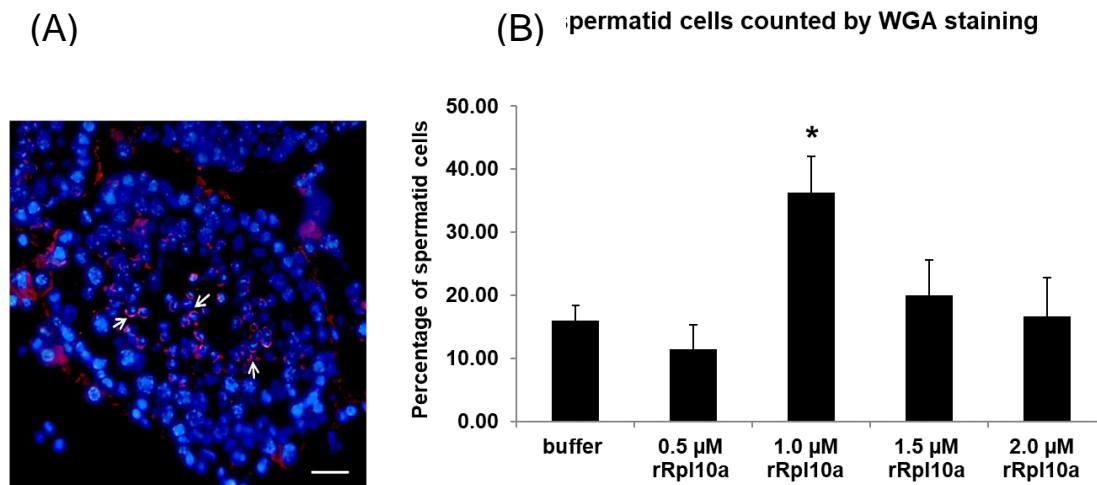


Figure 24. WGA lectin histochemistry confirmed the spermatid cells in seminiferous tubules. (A) The testis explants were stained with Alexa Fluor 594 WGA (Red) and Hoechst 33342 (blue). The acrosomal spermatids were detected (pointed by white arrows), original magnification $\times 400$, scale bars = 20 μm . (B) The percentage of spermatid cells under WGA histochemistry observation was presented. The significant differences were compared by one-way ANOVA test (mean \pm SD, n=4 and p<0.05).

2.4 Determination of early and late stage gene of spermatogenesis in mice testis

To confirm the percentage of spermatogenesis in mouse testis after incubation with rRp110a protein, the expression of the gene in early stage and late stage of spermatogenesis were determined. *Rhau* mRNA that highly expressed in spermatogonial stem cell and primary spermatocytes was selected to use as a marker for the early stage gene of spermatogenesis. Another gene, *Prm2* was also used to confirmed mature stage of spermatogenesis (Figure 25). Since the best concentration for spermatogenesis stimulation was 1 μ M, the early and late stage marker genes were evaluated. The expression levels of *Rhau* gene were significantly decreased in mouse testis treated with 1 μ M rRp110a when compared with buffer group (p-value <0.05). In contrast, the increasing of *Prm2* gene expression was detected in 1 μ M of rRp110a protein treated testes, compared to buffer group. This result showed that rRp110a protein treated group induced the cells to be spermatid cells better than the buffer group while, the cells in the early stage were reduced. This agreement result supported the evaluation stage of spermatogenesis using histological technique.

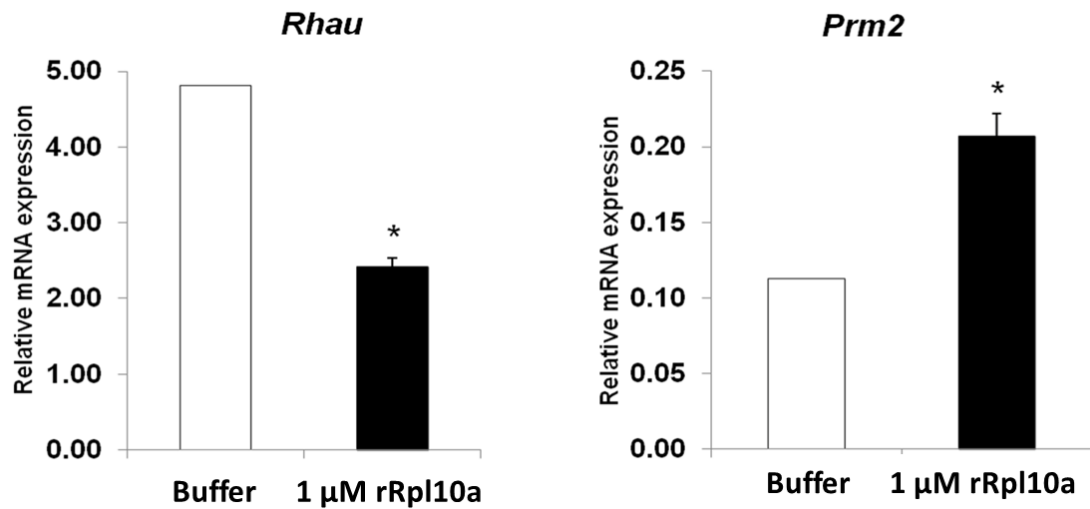


Figure 25. The levels of *Rhau* and *Prm2* mRNA expression in mice's testis explants after 1 μ M rRpl10a stimulation. The relative mRNA expression levels were normalized with β -actin (mean \pm SD, n=2 and p < 0.05). The significant differences in the expression of the gene were compared by t-test.

2.5 rRpl10a protein enhanced proliferation of spermatogonia cells

EdU assay was used to monitor proliferating cells in mouse testis after rRpl10a protein incubation. 5-ethynyl-2'-deoxyuridine (EdU) was used to label DNA in cells (Salic and Mitchison, 2008). The results was showed in Figure 24. We found that EdU was firmly incorporated into the DNA of the proliferating cell in mouse testis which treated with 1 μ M of rRpl10a protein. The dose of 1.5 and 2.0 μ M rRpl10a treated testes showed some intensity of DNA labeling, whereas 0.5 μ M and buffer group presented weak signal of EdU staining. The result revealed that rRpl10a protein promoted spermatogonia proliferation (Figure 26).

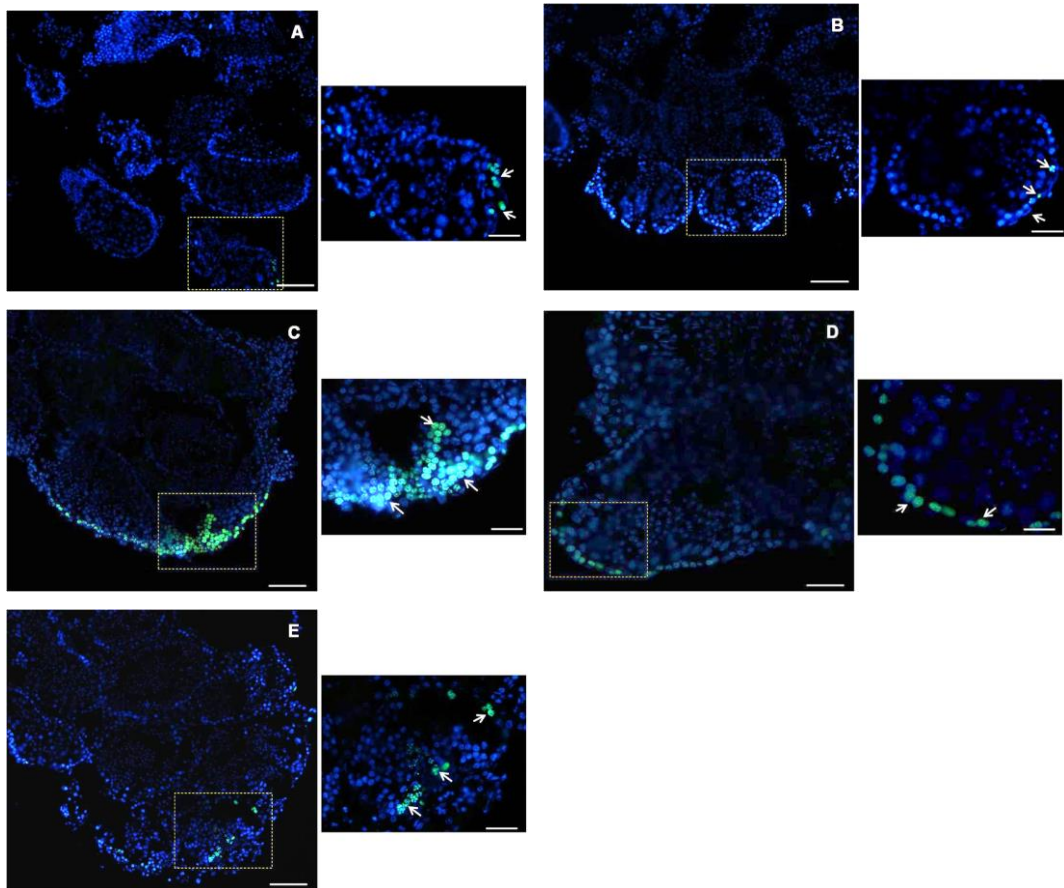


Figure 26. Effect of rRpl10a protein on cell proliferation. The testis explants were incubated with EdU and stained with Alexa Fluoro 488 (green) and DAPI (blue) staining. The mouse testes tissue incubated with different dose of rRpl10a protein; A. buffer as control, B. 0.5 μ M, C. 1.0 μ M, D. 1.5 μ M, E. 2.0 μ M. In figure A-E, original magnification $\times 200$, scale bars = 50 μ m. In the magnified inserts, original magnification $\times 400$, scale bars = 20 μ m.

Part III: The effects of *rpl10a* gene knockdown and knockout on abnormality development, reduction of hemoglobin and PGCs marker genes reduction

1. The effects of *rpl10a* gene knockdown using Morpholino antisense oligonucleotide

1.1 Zebrafish *rpl10a* gene structure of *rpl10a* MO-injected embryos

Zebrafish *rpl10a* gene contains six exons including 648 bp cDNA sequences and locates on chromosome 8. The *rpl10a* encodes up to 216 amino acids protein. To investigate the effect of *rpl10a* deficiency, we knocked down *rpl10a* gene using MOs injection to inhibit protein translation. The MOs target site is in the diagram (Figure 27A). Injection of the MO^{SP} that had specificity to exon 5 altered the splicing and resulted in the exclusion part of exon 5 from mature mRNA. Moreover, the expression of *rpl10a* gene was decreased which detected by RT-PCR. The DNA sequencing was confirmed in the splicing site of exon 5 after the MO^{SP} injection. We found that only 33 bp of exon 5 was deleted (Figure 27B).

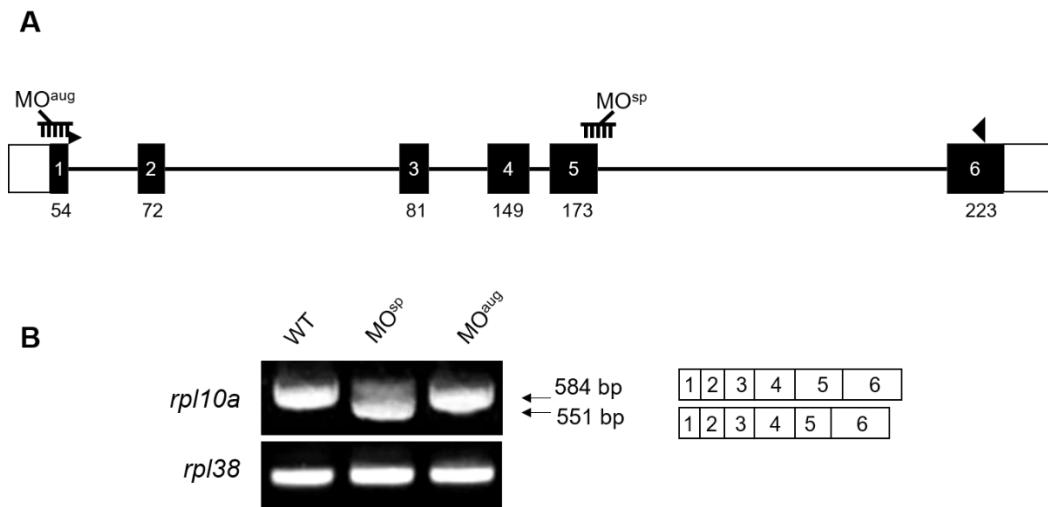


Figure 27. (A) Schematic presents zebrafish *rpl10a* gene structure. The white boxes represent the untranslated region. The translated region is shown with black boxes, and the arrows were marked at the start and stop codon, respectively. (B) RT-PCR analysis of *rpl10a* in MO-injected (MO^{aug} , MO^{sp}), rescued (MO^{sp} +mRNA) and wild-type embryos, *rpl38* was amplified as a control. The smaller PCR product size (551 bp) and decreased mRNA (584 bp) expression were observed in MO^{sp} injected embryos after 33 bp of exon 5 skipping. MO^{sp} : MO^{spE515}

1.2 The effect of *rpl10a* MO^{aug} on zebrafish embryos morphology

rpl10a MO^{aug} is antisense oligonucleotide which inhibits Rpl10a protein translation. The embryos were affected by *rpl10a* MO^{aug} showed different morphology from wild-type fish at various concentrations (0.5, 2.5 and 5 $\mu\text{g}/\mu\text{l}$). The morphology of 25-hpf *rpl10a* gene knockdown embryos was thinner yolk extension, smaller eyes, shorter body length and bent tail (Figure 28, left panel). At 50 hpf, the MO^{aug} injected embryos were bigger yolk sac, smaller eyes, reduced melanophore pigment, and a curved tail. Moreover, they had a severe phenotype and died after 3 dpf.

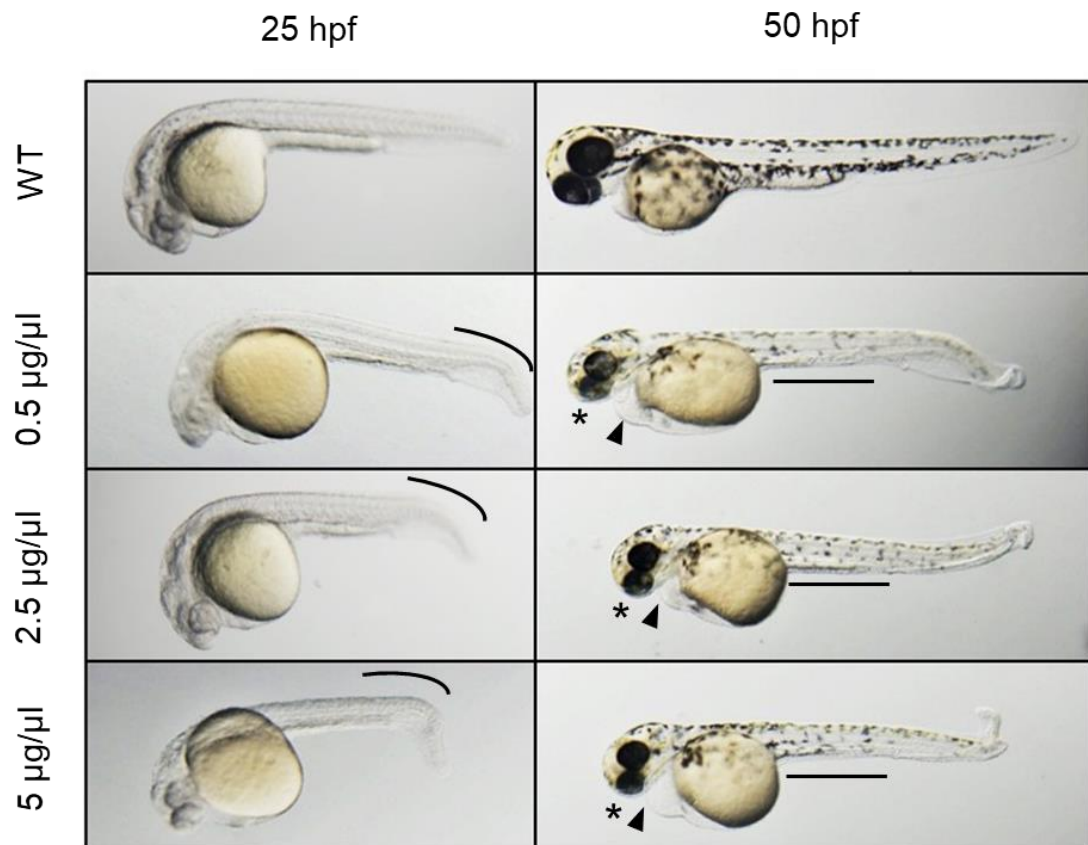


Figure 28. Morphology of zebrafish embryos after *rpl10a* MO^{aug} injection at 0.5, 2.5, 5 µg/µl after 25 and 50 hours post fertilization (hpf).

1.3 The effect of *rpl10a* MO^{sp} on zebrafish embryo morphology

The *rpl10a* MO^{sp} is antisense oligonucleotide which was designed to modify and the splicing events. In this study, both MO^{sp} for exon 4 and 5 skipping were designed. Also, *rpl10a* MO^{spE414} was designed for exon 4 and intron 4 skipping, but there were no different phenotypes with uninjected embryos. For exon 5 splicing embryos, their phenotypes were little smaller than wild-type. When the concentration was increased, the tail bending increased (Figure 29). Even though *rpl10a* MO^{spE515} morphants had similar phenotype with Rpl10a protein inhibiting embryos, they had more significant decreasing of yolk extension, pigmentation, smaller eyes and edema at 50 hpf. Therefore, we chose the concentration of *rpl10a* MO^{aug} and MO^{spE515} at 0.5 and 5 µg/µl for rescue experiment, respectively.

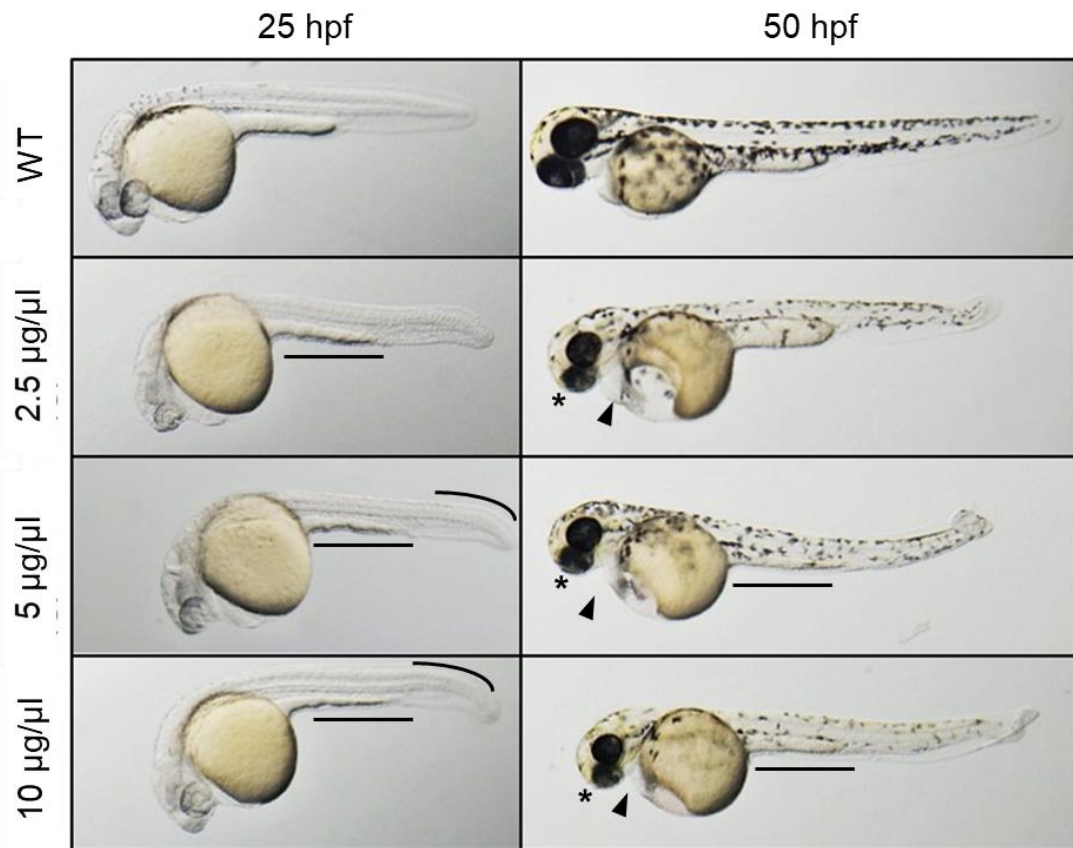


Figure 29. Morphology of zebrafish embryos after *rpl10a* MO^{spE515} injection at 2.5, 5, 10 µg/µl after 25 and 50 hours post fertilization (hpf).

1.4 Detection *rpl10a* gene splicing after *rpl10a* MO^{sp} injections using RT-PCR

To check the activity of Morpholinos, the PCR product from injected embryos were checked splice-modification after MO^{sp} injection by RT-PCR. The result showed double bands of PCR product with 584 and 684 bp in 40 µg/µl MO^{spE414} morphants (Figure 30B), but there was no shifted band at 20 µg/µl MO^{spE414} (Figure 30A). The size was increased 100 bp because of the intron 4 insertion. The maximum concentration of *rpl10a* MO^{spE414} affected to the PCR product size. For both concentrations of *rpl10a* MO^{spE515} (5 and 10 µg/µl), the PCR product size was shifted (Figure 30C). Moreover, the sequencing results were confirmed that the *rpl10a* gene sequences were deleted 33 bp (part of exon 5 and MO target region) (Figure 31). This

sequencing reduction caused 11 predicted amino acids reduction. (Figure 32). As the result was not successful using *rpl10a* MO^{spE414}, so the *rpl10a* MO^{spE515} was used to studied in next experiments. After this part, MO^{sp} was referred to MO^{spE515}.

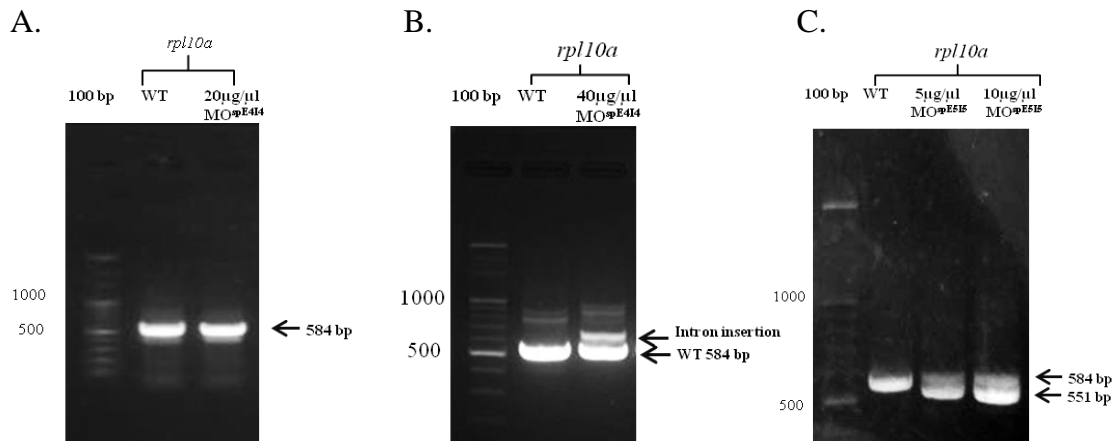


Figure 30. PCR product of morphants after MO^{spE414} injection at 20 µg/µl (A), 40 µg/µl (B) and MO^{spE515} at 5 and 10 µg/µl (C).

rpl10a sequences in MO^{spE515} morphants

```

CGTTGTACGAGGCCGTTAAGGAGGTCCAGGCCGTTCCCGTCGCAAGAAGAGAAAGTTCTTGAAACCGTGGAACTCCAGATCA
GCTTGAAGAACTACGACCCCTCAGAAGGACAAGCGTTTCTCAGGCACTGTCAGGCTGAAGACCACCCCGCGGCCCAAGTTCTCTG
TCTGCGTTCTTGGAGACCAGCAGCATTGTGATGAAGCAAAGGCCGCTGAAGTCCACACATGGACATTGAGGCTCTTAAGAAGC
TCAATAAGAACAAGAAGCTGGTCAAGAAGCTGGCAAAGAAGTACGATGCTTTCCTGGCCTCTGAGTCTCTGATCAAGCAGATTC
CTCGTATCCTGGGCCCTGGCCTCAACAAGGCAGGAAAAGTTCCCTCTCTGCTCACCCATAATGAGAACCCTGGGCACCAAGGTGG
ATGAGGTGAAATCCACCATCAAATTCAGATGAAGAAGGTTCTGTGTCTGGCTGTGGCCGTGGGTCATGTGAAGATGAGTGAGG
AAGAGCTGGTCTACAACATCCACTGGCTGTCAACTTCCTGGTGTCTCTGCTGAAGAAGAAGTGGCAAAACGTCAGAGCT

```

33 bp deleted sequences MO target

Figure 31. presented the sequence of *rpl10a* gene which was deleted after exon 5 splice-modification embryos.

```

      *      20      *      40      *      60      *      80      *      100      *
Rpl10a protein : MSKVSRDTLYFAVKEVÇAGSRRKRRKFLETVELÇISLKNYDPOKDRFSGTVRLKTTTPRPKFSVCVLGDÇÇHCDEARPAELPHMDTEALKKLNKNEKLVKKLARKYLAFIASESLIK : 117
Rpl10a deficiency : MSKVSRDTLYFAVKEVÇAGSRRKRRKFLETVELÇISLKNYDPOKDRFSGTVRLKTTTPRPKFSVCVLGDÇÇHCDEARPAELPHMDTEALKKLNKNEKLVKKLARKYLAFIASESLIK : 117
      *      120      *      140      *      160      *      180      *      200      *
Rpl10a protein : ÇIPRILGPGLNFAGKFPSLLTHNENLÇTKVDEVÇSTIKFCMKRLLCLAVAVGHVMMSEBELVYNIHLAVNELVSLLRKNWÇNVRALYIKSTMÇKÇQRLY : 216
Rpl10a deficiency : ÇIPRILGPGLNFAGKFPSLLTHNENLÇTKVDEV-----LCLAVAVGHVMMSEBELVYNIHLAVNELVSLLRKNWÇNVRALYIKSTMÇKÇQRLY : 205
      ÇIFFILSPGLNFAGKFPSLLTHNENLÇTKVDEILCLAVAVGHVMMSEBELVYNIHLAVNELVSLLRKNWÇNVRALYIKSTMÇKÇQRLY

```

Figure 32. Predicted amino acids after Rpl10a protein deficiency using *rpl10a* MO^{spE515} injection was 205 amino acids, in black box showed 11 amino acids were deleted.

1.5 Rescue experiment with full-length *rpl10a* mRNA

The result showed that there was no difference after rescue *rpl10a*MO^{aug} morphants with *rpl10a* mRNA at 24 and 48 hpf (Figure 33). It is possible that MO^{aug} sequences can bind with mRNA and block translation. The possible reason is that the target sequences of *rpl10a* MO^{aug} including 17 bp of *rpl10a* mRNA sequences. In contrast, after *rpl10a*^{spE515} morphants were rescued using *rpl10a* mRNA, the morphology of morphants was similar to wild-type embryos at 25 and 50 hpf. At 25 hpf, they showed the yolk extension became thicker than knockdown embryos (Figure 34). The result indicated that *rpl10a*^{spE515} morphants can rescue using full length of *rpl10a* mRNA.

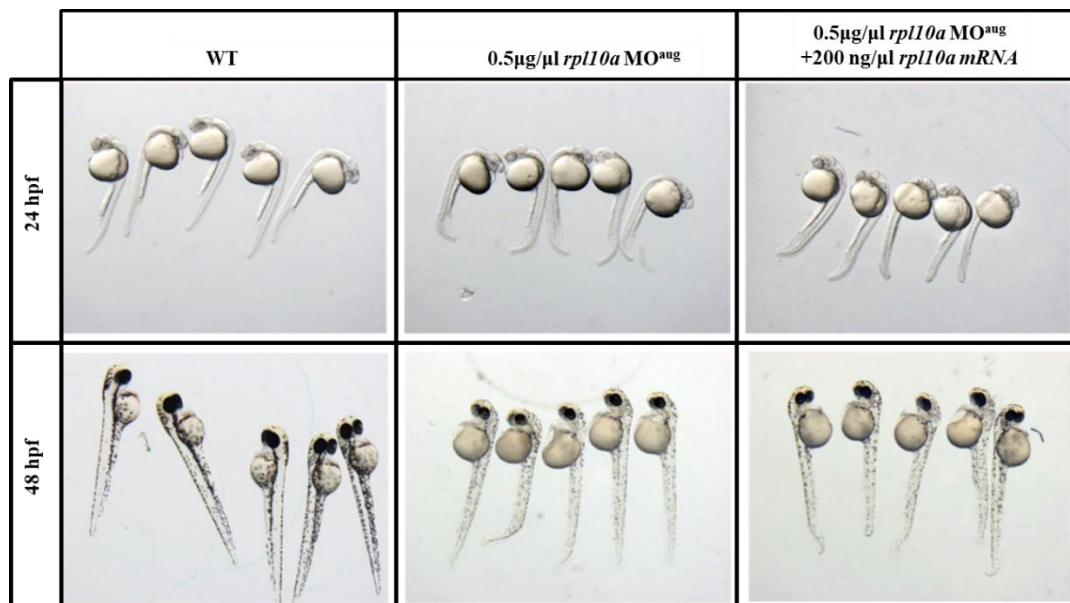


Figure 33. The morphology of rescued *rpl10a*MO^{aug} morphants with the synthetic full length of *rpl10a* mRNA at 24 and 48 hpf.

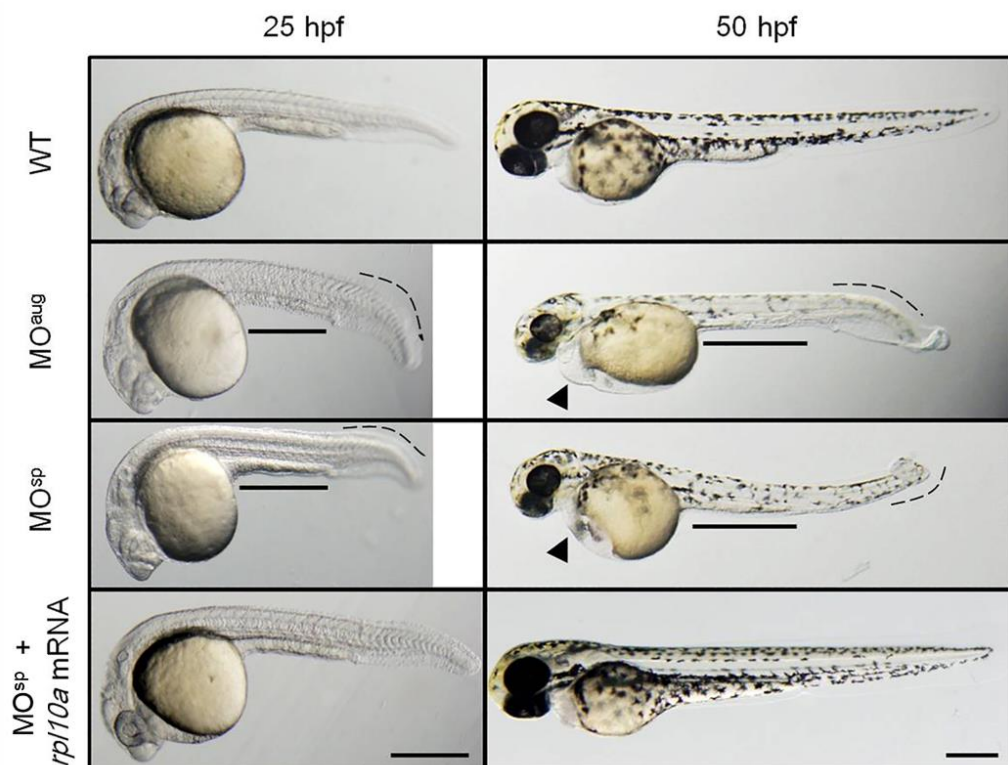


Figure 34. The zebrafish embryo morphology of morphants which rescued with the synthetic full length of *rpl10a* mRNA at 25 and 50 hpf. The black line showed smaller yolk sac extension. The edema of heart was pointed by the black arrow. The bent tails of morphants were indicated with curve line. Scale bar = 50 µm.

1.6 Hemoglobin staining

The hemoglobin staining was also performed. At 50 hpf, the reduction of hemoglobin staining and pigmentation were observed in knockdown samples, similar to *rps19* MO-injected embryos. The pigments were recovered after *rpl10a* mRNA co-injection, as well as the red blood cell, increasing. This result indicated that zebrafish *rpl10a* gene might have a secondary function in anemia (Figure 35).

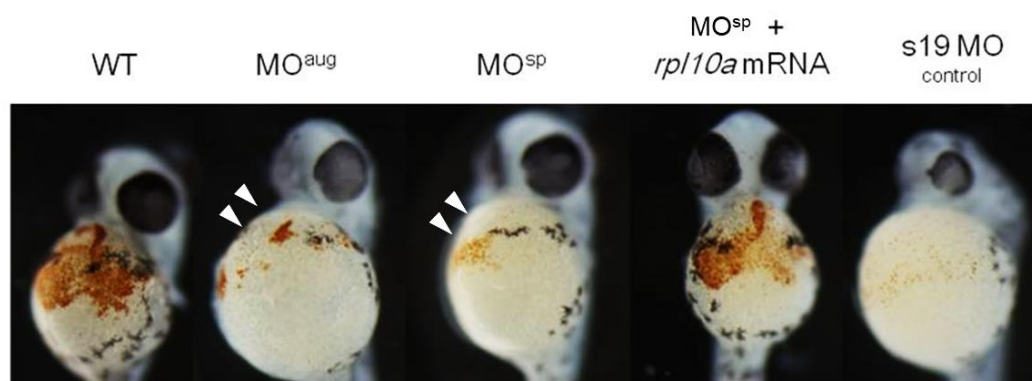


Figure 35. Hemoglobin staining after *rpl10a* MO^{spE515} recovery with *rpl10a* mRNA at 50 hpf. The figure showed the hemoglobin stained-embryos including WT, MO^{aug}, MO^{sp}, MO^{sp}+*rpl10a* mRNA and *rps19* MO as a positive control.

1.7 *rpl10a*-deficient embryos affect to number of PGCs marker genes reduction

1.7.1 Relative expression of PGCs marker genes in *rpl10a* gene knockdown embryos

The fold change expression of PGCs marker genes after *rpl10a* gene knockdown was presented, compared with WT and *rps19* gene knockdown at 25 hpf. The results showed the gene expression of *nanos1* and *vasa* were significantly decreased after inhibiting Rpl10a protein translation, compared to WT and *rps19* gene knockdown. The expression of *nanos1* and *vasa* transcripts were significantly reduced 0.42 and 0.37 fold from WT in *rpl10a*-deficient embryos, respectively. The relative

expression of *nanos1* and *vasa* transcript were also significantly declined, compared to *rps19* deficiency. However, the expression of *nanos1* in *rps19*-deficient embryos were little different with WT (Figure 36).

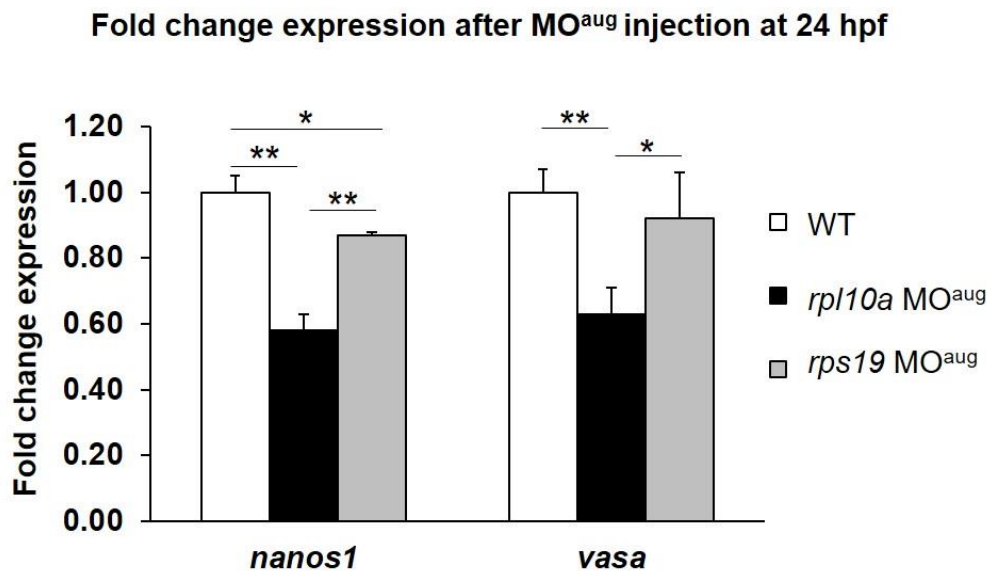


Figure 36. Fold change expression of *nanos1* and *vasa* gene in *rpl10a* knockdown embryos compared to WT and *rps19*-deficient embryos as a control. The pooled embryos were used 20 embryos each group (replication = 4). The data was analyzed statistical significance by one-way ANOVA, compared to WT. (*: p-value \geq 0.05, ** p-value \geq 0.001)

1.7.2 Relative expression of PGCs marker genes after *rpl10a* mRNA rescue

In addition, the effect of the PGCs marker genes expression after mRNA rescue was performed. The 25 hpf embryo samples included 5 $\mu\text{g}/\mu\text{l}$ of *rpl10a* MO^{spE515}, 5 $\mu\text{g}/\mu\text{l}$ of *rpl10a* MO^{spE515} with various mRNA concentration (100, 200 and 400 ng/ μl). The results showed that after *rpl10a* MO^{spE515} affected to low expression of *nanos1*. The *rpl10a* mRNA rescue showed increasing of *nanos1* mRNA expression depend on increasing *rpl10a* mRNA dose. The *vasa* gene slightly decreased expression in splicing *rpl10a* morphants. However, the expression of *vasa* in MO^{sp}

embryos were not significantly decreased. The 200 ng/ μ l of *rpl10a* mRNA rescue showed high expression of *nanos1* and *vasa* (Figure 37).

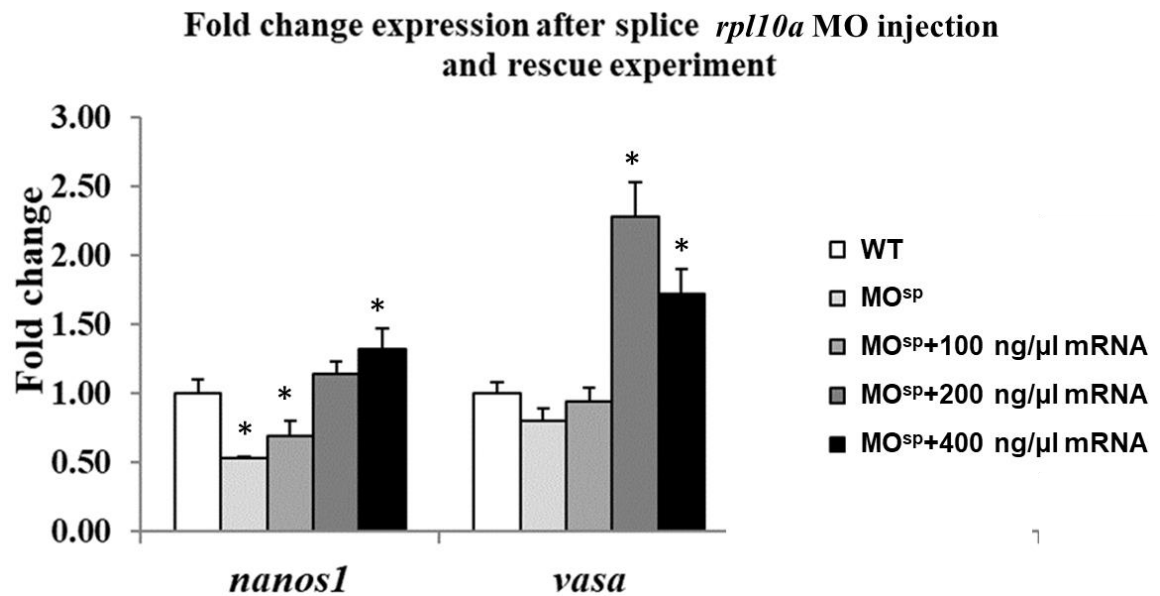


Figure 37. Fold change expression level of PGCs marker genes after *rpl10a* MO^{sp} (exon 5) injection and rescue experiment with *rpl10a* mRNA co-injection. (pool RNA from 15 embryos, replication = 4)

1.8 Effect of *rpl10a* gene knockdown on hemoglobin related transcripts

1.8.1 Expression of *gata1* and *tp53* after *rpl10a* gene knockdown

The fold change expression of *gata1* gene which is involved in blood cell maturation was decreased in MO-injected embryos at 24 hpf (Figure 38). Whereas, the high expression of the *tp53* gene was detected in *rpl10a*-deficient embryos compared to wild-type. These results had a similar trend of the expression with *rps19* MO injection. This qPCR result suggested that the erythroid involved gene had low expression in *rpl10a*-deficient embryos and implied that it might play a role in anemia.

Also, the *tp53* gene expression was increased similar to others ribosomal protein knockdown. This indicated that decreasing of *tp53* caused from the *rpl10a* defects.

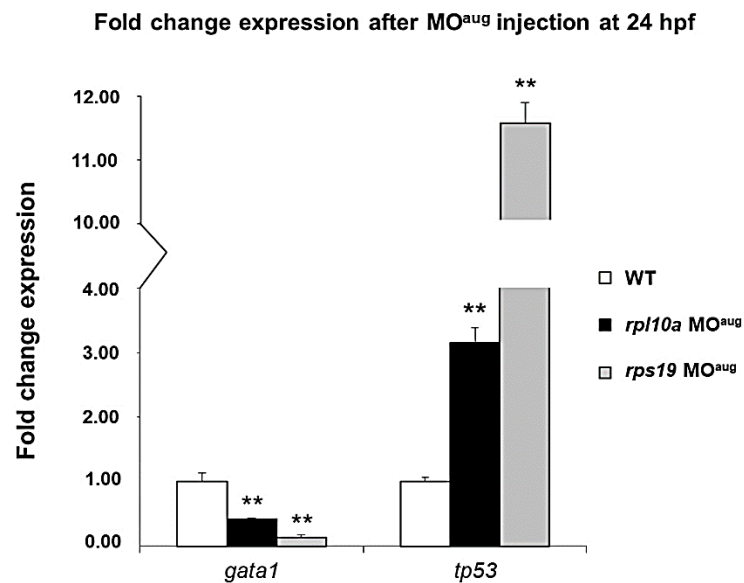


Figure 38 qRT-PCR results presented fold change expression of *gata1* and *tp53* gene in *rpl10a* knockdown embryos compared to wild-type and *rpls19* knockdown as a control. The pooled embryos were used 20 embryos each group (replication = 4). The data was analyzed statistical significance by one-way ANOVA, compared to WT (** p-value ≥ 0.001).

1.8.2 Expression of *hbae3* and *hbbe1* in *rpl10a*-deficient embryos

To check expression of other erythroid marker cells, the globin gene in embryonic stage (*hbae3* and *hbbe1*) in *Rpl10a*-deficiency zebrafish presented decreasing of transcript levels significantly compared to wild-type at 48 hpf. The results showed that *zhbae3* and *zhbbe1* gene were downregulated 0.74 and 0.78 folds, respectively (Figure 39).

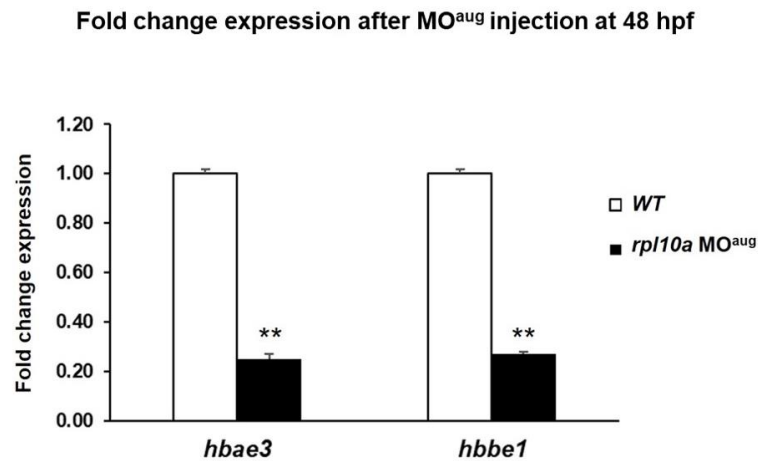


Figure 39. Fold change expression of *hbae3* and *hbbe1* mRNA in Rpl10a-deficient embryos at 48 hpf. Wild-type embryos were used as control. The pooled embryos used 20 embryos in each group (replication = 4). The data was analyzed statistical significance by one-way ANOVA, compared to WT (** p-value ≥ 0.001).

1.9 Effect of *rpl10a* gene knockdown on germline detected using the whole mount *in situ* hybridization (WISH)

To study the effect of *rpl10a* gene knockdown on germline, the PGCs marker genes in zebrafish embryos were detected using whole-mount *in situ* hybridization. We selected the *vasa* and *nanos1* gene for PGCs marker observation after *rpl10a* gene knocking down at 24 hpf. Also, *myoD*, a skeletal muscle-specific marker was used as a control. The *rps19* gene knockdown morphants was as a control. From this result found that *vasa* and *nanos1* gene which localized in PGCs were reduced after *rpl10a* gene knockdown. Although most of *rpl10a* morphants had reduced PGCs marker genes expression, some of them showed the mRNA expression pattern seemed as wild-type. In *rps19* morphants seemed no difference of the expression levels with wild-type. *MyoD* gene had not different expression in both morpholino-injected embryos and WT (Figure 40). In addition, the expression of *fli1* (markers specific to the endothelium) was used as a control gene. The *fli1* expression showed no differences (Figure 41). From qPCR results revealed that the PGCs marker genes were reduced when the *rpl10a* gene was knocked down both MO^{aug} and MO^{sp}.

Whereas, the expression of *vasa* and *nanos1* was recovered using co-injection with 200 ng/ μ l of *rpl10a* mRNA. The gene expression quantification related to the *nanos1* gene expression result by *in situ* hybridization.

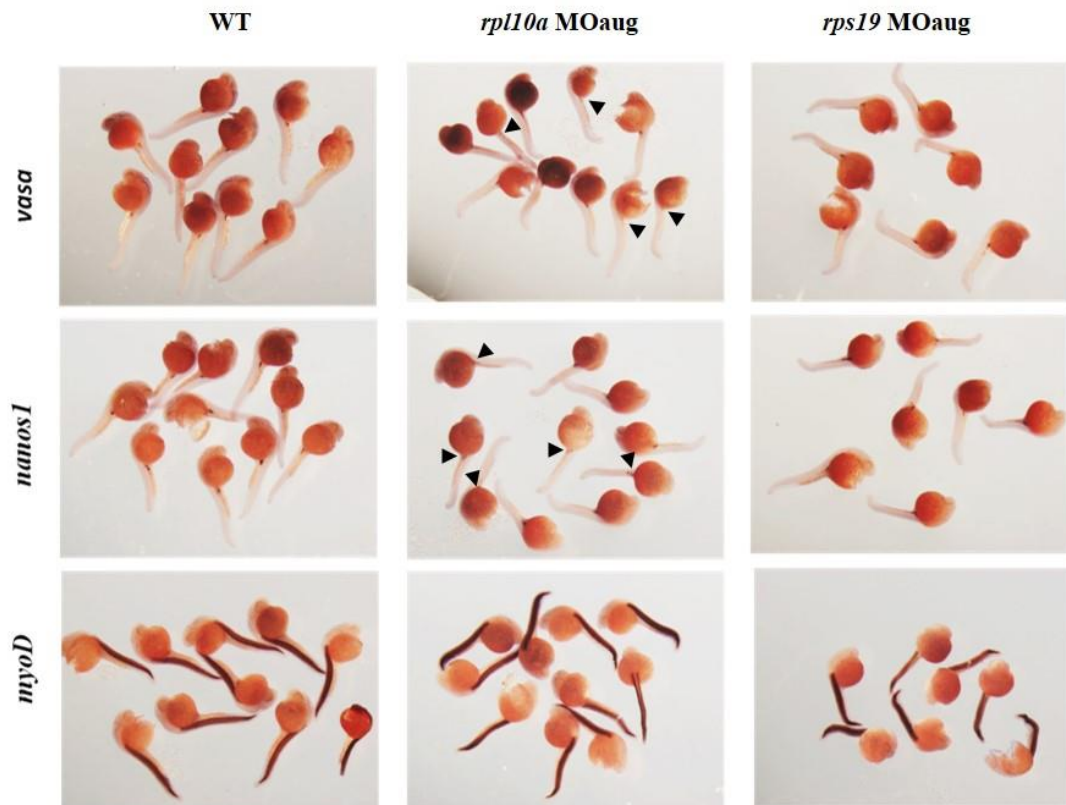


Figure 40. The expression of *vasa*, *nanos1*, *myoD* and gene in zebrafish using WISH assay after MO injection at 24 hpf.

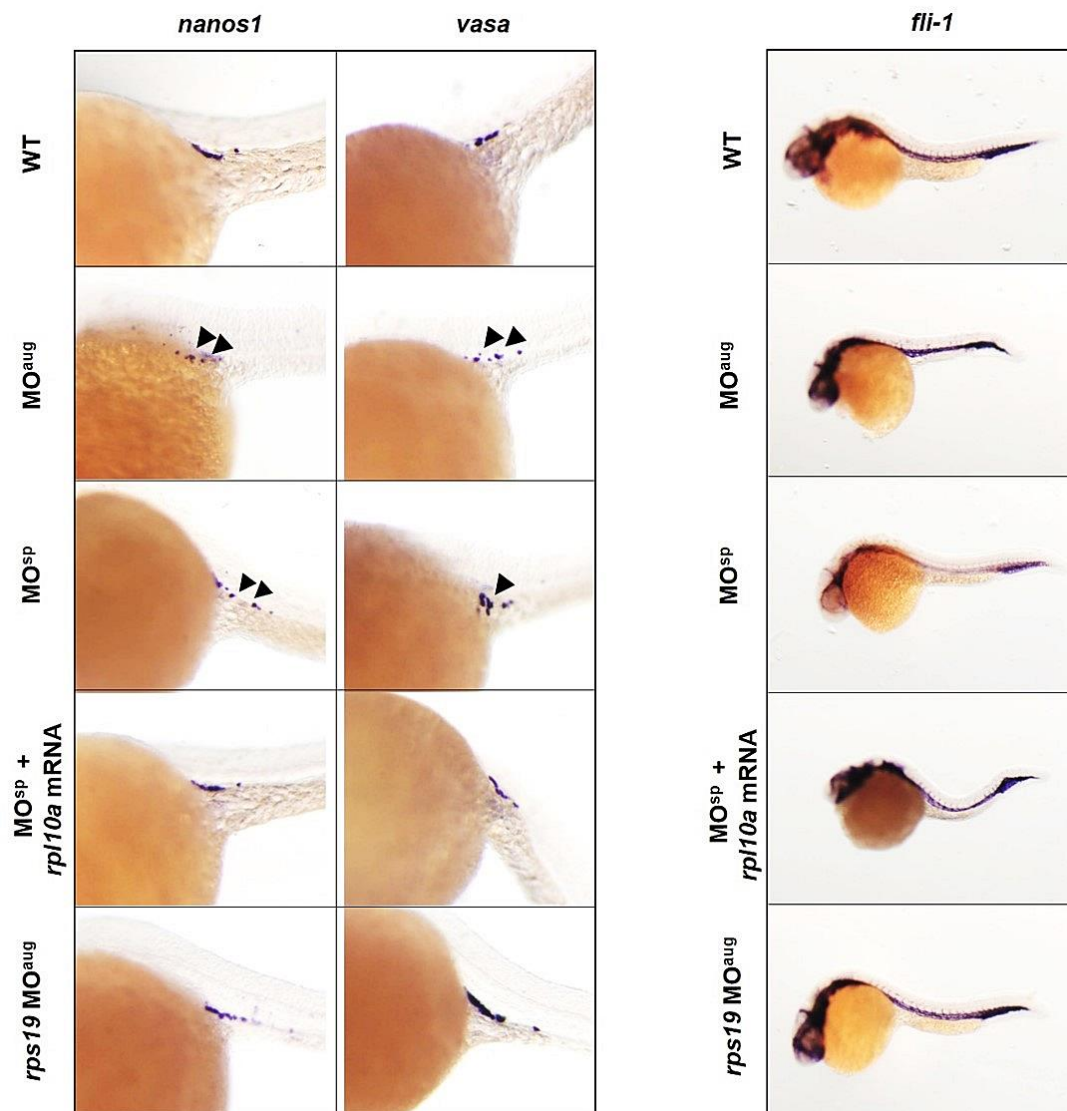


Figure 41. Whole-mount *in situ* hybridization presented the expression of PGCs marker genes including *nanos1* and *vasa* after morpholinos injection at 25 hpf. *fli-1* gene expression was used as a control.

In addition, the expression signal of *nanos1* and *vasa* gene were divided into 3 groups for estimation the effect of knocking down. The level of estimation was divided into low, medium and high expression level (Figure 42 right panel). We graded and counted in percentage. The result showed that *nanos1* had low expression in *rpl10a* MO^{aug} and MO^{spE515} injected embryos, compared to other groups. The rescued embryos using *rpl10a* mRNA showed higher *nanos1* expression, and expression

pattern was similar with the wild-type group. Whereas, there was no much different of *vasa* gene expression in $5\mu\text{g}/\mu\text{l}$ of *rpl10a* MO^{spE515} and rescue experiment or control groups. However, $0.5\mu\text{g}/\mu\text{l}$ of *rpl10a* MO^{aug} was slightly lower expression than other groups. From these results indicated that *rpl10a* gene knockdown affected to the reduction of PGCs marker gene expression especially *nanos1*. Moreover, there was no effect of PGCs maker genes declination in *rps19* AUG MO morphants (Figure 42 left panel). This whole-mount *in situ* hybridization result also showed the same expression trend with qPCR results.

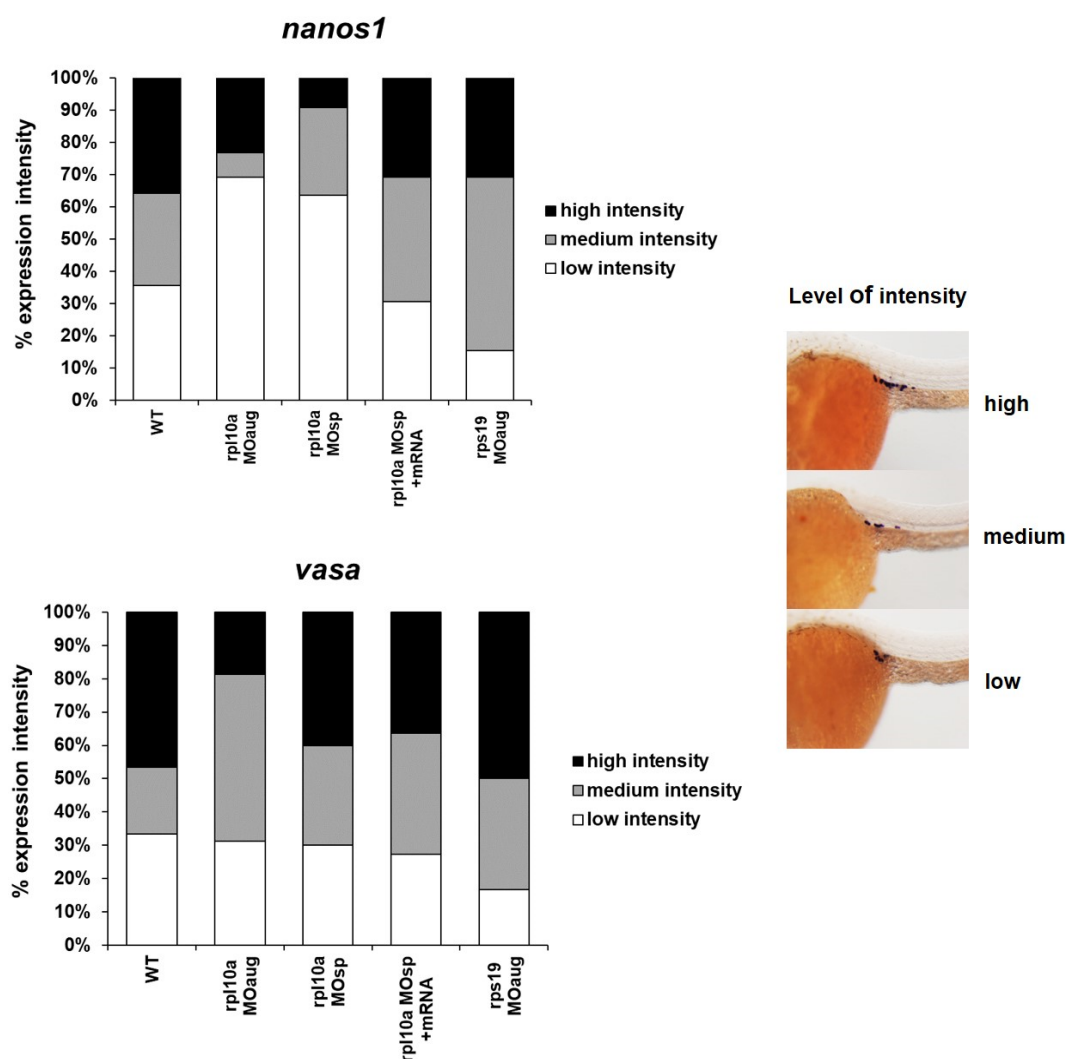


Figure 42. The percentage of expression intensity of PGCs marker genes (*nanos1* and *vasa*) after whole-mount *in situ* hybridization performing. The percentage was calculated by graded the intensity expression level as 3 groups as right panel.

2. *rpl10a* gene knockout using the CRISPR-Cas9 system

2.1 Heteroduplex mobility assay (HMA)

The guide RNA (*rpl10a* exon5 crRNA and tracrRNA) and Cas9 protein complex was injected into 1-cell stage embryos and collected 24 hpf embryos for HMA assay. At 24 hpf, the morphology of injected embryos was similar to uninjected embryos (Figure 43A), however, the HMA showed heteroduplex pattern because of mobility after CRISPR-cas9 injection (Figure 43B). The result indicated that these embryos were edited genome by CRISPR-Cas9.

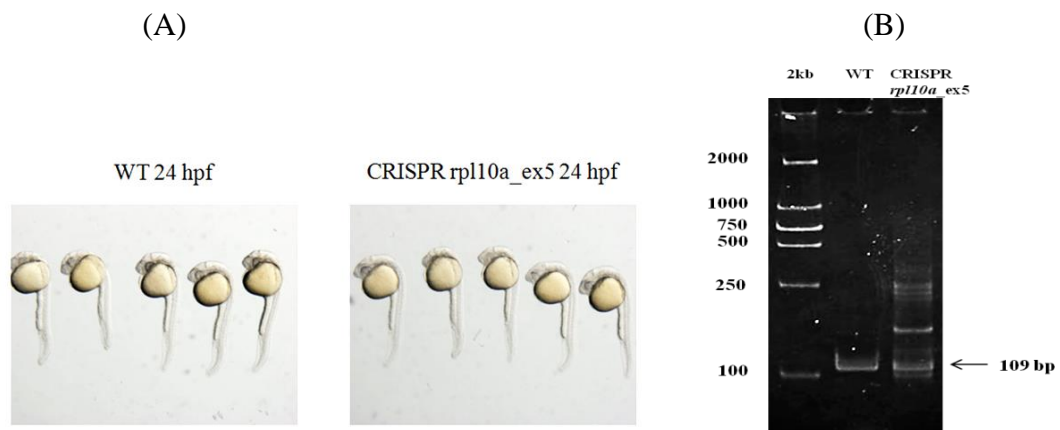


Figure 43 The morphology of zebrafish embryos after CRISPR *rpl10a* exon5 injection (A) and HMA assay showing heteroduplex pattern under 15% acrylamide gel analysis in mutant embryos (B).

2.2 The efficiency of crRNA and mutation pattern in F0 embryos

To evaluate the efficiency of crRNA and check mutation pattern, the sequencing was performed in embryos after *rpl10a* exon5 CRISPR injection. The figure showed the pattern of insertion/deletion mutation. We found that 20 from 29 colonies were mutated and calculated crRNA efficiency was 69%. From these colonies, the 14 patterns of mutation occurred, and a number of each pattern was shown in figure 44.

	PAM	Target Sequence		No. of colony
WT :	CCTGGGCCCTGG	CCTCAACAAGGCAGGAAAGTTTCC CCCTCTCTGCT	→ WT	= 9
C1 :	CCT-----	----- GTTTCC CCCTCTCTGCT	→ 27 bp del	= 1
C3,54,55,58:	CCTGGGCCCTGG C -----	----- AGGAAAGTTTCC CCCTCTCTGCT	→ 11 bp del	= 4
C4 :	CCTGGGCCCTGG-----	----- AGGCAGGAAAGTTTCC CCCTCTCTGCT	→ 8 del + 2 ins	= 1
	AAAGTATCCT			
C6 :	CCTGGGCCCTGG CCT -----	----- AGGCAGGAAAGTTTCC CCCTCTCTGCT	→ 5 bp del	= 1
C11 :	CCTGGGCCCTGG CCTCAA - λ	- GGCAGGAAAGTTTCC CCCTCTCTGCT	→ 3 del + 9 ins	= 1
	AAAATTAAA			
C24 :	CCTGGGCCCT-----	----- CAAGGCAGGAAAGTTTCC CCCTCTCTGCT	→ 8 bp del	= 1
C30 :	CCTGGGCCCTGG CCTCA ---	--- AGGCAGGAAAGTTTCC CCCTCTCTGCT	→ 3 bp del	= 1
C38,40 :	CCTGGGCCCTGG CCTCAA - λ	- GGCAGGAAAGTTTCC CCCTCTCTGCT	→ 3 del + 30 ins	= 2
	TCATTCAAACCTTCAATCAAACCTTCTCA			
C39 :	CCTGGGCCCTGG CC - λ	- AAGGCAGGAAAGTTTCC CCCTCTCTGCT	→ 5 del + 8 ins	= 1
	CTGGCCC			
C41 :	CCTGGGCCCTGG CC -----	----- AAGGCAGGAAAGTTTCC CCCTCTCTGCT	→ 5 bp del	= 1
C43,48,52:	CCTGGGCCCTGG- λ	- CAACAAGGCAGGAAAGTTTCC CCCTCTCTGCT	→ 3 del + 9 ins	= 3
	AAAGTTCCT			
C44 :	CCTGGGCCCTGG CCTCA ----	---- GGCAGGAAAGTTTCC CCCTCTCTGCT	→ 4 bp del	= 1
C46 :	CCTGGGCCCTGG CCTCA ---	--- AGGCAGGAAAGTTTCC CCCTCTCTGCT	→ 5 bp del	= 1
C53 :	CCTGGGCC-----	----- CAAGGCAGGAAAGTTTCC CCCTCTCTGCT	→ 10 del + 3 ins	= 1
	ATT			

crRNA efficiency = 20/29 \approx 69 %

Figure 44. presented insertion/deletion mutation patterns after *rpl10a* exon5 CRISPR injection (F0 embryos).

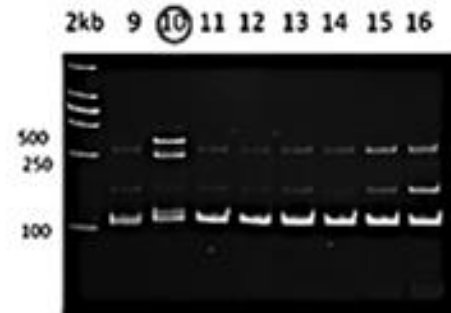
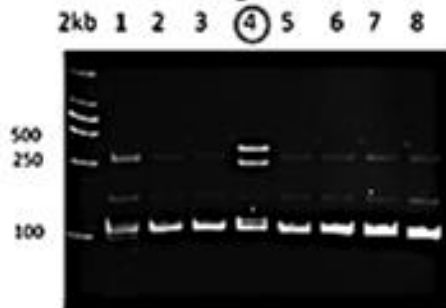
2.3 Mutation pattern in F1 heterozygous embryos

After F0 fish were grown and mated with wild-type fish for getting F1 embryos. The HMA pattern in F1 embryos was showed different patterns of mutation including 3 bp deletion, 4 bp deletion, 5 bp deletion, 11 bp deletion and 7 bp insertion. We observed that the germline transmission rate (indel mutation) was low in F1 embryos which had the frameshift mutation (Figure 45). Moreover, the predicted amino acids after mutation were shown in the figure. We found 5 patterns of mutation and 4 frameshift mutations were occurred (Figure 46).

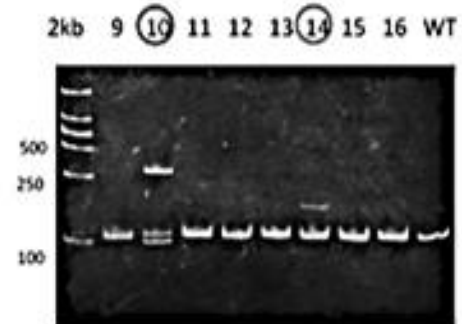
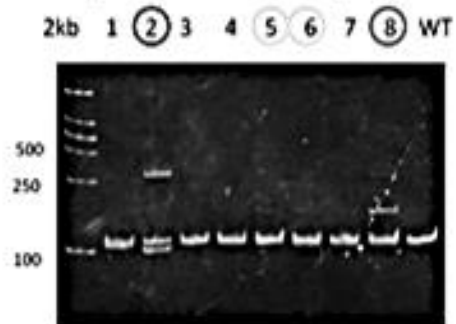
3 bp deletion



5 bp deletion



11 bp deletion 3 bp deletion



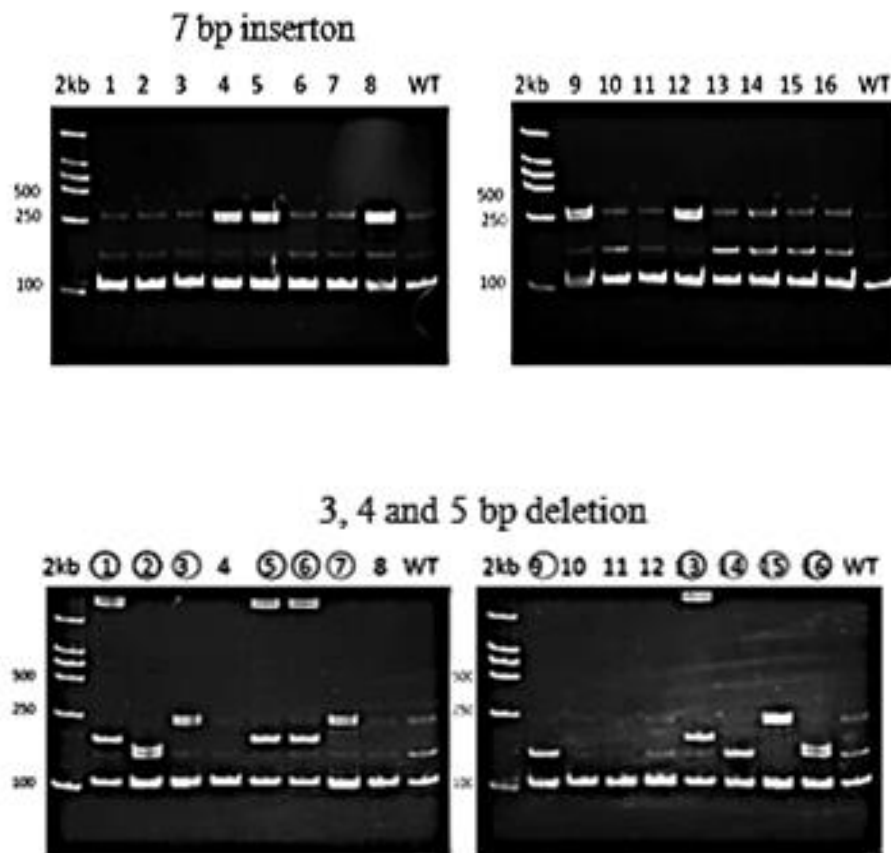


Figure 45. The picture presented HMA patterns of each F1 embryo mutation. There were many mutation patterns that found in heterozygous F1 embryos for example 3, 4, 5 or 11 bp deletion, and 7 bp insertion.

Mutation pattern	Amino acid changing	aa
<div style="display: flex; justify-content: space-around; border: 1px solid black; padding: 2px;"> PAM Target Sequence </div> <p>CCTGGGCCCTGG<u>CCT</u>CAACAAGGCAGGAAAGTTTCCCTCTCTGCT → WT</p> <p>CCTGGGCCCTGG<u>CCT</u>---CAAGGCAGGAAAGTTTCCCTCTCTGCT → 3 bp del</p> <p>CCTGGGCCCTGG<u>C</u>-----AGGAAAGTTTCCCTCTCTGCT → 11 bp del</p> <p>CCTGGGCCCTGG<u>CC</u>----AAGGCAGGAAAGTTTCCCTCTCTGCT → 5 bp del</p> <p>CCTGGGCCCTGG<u>CCT</u>CAACAAGGCAGGAAAGTTTCCCTCTCTGCT → 7 bp ins</p> <p style="margin-left: 100px;">A ACCTCGG</p> <p>CCTGGGCCCTGG<u>CCT</u>CA---GGCAGGAAAGTTTCCCTCTCTGCT → 4 bp del</p>	<p>118</p> <p>QIPRILGPGLNKAGKFPSSLTHNENLG</p> <p>QIPRILGPGL_KAGKFPSSLTHNENLG</p> <p>QIPRILGPGQGRKVSLSAHP*</p> <p>QIPRILGPGRKVSLSAHP*</p> <p>QIPRILGPGLKGRNGRKVSLSAHP*</p> <p>QIPRILGPGTRQESFPLCSPIMRTWAPRWMR*</p>	<p>216</p> <p>215</p> <p>136</p> <p>134</p> <p>141</p> <p>148</p>

Figure 46. The picture presented mutation patterns and amino acid changing in F1 embryos. The PAM sequence (CCT) was highlighted as underline. The target sequence was labelled with black bond letters. The nucleotide which was deleted in target sequence was marked by hyphen. The predicted amino acids that were changed and stop codon were marked by gray letters and star, respectively.

2.4 Mutation pattern in F2 heterozygous embryos

After F0 fish were grown and mated with same mutant fish for breeding F2 embryos. The HMA pattern in F0, F1 and F2 embryos were showed 5 deletion pattern (Figure 47A-B). The result of direct sequencing was confirmed by the changing of nucleotides that found in F1 (Figure 47C). Furthermore, the predicted amino acids after mutation were shown in the Figure 47D. We found that after 3, 5, 11, 15, 17 bp deletion were occurred, they caused amino acids reduce to 215, 134, 136, 211, 133 amino acids, respectively. While, the 7 bp insertion showed the predicted amino acids reduced to 141 bp.

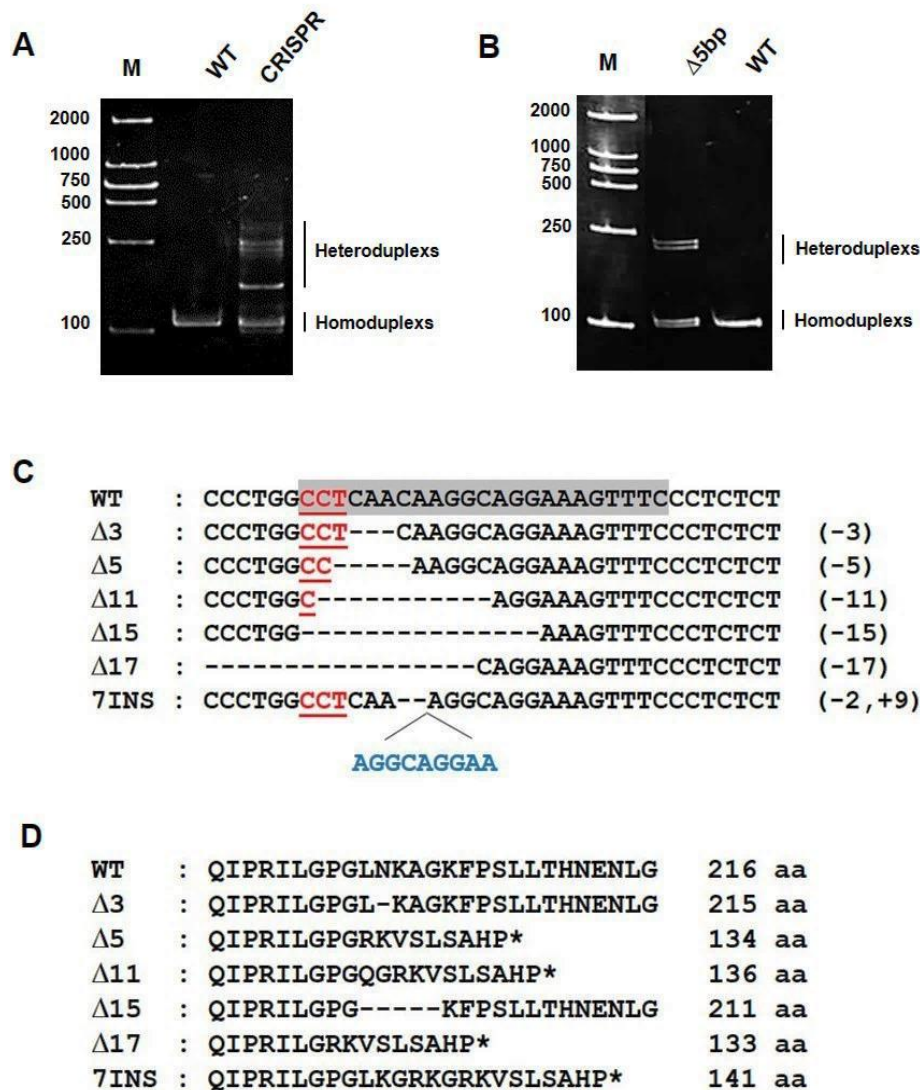


Figure 47 (A) Heteroduplex pattern was observed after crRNA-trancrRNA-Cas9 complex (CRISPR- Cas9) injection. (B) HMA patterns displayed different heteroduplex pattern in 5 bp deletion mutation compared to WT. (C) The patterns of mutation which obtained from genome editing are presented. The crRNA target site and PAM sequences are presented in gray highlighted and red letters, respectively. The deleted nucleotide was shown in hyphen whereas the inserted nucleotides are presented in blue letters. (D) Predicted amino acid sequences after *rpl10a* gene knockout by CRISPR-Cas9 are started from amino acid position at 190. Deleted sequence and stop codon are marked by hyphen and star, respectively.

2.5 The effects *rpl10a* knockout embryos on phenotype and morphology

The mutant embryos at 3 dpf were observed abnormal phenotypes including smaller eyes, severe edema, big yolk sac, smaller yolk extension, reduced pigmentation and bent tail. Whereas, heterozygous and wild-type embryos were shown no significant difference. Morphology of mutant embryos was also stained with H&E staining. The muscle of mutant fish was observed low staining. This result may cause to bent tail phenotype. The mutant embryos were not swimming and had low metabolism; therefore, the mutant fish died within 3-5 days. However, the heterozygous and wild-type fish can grow to be adulthood (Figure 48).

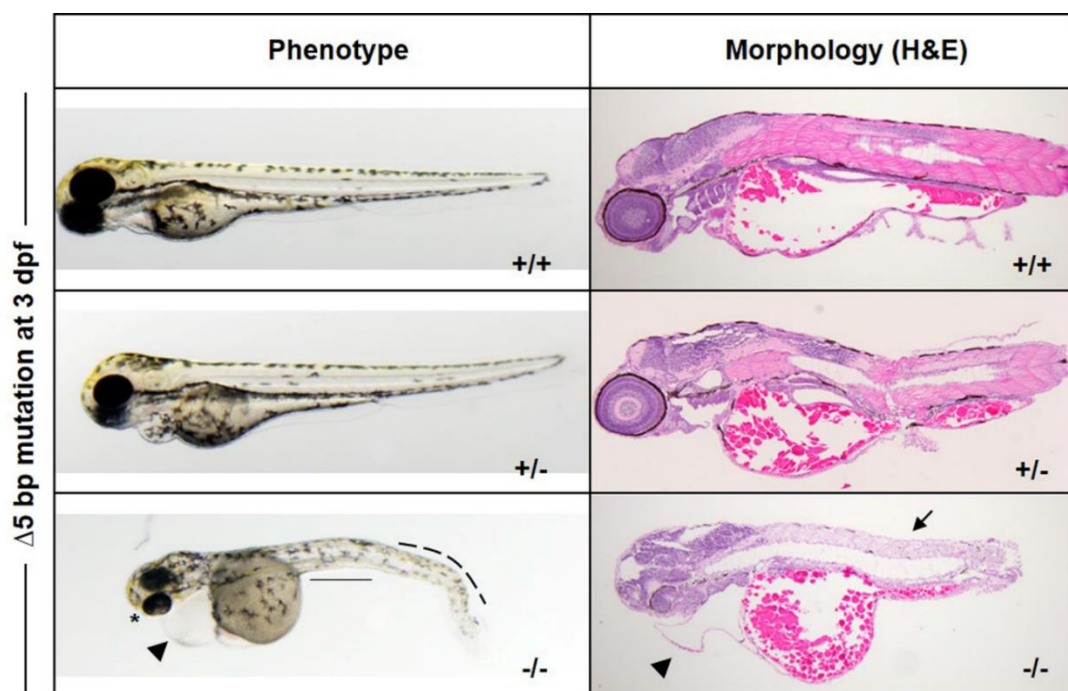


Figure 48. Abnormality phenotype and morphology of homozygous 5-bp deletion mutation (-/-) embryos. Wild-type (+/+) embryos and heterozygous (+/-) at 3 dpf were presented in H&E staining.

2.6 The *rpl10a* knockout embryos caused by hemoglobin staining reduction

The hemoglobin staining was performed after *rpl10a* gene knockout using CRISPR-Cas9 at 48 hpf. The 5 bp deletion homozygous and heterozygous mutant embryos were clearly observed hemoglobin reduction, compared to wild-type (Figure 49).

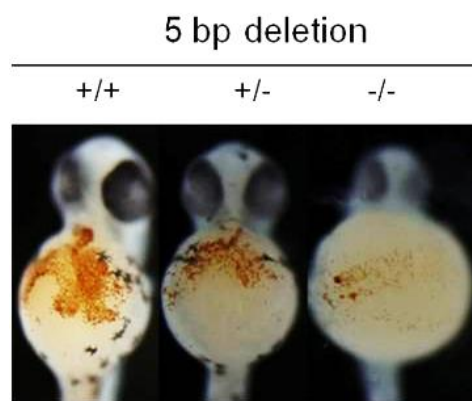


Figure 49. Hemoglobin staining of 5 bp deletion homozygous mutation (-/-). Wild-type (+/+) embryos and heterozygous (+/-) at 50 hpf were presented. The reduction of hemoglobin was observed significantly in mutant embryos.

CHAPTER 5

DISCUSSION

Part I: The effect of rRpl10a protein on shrimp ovarian maturation

From many pieces of evidence indicated that *rpl10a* gene might play a role as extra-ribosomal function. In the previous study, *rpl10a* gene in cancer cells reacts with radiation (Balcer-Kubiczek et al., 1997; Lee et al., 2006). The production of Rpl10a also related to lymphoid cells maturation and embryogenesis (Fiscaro et al., 1995). The report in banana shrimp indicated that *rpl10a* gene was expressed differentially during ovarian maturation especially the early stage of vitellogenesis (Wonglapsuwan et al., 2009). Rpl10a protein plays a function during the ovarian development process in the *Drosophila* (Wonglapsuwan et al., 2011). In rainbow trout, the Rpl10a expression was associated with the regulation of gonadal development (Makkapan et al., 2014). As above reports can assume that the Rpl10a protein had a secondary function to control the ovarian development.

To study the ovarian development, the rRpl10a protein was used for stimulation. Tiu and Chan (2007) studied the recombinant molt-inhibiting hormone (MeMIH) was produced and used for reproductive stimulation in the shrimp *M. ensis*. The result indicated that MeMIH affected to a gonad stimulatory and play function as a gonad-stimulating hormone. In addition, the exogenous GnRH was handled in black tiger shrimp to study the effect on ovarian development. That report revealed that the ovarian maturation was occurred significantly shorten (Ngersounnern et al., 2008). Our results suggested that the 180 µg per shrimp was optimal dosage to stimulate the early stages of shrimp ovarian development after 7 days induction. However, no observation in the mature stage of vitellogenesis after rRpl10a stimulation. Also, we found that longer received the rRpl10a (at 15 days after induction) could not reach the mature stage, it was possible that the ovaries were turned back to the immature stage. The suitable amount of rRpl10a was required for normal development. Previous result showed the excess *rpl10a* in *Drosophila* led to the death of cells in germline and the eyes (Wonglapsuwan et al., 2011). Therefore, it is possible to use rRpl10a at the initial

for early ovarian development stimulation. This method will be more proper than stimulation by eyestalk ablation, and it may be applied for vitellogenesis stimulation in shrimp aquaculture in the future.

Part II: The effect of rRpl10a protein on shrimp spermatogenesis comparative to mouse

In this study, the rRpl10a protein was examined as a stimulator for spermatogenesis in shrimp and mice. The observation found that rRpl10a was able to induce the spermatogenesis from spermatogonia cells into spermatid cells within 4 h, *in vitro*. Therefore, the rRpl10a might involve spermatogonia proliferation which occurred in the early stage of spermatogenesis. The optimal dosage of rRpl10a for spermatogenesis in shrimp and mouse was 1.0 μ M. Our result agreed with the result of treatment of the shrimp's ovarian explants at 1.0 μ M rRpl10a protein for 4 h. After Rpl10a incubation, the genes which related to early vitellogenesis including, *sop*, *tctp*, and *hsp70* gene were upregulated in ovarian tissue at a maximum level at 4 h (Wonglapsuwan et al., 2010).

From our study, we also confirmed the H&E evaluation using WGA lectin histochemistry. Lectins are bound with spermatogenic cell because in the modification process, the intracellular glycoprotein during germ cell differentiation is changed (Koehler, 1981). Therefore, lectins are useful for spermatozoa detection. Lee and Damjanov (1984) reported that WGA reacted with all mouse spermatogenic cells, but the intensity was increased in the late stage of spermatogenesis. Increasing of WGA receptor appeared on the cell surface of late spermatids. However, during spermiogenesis, WGA lectin staining was detected in the boundary of spermatid cells. WGA was also positive in acrosomal granules of Golgi-phase spermatid (Arya and Vanha-Perttula, 1986). Similarly, Söderström et al. (1984) indicated that WGA was stained in the acrosome of late spermatids after formalin fixation. The acrosome of spermatids was bound specifically with WGA lectin because of the presence of N-acetyl-D-glucosamine sugar residues. Also, increasing the intensity of WGA binding in spermatid development indicated that the WGA receptors were continuously

formed during spermatogenesis. The result observed that H&E assessment and WGA result had the similar trend that rRpl10a can induce the mouse spermatogenesis. Moreover, the EdU assay was confirmed the cell proliferation. The result found that the rRpl10a protein affects to the replication of spermatogonia cells.

Besides, we confirmed the result by determining the expression level of the marker gene in the early stage of spermatogenesis. *Dmrt1* gene in crustacean (*Eriocheir sinensis*) was more expressed in immature testis than mature stage (spermatozoa) due to *Dmrt1* is an essential gene for the early stage of spermatogenesis (Zhang and Qiu, 2001). Our result indicated that rRpl10a-incubated shrimp testis showed decreasing of *Dmrt1* expression level. In the parallel result, RNA helicase associated with AU- rich element (*Rhau*) gene expression that required for spermatogonia differentiation was also determined in rRpl10a treated mice testis. Gao et al. (2015) reported that *Rhau* gene was upregulated in mouse testis higher than in other tissues. They also found that *Rhau* was expressed at high levels in spermatogonia stem cells and primary spermatocytes, but expressed at low levels in spermatid cells. In mice *Rhau* knockout testes, the percentage of primary spermatocytes was decreased, resulting in abnormal cell proliferation during spermatogonia differentiation. Therefore, *Rhau* plays an important role in spermatogonia differentiation.

In addition, both protamine (*Prm1* and *Prm2*) mRNAs are detected in round spermatid stage and translated during elongating spermatid stage (Bower et. al., 1987). When the mouse *Prm1* or *Prm2* gene was interrupted, leading to the reduction of specific protein quantity. Furthermore, *Prm2* defective sperm caused the blastocyst development of mouse eggs were less. The results indicated that *Prm2* plays a function in sperm chromatin maintenance (Cho et al., 2003). The infertility in man was interrupted by alteration of *Prm1* and *Prm2* gene expression and mutation of protamine gene (Oliva, 2006). Moreover, protamine deficiency caused the decrease of number, motility and spermatozoa morphology (Akmal et. al., 2016). From these reports indicated that *Prm2* gene is an essential gene in the late stage of spermatogenesis. Our results revealed that after incubating with rRpl10a protein for 4

h, the expression of *Prm2* gene was upregulated, while the *Rhau* gene expression was downregulated.

From these finding, we can assume that rRpl10a protein increases the efficiency of spermatogenesis via stimulation activity of spermatogonia replication. Beyond the function in the ribosome, many ribosomal proteins played secondary functions (Wool, 1996). Therefore, it is possible that Rpl10a protein might be extra play function in spermatogenesis in shrimp and mouse.

Part III. The effects of *rpl10a* gene knockdown and knockout on abnormality development, reduction of hemoglobin and PGCs marker genes reduction

Ribosomopathies or ribosomal protein diseases such as DBA anemia have been studied. Deficiency of ribosomal protein S19 leads to anemia inpatient (Draptchinskaia et al., 1999). The other ribosomal proteins have also been identified including *RPL11*, *RPL5*, *RPL35A*, *RPS24*, *RPS7*, *RPS17*, *RPS10*, *RPS26*, and *RPL26* (Gadav et al., 2006, Gadav et al., 2008; Cmejla et al., 2007; Farrar et al., 2008; Doherty et al., 2010).

RPs genes mutations whether small or large subunit ribosome was affected by alteration of rRNA and erythroid precursor defects (Costa et al., 2010). Insufficiency of RPs caused the translation efficiency decline. The failure of the 40s or 60s subunit led to the reduction of protein translation; therefore, downstream of the protein related with the erythroid defect was specifically expressed in erythroid progenitor cell (Farrar et al., 2008; Yadav et al., 2014). Rpl10a is also known as cyclosporin-A 19 (CsA-19); an immunosuppressive drug. CsA-19 expression in mice liver which acts as a source of hematopoietic progenitors was observed to be regulated (Fisicaro et al., 1995). Our result indicated that *rpl10a*-deficient zebrafish resulted in hemoglobin reduction.

The expression of *tp53*, apoptotic gene, was increased due to loss of *rpl10a* similar to *rps19* deficiency. Although, the morphological abnormalities were dependent on *tp53* activation, in the *rps19* deficient-embryos, the *tp53* independent pathway is more important to the anemic phenotype (Torihara et al., 2011). However,

the exact role of *tp53* in *rpl10a*-deficient zebrafish that caused to anemia still unknown. Moreover, ribosomal protein deficiency might be a proapoptotic defect due to ribosome assembly defect; furthermore, it causes the *tp53* level increasing and proapoptotic phenotype stimulation (Farrar et al., 2008). Also, dysfunction of *rpl10a* gene affected the morphological abnormalities and growth retardation. The lethal day of *rpl10a*-deficient zebrafish was between 3-7 dpf. Ribosomal proteins deficiency led to abnormal morphology and development in zebrafish (Uechi et al., 2006). Moreover, the expression of *gata1*, *hbae3* and *hbbe1* mRNA which are erythroid marker genes had significant fold change reduction in *rpl10a*-deficient embryos.

Furthermore, the primordial germ cell marker gene expression including *nanos1* and *vasa* were determined. Primordial germ cells or PGCs during early embryogenesis are the precursors to spermatozoa and oocytes which are reproductive gametes. The *vasa* gene was identified as a marker for PGCs in zebrafish (Yoon et al., 1997). Also the *nanos1*, a germplasm gene was essential for the PGC migration and viability (Köprunner et al., 2001). Our result found that the expression of *nanos1* and *vasa* gene were declined in *rpl10a*-deficient embryos. Therefore, this result suggested that Rpl10a might be involved with PGCs migration to germ cell and viability.

Overall results suggested that *rpl10a* insufficient may lead to delay in embryogenic development, caused to anemia and might be interrupted primordial germ cell development.

CHAPTER 6

CONCLUSIONS

1. Stimulation on ovarian development in *F. merguensis* with rRp110a protein

The rRp110a protein promoted the early ovarian development stages of shrimps. At 180 µg of Rp110a/shrimp was the effective dose to stimulate ovaries to reach to stages I and II of vitellogenesis (28.57% and 28.57%, respectively) within 7-days post injection.

2. Induction of spermatogenesis in *P. monodon* and *M. musculus* with rRp110a protein

This report revealed that rRp110a protein play an important function in spermatogenesis in both shrimp and mouse. The effective dose for shrimp testicular development was 1.5 µM (52.94% of the mature stage) to stimulated the spermatogonia cell into spermatid cells. While the dose of rRp110a at 1 µM showed the effective stimulation of spermatogenesis in mouse at 4 h both H&E staining and WGA lectin histochemistry evaluation. Moreover, the expression of *Dmrt1* gene which was detected in the early stage of spermatogenesis in shrimp was low. The expression of early stage marker gene (*Rhau*) was decreased, the level of the late stage marker gene (*Prm2*) was upregulated. The cell proliferation was also confirmed by the presence of a strong signal of fluorescence in 1 µM of rRp110a using EdU detection. The results of these study may be used to develop sperm maturation of animal as well as a human *in vitro* in the future.

3. Loss activity of *rpl10a* gene on abnormality development in zebrafish

The phenotype of zebrafish which loss the activity of *rpl10a* gene showed thinner yolk extension, smaller eyes, shorter body length and bent tail at 25 hpf. At 50 hpf, *rpl10a* gene defect embryos were bigger yolk sac, edema, smaller eyes, melanophore pigment reduction, and a curved tail. After rescued with *rpl10a* mRNA, the abnormal phenotype was recovered to be the same as wild-type. This result revealed that *rpl10a* gene is essential for early embryogenic development. Histological morphology at 3 dpf also indicated severe abnormal development and low staining of muscle. The *rpl10a*-defect embryos presented a slow growth and embryonic lethality within 5-7 dpf. The knockdown and knockout *rpl10a* gene showed the same abnormality development.

4. Dysfunction of *rpl10a* gene on anemia in zebrafish

Five base pair deletion homozygous mutant embryos also showed the reduced red blood cell and hemoglobin. Furthermore, *gata1* mRNA expression declined and *tp53* gene expression increased in *rpl10a* gene knockdown. Moreover, the embryonic globin gene expression including *hbae3* and *hbbe1* were significantly decreased in 48-hpf-embryos. These results supported that Rpl10a protein might play a secondary role in anemia.

5. Defective of *rpl10a* gene on PGCs marker genes

The *rpl10a* deficiency (knockdown) in zebrafish affected on primordial germ cell development and showed low expression of PGCs marker genes especially *nanos1*.

Future works

1. Test activity of His-Rp110a protein to stimulate the spermatogenesis *in vivo*.
2. Study mechanism of *rpl10a* gene knockout on anemia and used mutant fish as a model for disease study.

REFERENCES

- Agungpriyono, S., Kurohmaru, M., Prasetyaningtyas, W. E., Kaspe, L., Leus, K. Y., Sasaki, M., Kitamura, N., Yamada, J. and Macdonald, A. A. (2007) A Lectin Histochemical Study on the Testis of the Babirusa, *Babyroussa babyroussa* (Suidae). *Anatomia, Histologia, Embryologia*, 36: 343-348.
- Agungpriyono, S., Kurohmaru, M., Kimura, J., Wahid, A. H., Sasaki, M., Kitamura, N., Yamada, J., Fukuta, K. and Zuki, A. B. (2009) Distribution of Lectin-Bindings in the Testis of the Lesser Mouse Deer, *Tragulus javanicus*. *Anatomia, Histologia, Embryologia*, 38: 208-213.
- Akmal M., Widodo M. A., Sumitro S. B., Purnomo B. B. (2016) The important role of protamine in spermatogenesis and quality of sperm: A mini review. *Asian Pacific Journal of Reproduction* 5(5): 357-60.
- Amatruda, J. F., Shepard, J. L., Stern, H. M., & Zon, L. I. (2002) Zebrafish as a cancer model system. *Cancer cell*, 1(3): 229-231.
- Arya, M., Vanha-Perttula, T. (1986) Comparison of lectin-staining pattern in testis and epididymis of gerbil, guinea pig, mouse, and nutria. *American journal of anatomy*, 175(4): 449-469.
- Balcer-Kubiczek, E. K., Meltzer, S. J., Han, L. H., Zhang, X. F., Shi, Z. M., Harrison, G. H., Abraham, J. M. (1997) Csa-19, a radiation-responsive human gene, identified by an unbiased two-gel cDNA library screening method in human cancer cells. *Oncogene*, 14(25), 3051.
- Bill, B. R., Petzold, A. M., Clark, K. J., Schimmenti, L. A., & Ekker, S. C. (2009) A primer for morpholino use in zebrafish. *Zebrafish*, 6(1), 69-77.
- Bower P. A., Yelick P. C., Hecht N. B. (1987) Both P1 and P2 protamine genes are expressed in mouse, hamster, and rat. *Biology of reproduction* 37: 479-488.
- Braat A. K., van de Water, S, Korving J., Zivkovic, D. (2001) A zebrafish vasa morphant abolishes vasa protein but does not affect the establishment of the germline. *genesis*, 30(3): 183-185.
- Brown, A. JR., Patlan, D. (1974) Color Changes in the Ovaries of Penaeid Shrimp as a Determinant of Their Maturity. *Marine Fisheries Review* 36 (7).

- Brownlie, A., Hersey, C., Oates, A.C., Paw, B.H., Falick, A.M., Witkowska, H.E., Flint, J., Higgs, D., Jessen, J., Bahary, N., Zhu, H. (2003) Characterization of embryonic globin genes of the zebrafish. *Developmental biology*, 255(1): 48-61.
- Dall, W., Hill, J. B., Rothlisberg, C. P., Sharples, J. D. (1990) *The Biology of the Penaeidae. Advances in Marine Biology* 27.
- Cho, C., Willis, W. D., Goulding, E. H., Jung-Ha, H., Choi, Y. C., Hecht, N. B., Eddy, E. M. (2001) Haploinsufficiency of protamine-1 or-2 causes infertility in mice. *Nature genetics*, 28(1): 82.
- Cho, C., Jung-Ha, H., Willis, W.D., Goulding, E.H., Stein, P., Xu, Z., Schultz, R.M., Hecht, N.B. and Eddy, E.M. (2003) Protamine 2 deficiency leads to sperm DNA damage and embryo death in mice. *Biology of reproduction*, 69(1): 211-217.
- Cmejla, R., Cmejlova, J., Handrkova, H., Petrak, J., Pospisilova, D. (2007) Ribosomal protein S17 gene (RPS17) is mutated in Diamond-Blackfan anemia. *Human Mutation* 28: 1178-1182.
- Detrich, H.W., Kieran, M.W., Chan, F.Y., Barone, L.M., Yee, K., Rundstadler, J.A., Pratt, S., Ransom, D., Zon, L.I. (1995) Intraembryonic hematopoietic cell migration during vertebrate development. *Proceedings of the National Academy of Sciences of the United States of America* 92: 10713-10717.
- Doherty, L., Sheen, M.R., Vlachos, A., Choessel, V., O'Donohue, M.-F., Clinton, C., Schneider, H.E., Sieff, C.A., Newburger, P.E., Ball, S.E., Niewiadomska, E., Matysiak, M., Glader, B., Arceci, R.J., Farrar, J.E., Atsidaftos, E., Lipton, J.M., Gleizes, P.-E., Gazda, H.T. (2010) Ribosomal Protein Genes RPS10 and RPS26 Are Commonly Mutated in Diamond-Blackfan Anemia. *American Journal of Human Genetics* 86: 222-228.
- Doudna, J. A., & Charpentier, E. (2014). The new frontier of genome engineering with CRISPR-Cas9. *Science*, 346(6213), 1258096.
- Draper, B. W., McCallum, C. M., Moens, C. B. (2007) *nanos1* is required to maintain oocyte production in adult zebrafish. *Developmental biology*, 305(2): 589-598.

- Draptchinskaia, N., Gustavsson, P., Andersson, B., Pettersson, M., Willig, T.-N., Dianza, I., Ball, S., Tchernia, G., Klar, J., Matsson, H., Tentler, D., Mohandas, N., Carlsson, B., Dahl, N. (1999) The gene encoding ribosomal protein S19 is mutated in Diamond-Blackfan anaemia. *Nature Genetics* 21: 169.
- Farrar, J.E., Nater, M., Caywood, E., McDevitt, M.A., Kowalski, J., Takemoto, C.M., Talbot, C. C., Meltzer, P., Esposito, D., Beggs, A. H., Schneider, H. E., Grabowska, A., Ball, S.E., Niewiadomska, E., Sieff, C. A., Vlachos, A., Atsidaftos, E., Ellis, S.R., Lipton, J.M., Gazda, H. T., Arceci, R.J. (2008) Abnormalities of the large ribosomal subunit protein, Rpl35a, in Diamond-Blackfan anemia. *Blood* 112: 1582-1592.
- Fiscaro N., Katerelos M., Williams J., Power D., D'Apice A., Pearse M. (1995) Identification of genes downregulated in the thymus by cyclosporin-A: preliminary characterization of clone CSA-19. *Molecular immunology* 32: 565-572.
- Jiang, F. J., Yun, L. L., Xiu, L. G. (2002) Molecular Cloning and Characterization of Human DDX36 and Mouse Ddx36 Genes, New Members of the DEAD/H Box Superfamily [J]. *Acta Biochimica Et Biophysica Sinica*, 5: 020.
- Gao X., Ma W., Nie J., Zhang C., Zhang J., Yao G., Han J., Xu J., Hu B., Du Y., Shi Q. (2015) A G-quadruplex DNA structure resolvase, RHAU, is essential for spermatogonia differentiation. *Cell death & disease* 6: e1610.
- Gartner L.P., Hiatt J.L. (2012) *Color atlas and text of histology*. Lippincott Williams & Wilkins: 434-452.
- Gazda, Hanna T., Grabowska, A., Merida-Long, Lilia B., Latawiec, E., Schneider, Hal E., Lipton, Jeffrey M., Vlachos, A., Atsidaftos, E., Ball, Sarah E., Orfali, Karen A., Niewiadomska, E., Da Costa, L., Tchernia, G., Niemeyer, C., Meerpohl, Joerg J., Stahl, J., Schratt, G., Glader, B., Backer, K., Wong, C., Nathan, David G., Beggs, Alan H., Sieff, Colin A. (2006) Ribosomal Protein S24 Gene Is Mutated in Diamond-Blackfan Anemia. *American Journal of Human Genetics* 79: 1110-1118.

- Gazda, H.T., Sheen, M.R., Vlachos, A., Choessel, V., O'Donohue, M.-F., Schneider, H., Darras, N., Hasman, C., Sieff, C. A., Newburger, P. E., Ball, S. E., Niewiadomska, E., Matysiak, M., Zaucha, J. M., Glader, B., Niemeyer, C., Meerpohl, J.J., Atsidaftos, E., Lipton, J.M., Gleizes, P.-E., Beggs, A.H. (2008) Ribosomal Protein L5 and L11 Mutations Are Associated with Cleft Palate and Abnormal Thumbs in Diamond-Blackfan Anemia Patients. *American Journal of Human Genetics* 83: 769-780.
- Goodman M., Moore G. W., Matsuda G. (1975) Darwinian evolution in the genealogy of haemoglobin. *Nature*, 253(5493): 603.
- Gruidl M. E., Smith P. A., Kuznicki K. A., McCrone J. S., Kirchner J., Roussel D. L., Strome S., Bennett K. L. (1996) Multiple potential germ-line helicases are components of the germ-line-specific P granules of *Caenorhabditis elegans*. *Proceedings of the National Academy of Sciences* 26;93(24):13837-13842.
- Herpin, A. and Scharl, M. (2011) Dmrt1 genes at the crossroads: a widespread and central class of sexual development factors in fish. *FEBS Journal* 278: 1010–1019.
- Ikhwanuddin, M., Lyana, N.A., Bakar, N.H.A., Jasmani, S., Bolong, A-M.A. (2012) Stimulation of Ovarian Maturation Using Serotonin (5-Hydroxytryptamine) Hormone on Banana Shrimp, *Fenneropenaeus merguensis* (De Man, 1888). *World Applied Sciences Journal* 18 (3): 436-445.
- Jiang, F., Doudna, J. A. (2017) CRISPR–Cas9 structures and mechanisms. *Annual review of biophysics*, 46, 505-529.
- Johnson L., Chaturvedi P. K., Williams J. D. (1992) Missing generations of spermatocytes and spermatids in seminiferous epithelium contribute to low efficiency of spermatogenesis in humans. *Biology of reproduction* 47: 1091-1098.
- Kim, M., Denlinger, D. L. (2010) A potential role for ribosomal protein S2 in the gene network regulating reproductive diapause in the mosquito *Culex pipiens*. *Journal of Comparative Physiology B*, 180(2): 171-178.

- Kimmel C. B., Ballard W. W., Kimmel S. R., Ullmann B., Schilling, T. F. (1995) Stages of embryonic development of the zebrafish. *Developmental dynamics*, 203(3): 253-310.
- King, E. J. (1948) A Study of the Reproductive Organs of the Common Marine Shrimp, *Penaeus setiferus* (Linnaeus). *Biological Bulletin* 94 (3): 244-262.
- Koehler, J. K. (1981) Lectins as probes of the spermatozoon surface. *Archives of andrology*, 6(3): 197-217.
- Köprunner, M., Thisse, C., Thisse, B., Raz, E. (2001) A zebrafish nanos-related gene is essential for the development of primordial germ cells. *Genes & Development* 15: 2877-2885.
- Lasko, P. F., Ashburner, M. (1990) Posterior localization of vasa protein correlates with, but is not sufficient for, pole cell development. *Genes & development*, 4(6): 905-921.
- Lee, M. C., Damjanov, I. (1984) Anatomic distribution of lectin-binding sites in mouse testis and epididymis. *Differentiation*, 27(1-3): 74-81.
- Lee, Y.S., Choi, D.K., Kim, C.D., Im, M., Mollah, M.L., Jang, J.Y., Oh, T.J., An, S., Seo, Y.J., Hur, G.M., Cho, M.J. (2006) Expression profiling of radiation-induced genes in radiodermatitis of hairless mice. *British Journal of Dermatology*, 154(5): 829-838.
- Marchand O, Gororoun M, D’Cotta H, McMeel O, Lareyre JJ, Bernot A, Laudet V, Guiguen Y. 2000. *DMRT1* expression during gonadal differentiation and spermatogenesis in the rainbow trout, *Oncorhynchus mykiss*. *Biochimica et Biophysica Acta*, 1493(1-2):180-187.
- Makkapan W., Yoshizaki G., Tashiro M., Chotigeat W. (2014) Expression profile of ribosomal protein L10a throughout gonadal development in rainbow trout (*Oncorhynchus mykiss*). *Fish physiology and biochemistry* 40: 1069-1081.
- Mota, M. I., Tome, G. S. (1965) On the histological structure of the gonads of *Panulirus Argus* (LATR.). *Arq. Est. Biol. Mar. Univ. Ceara*, 5 (1): 15-26.

- Motoh, H. (1981). Studies on the fisheries biology of the giant tiger prawn, *Penaeus monodon* in the Philippines. (Technical Report No. 7). Tigbauan, Iloilo, Philippines: Aquaculture Department, Southeast Asian Fisheries Development Center.
- Ngernsoungnern, A., Ngernsoungnern, P., Weerachatanukul, W., Chavadej, J., Sobhon, P., Sretarugsa, P. (2008) The existence of gonadotropin-releasing hormone (GnRH) immunoreactivity in the ovary and the effects of GnRHs on the ovarian maturation in the black tiger shrimp *Penaeus monodon*. *Aquaculture*, 279(1-4): 197-203.
- Ohashi H., Umeda N., Hirazawa N., Ozaki Y., Miura C., Miura, T. (2007) Expression of vasa (vas)-related genes in germ cells and specific interference with gene functions by double-stranded RNA in the monogenean, *Neobenedenia girellae*. *International journal for parasitology*, 37(5): 515-523.
- Oliva, R. (2006) Protamines and male infertility. *Human reproduction update*, 12(4): 417-435.
- Oliver, E. R., Saunders, T. L., Tarlé, S. A., & Glaser, T. (2004) Ribosomal protein L24 defect in belly spot and tail (Bst), a mouse Minute. *Development*, 131(16): 3907-3920.
- O'shaughnessy P. J., Monteiro A., Verhoeven G., De Gendt K., Abel M. H. (2010) Effect of FSH on testicular morphology and spermatogenesis in gonadotrophin-deficient hypogonadal mice lacking androgen receptors. *Reproduction* 139: 177-184.
- Ota, S., Hisano, Y., Muraki, M., Hoshijima, K., Dahlem, T.J., Grunwald, D.J., Okada, Y. and Kawahara, A. (2013) Efficient identification of TALEN-mediated genome modifications using heteroduplex mobility assays. *Genes to Cells*, 18(6): 450-458.
- Ota S., Kawahara A. (2016) Detection of Multiple Genome Modifications Induced by the CRISPR/Cas9 System. *Zebrafish*. Humana Press, New York, NY: 53-63.

- Ransom, D. G., Haffter, P., Odenthal, J., Brownlie, A., Vogelsang, E., Kelsh, R.N., Brand, M., Van Eeden, F. J., Furutani-Seiki, M., Granato, M. and Hammerschmidt, M. (1996) Characterization of zebrafish mutants with defects in embryonic hematopoiesis. *Development*, 123(1): 311-319.
- Rastelli, L., and Kuroda, M. I. (1998) An analysis of maleless and histone H4 acetylation in *Drosophila melanogaster* spermatogenesis. *Mechanisms of development*, 71(1-2): 107-117.
- Raymond C. S., Kettlewell J. R., Hirsch B., Bardwell V. J., Zarkower D. (1999) Expression of *Dmrt1* in the Genital Ridge of Mouse and Chicken Embryo Suggests a Role in Vertebrate Sexual Development. *Developmental Biology* 215:208-220.
- Salic, A., Mitchison, T. J. (2008) A chemical method for fast and sensitive detection of DNA synthesis *in vivo*. *Proceedings of the National Academy of Sciences*, 105(7), 2415-2420.
- Söderström K. O., Malmi R., Karjalainen K. (1984) Binding of fluorescein isothiocyanate conjugated lectins to rat spermatogenic cells in tissue sections. *Histochemistry* 80: 575-579.
- Sunanaga T., Watanabe A., Kawamura K. (2007) Involvement of vasa homolog in germline recruitment from coelomic stem cells in budding tunicates. *Development genes and evolution*, 217(1): 1-11.
- Timme-Laragy, A. R., Karchner, S. I., Hahn, M. E. (2012) Gene knockdown by morpholino-modified oligonucleotides in the zebrafish (*Danio rerio*) model: applications for developmental toxicology. In *Developmental Toxicology*, Humana Press, Totowa, NJ: 51-71.
- Tiu, S. H. K., Chan, S. M. (2007) The use of recombinant protein and RNA interference approaches to study the reproductive functions of a gonad-stimulating hormone from the shrimp *Metapenaeus ensis*. *The FEBS journal*, 274(17): 4385-4395.

- Torihara, H., Uechi, T., Chakraborty, A., Shinya, M., Sakai, N., Kenmochi, N. (2011) Erythropoiesis failure due to RPS19 deficiency is independent of an activated Tp53 response in a zebrafish model of Diamond–Blackfan anaemia. *British journal of haematology*, 152(5): 648-654.
- Torregrosa, N., Domínguez-Fandos, D., Camejo, M. I., Shirley, C. R., Meistrich, M. L., Ballescà, J. L., Oliva, R. (2006) Protamine 2 precursors, protamine 1/protamine 2 ratio, DNA integrity and other sperm parameters in infertile patients. *Human Reproduction* 21(8): 2084-2089.
- Uechi, T., Nakajima, Y., Chakraborty, A., Torihara, H., Higa, S., Kenmochi, N. (2008) Deficiency of ribosomal protein S19 during early embryogenesis leads to reduction of erythrocytes in a zebrafish model of Diamond-Blackfan anemia. *Human Molecular Genetics* 17: 3204-3211.
- Weidinger, M., Varcoe, B. T., Heerlein, R., Walther, H. (1999) Trapping states in the micromaser. *Physical Review Letters*, 82(19), 3795.
- Wonglapsuwan, M., Phongdara, A., Chotigeat, W. (2009) Dynamic changes in gene expression during vitellogenic stages of the white shrimp: *Fenneropenaeus merguensis* de Man. *Aquaculture Research* 40: 633-643.
- Wonglapsuwan, M., Miyazaki, T., Loongyai, W., Chotigeat, W. (2010) Characterization and Biological Activity of the Ribosomal Protein L10a of the White Shrimp: *Fenneropenaeus merguensis* De Man During Vitellogenesis. *Mar Biotechnol* 12: 230–240.
- Wonglapsuwan, M., Chotigeat, W., Timmons, A., McCall, K. (2011) RpL10A regulates oogenesis progression in the banana prawn *Fenneropenaeus merguensis* and *Drosophila melanogaster*. *General and Comparative Endocrinology* 173: 356–363.
- Wool, I. G. (1996) Extraribosomal functions of ribosomal proteins. *Trends in Biochemical Sciences* 21: 164-165.
- Xia, X., Hou, F., Li, J. and Nie, H. (2005) Ribosomal protein L10a, a bridge between trichosanthin and the ribosome. *Biochemical and Biophysical Research Communications* 336:281–286.

- Yadav, G. V., Chakraborty, A., Uechi, T., Kenmochi, N. (2014) Ribosomal protein deficiency causes Tp53-independent erythropoiesis failure in zebrafish. *The International Journal of Biochemistry & Cell Biology* 49: 1-7.
- Yamaguchi, A., Lee, K. H., Fujimoto, H., Kadomura, K., Yasumoto, S., Matsuyama, M. (2006) Expression of the *DMRT* gene and its roles in early gonadal development of the Japanese pufferfish *Takifugu rubripes*. *Comparative Biochemistry and Physiology, Part D* 1: 59 - 68.
- Yoon C., Kawakami K., Hopkins, N. (1997) Zebrafish vasa homologue RNA is localized to the cleavage planes of 2-and 4-cell-stage embryos and is expressed in the primordial germ cells. *Development*, 124(16): 3157-3165.
- Zhang E. F. and Qiu G. F. (2010) A novel Dmrt gene is specifically expressed in the testis of Chinese mitten crab, *Eriocheir sinensis*. *Dev Genes Evol* 220: 151-159.
- Zhang, Z., Wang, Y., Jiang, Y., Lin, P., Jia, X., & Zou, Z. (2007) Ribosomal protein L24 is differentially expressed in ovary and testis of the marine shrimp *Marsupenaeus japonicus*. *Comparative Biochemistry and Physiology Part B: Biochemistry and Molecular Biology*, 147(3): 466-474.

APPENDIX

APPENDIX A

1. Agarose gel electrophoresis

For the gel, a 1.2% (w/v) of agarose gel in 0.5x TAE buffer (20 mM Tris-acetate, 0.5 mM EDTA) was melted and poured on a plastic tray, a comb was placed in the gel. After the agarose gel was completely set, the comb was carefully removed and the gel was installed on the platform in the electrophoresis tank containing 0.5x TAE buffer. The RNA samples were mixed with 30% (v/v) gel-loading buffer (25% (v/v) glycerol, 60 mM EDTA, 0.25% (w/v) bromophenol blue) and slowly loaded into the slots of the submerged gel using an automatic micropipette. The electrophoresis was carried out at a constant 120 V for 1 h. Next, the gel was stained with 2.5 µg/ml of ethidium bromide solution for 5 min and destained with water for 15 min. After that the RNA patterns was observed under UV light box (Quantity One Gel Doc model) (BIO-RAD, USA).

2. SDS-polyacrylamide gel electrophoresis (SDS-PAGE)

SDS-PAGE was performed as described by Laemmli, 1970. The gel solution is shown in the Table 11. Electrophoresis was carried out in the descending direction with Tris-glycine buffer (25 mM Tris-HCl, pH 6.8, 192 mM glycine and 0.1% (w/v) SDS) using a constant 100 V for 150 min or until the tracking dye reached the edge of the gel. The protein patterns were visualized by Coomassie blue staining.

Table 14 Composition of 12% SDS-polyacrylamide gel

Solution	Separating Gel (5 ml)	Stacking Gel (3 ml)
Water	1.7	2.1
30% Acrylamide mix ^a	2.0	0.5
1.5 M Tris (pH 8.8)	1.3	–
1.0 M Tris (pH 6.8)	–	0.38
10% SDS ^b	0.05	0.03
10% APS ^c	0.05	0.03
TEMED ^d	0.002	0.003

^aA = 30% Acrylamide (acrylamide: N,N'-methylenebisacrylamide, 29:1)

^bSDS = sodium dodecyl sulfate

^cAPS = ammonium persulfate

^dTEMED = N,N,N',N' – tetramethylethylenediamine

3. Protein measurement, Lowry's method (Lowry et al., 1951)

Bovine serum albumin (BSA) was used as a protein standard. Working standard of BSA (20, 40, 60, 80, 100 µg/ml) was diluted from BSA stock (1 mg/ml) for 1 ml. Protein samples were diluted (1: 100). The BSA standard and protein sample were mixed with 1 ml of reagent A and allow standing for 10 min at room temperature. Then, 0.5 ml of reagent B was added very rapidly and mixed using vortex. After place at room temperature for 30 min, the sample was measured by a spectrophotometer at OD750. Concentration of protein sample was determined by calculating from BSA standard curve.

APPENDIX B

1. Chemical stock solution and buffer

1 M Tris-HCl pH 6.8

Tris-HCl 121.1 g

Dissolve 121.1 g of Tris base in 800 ml of distilled water. Adjust the pH to the desired value by adding concentrated HCl. Adjust the volume of the solution to 1000 ml with distilled water and sterilize by autoclaving.

1.5 M Tris-HCl pH 8.8

Tris-HCl 181.7 g

Dissolve 181.7 g of Tris base in 800 ml of distilled water. Adjust the pH to the desired value by adding concentrated HCl. Adjust the volume of the solution to 1000 ml with distilled water and sterilize by autoclaving.

0.5 M EDTA (pH 8.0)

EDTA 186.12 g

Dissolve 186.12 g of EDTA in 800 ml of distilled water. Adjust the pH to 8.0 by adding concentrated HCl. Adjust the volume of the solution to 1000 ml with distilled water and sterilize by autoclaving.

1 N NaOH

NaOH 40 g

Prepare this solution with extreme care in plastic beakers. Dissolve in 800 ml of distilled water and adjust the volume to 1000 ml with distilled water. Store the solution in a plastic container at room temperature.

0.2 M NaH₂PO₄

NaH₂PO₄ 13.8 g

Dissolve 13.8 g in 400 ml of distilled water. Adjust the volume of the solution to 500 ml with distilled water and sterilize by autoclaving.

0.2 M Na₂HPO₄

Na₂HPO₄ 14.2 g

Dissolve 14.2 g in 400 ml of distilled water. Adjust the volume of the solution to 500 ml with distilled water and sterilize by autoclaving.

1 M DTT

DTT 15.43 g

Dissolve in 100 ml with distilled water and sterilize by filtration.

1 M IPTG

IPTG 2.38 g

Dissolve in 10 ml with distilled water and sterilize by filtration.

10% SDS (w/v)

SDS 100 g

Dissolve in 900 ml of distilled water. Heat to 68 °C and stir with a magnetic stirrer to assist dissolution. Adjust the volume to 1000 ml with distilled water and store at room temperature. Sterilization is not necessary.

Ammonium persulfate (10% w/v)

Ammonium persulfate 10 g

Dissolve 10 g ammonium persulfate in 100 ml of distilled water and store at -20 °C.

Ethidium bromide (10 mg/ml)

Ethidium bromide	1 g
Distilled water	100 ml

Stir on a magnetic stirrer for several hours to ensure that the dye has dissolved. Wrap the container in aluminum foil or transfer the solution to a dark bottle and store at room temperature.

Phosphate-buffered saline (PBS, pH 7.4)

NaCl	8 g
KCl	0.2 g
Na ₂ HPO ₄	1.44 g
KH ₂ PO ₄	0.24 g

Dissolve the ingredients in 800 ml of distilled water. Adjust the pH to 7.4 with HCl. Add distilled water to 1000 ml. Sterilize the buffer by autoclaving and store at room temperature

RNase A (10 mg/ml)

RNase A	10 mg
---------	-------

Dissolve and bring up to 1 ml with sterile distilled water. Boil in water for 5 min and store at -20 °C

2. Chemical and solutions for histological**Buffered neutral formalin solution**

0.2 M NaH ₂ PO ₄	165 ml
0.2 M Na ₂ HPO ₄	225 ml
100% formalin (formaldehyde 37-39%)	100 ml
Distilled water	510 ml

Mix the solutions well and store at room temperature.

4% Paraformaldehyde (PFA)

Paraformaldehyde 4 g

Dissolve with warm distilled water (60°C) and drop 1 N NaOH carefully until solution is clear. Adjust pH to 7.4 by adding 1 N HCl and add PBS buffer volume to 100 ml

Working eosin solution

Stock 1% eosin 100 ml

95% ethyl alcohol 120 ml

Glacial acetic acid 1 ml

Distilled water 30 ml

Mix the solutions and store at room temperature

3. Chemicals and solutions for western blot**Transfer buffer (Nitrocellulose membrane)**

Tris base 3.03 g

Glycine 14.42 g

Dissolve the ingredients in 700 ml of distilled water. Adjust the volume to 800 ml with distilled water. Add 200 ml of 100% methanol before use.

Detection buffer (pH 9.5)

Tris-HCl 1.21 g

NaCl 0.58 g

MgCl₂ 1.02 g

Dissolve Tris-HCl and NaCl in 80 ml of distilled water. Adjust the pH to 9.5 by adding concentrated HCl. Adjust the volume of the solution to 100 ml with distilled water and sterilize by autoclaving. Add MgCl₂ before use.

Colour substrate solution**NBT**

NBT 30 mg

Dissolve NBT in 700 μ l of dimethyl formamide (DMF) and 300 μ l of distilled water. Sterilization is not necessary.

BCIP

BCIP 15 mg

Dissolve BCIP in 1000 ml of distilled water. Sterilization is not necessary.

4. Solutions for electrophoresis**30% Acrylamide solution**

Acrylamide 29 g

N, N' methylene bisacrylamide 1 g

Dissolve acrylamide in 80 ml of distilled water and N,N' methylene bisacrylamide. Adjust volume with distilled water to 100 ml.

2X SDS Gel loading buffer

10% SDS 4 ml

Glycerol 2 ml

1 M Tris-HCl (pH 6.8) 1.2 ml

1 M DTT 2 ml

0.01% (w/v) bromophenol blue

Adjust the volume of the solution to 10 ml with distilled water and store at 4 °C.

4X SDS Gel loading buffer

40% SDS	2 ml
Glycerol	4 ml
2 M Tris-HCl (pH 6.8)	1.2 ml
2 M DTT	2 ml
0.01% (w/v) bromophenol blue	

Adjust the volume of the solution to 10 ml with distilled water and store at 4 °C

50X TAE, Electrophoresis buffer

Tris-base	242 g
Glacial acetic acid	57.1 ml
0.5 M EDTA, pH 8.0	100 ml

Dissolve the ingredients in distilled water and bring up to volume 1000 ml. Working solution for gel preparation and the buffer is 0.5X.

10X Formaldehyde gel running buffer (pH 7.0)

MOPS	44 g
Sodium acetate	10.88 g
0.5 M EDTA	20 ml

Dissolve the ingredients in RNase-free water. Adjust the pH to 7.0 with NaOH. Adjust the volume of the solution to 1000 ml. Sterilize the solution by autoclaving, and store at room temperature protected from light.

Tris-glycine buffer (pH 8.3)

Tris base	3.03 g
Glycine	14.42 g
SDS	1 g

Dissolve the ingredients in 800 ml of distilled water. Adjust the volume to 1000 ml with distilled water.

5. SDS-PAGE gel staining

Brilliant Coomassie Blue

Brilliant Coomassie Blue R	1 g
Methanol	212.5 ml
Acetic acid	37.5 ml
Distilled water	250 ml

Mix the ingredients together and store at room temperature protected from light.

Destaining

Methanol	500 ml
Acetic acid	75 ml
Distilled water	425 ml

Mix the ingredients together and store at room temperature.

Destaining II

Methanol	50 ml
Acetic acid	75 ml
Distilled water	875 ml

6. Media and antibiotics for bacterial

Ampicillin (50 mg/ml)

Ampicillin	50 mg
------------	-------

Dissolve in 1 ml of sterile distilled water. Store at -20 °C.

Kanamycin (20 mg/ml)

Kanamycin 20 mg

Dissolve in 1 ml of sterile distilled water. Store at -20 °C.

LB (Luria-Bertani) broth (supplement with 100 µg/ml ampicillin)

Tryptone 10 g

Yeast extract 5 g

NaCl 5 g

Adjust the volume of the solution to 1000 ml with distilled water and sterilize by autoclaving for 20 min at 15 psi. Add 2 ml of ampicillin (50 mg/ml) into warm medium (50 °C).

LB agar (supplement with 100 µg/ml ampicillin)

Tryptone 10 g

Yeast extract 5 g

NaCl 5 g

Agar 15 g

Adjust the volume of the solution to 1000 ml with distilled water and sterilize by autoclaving for 20 min at 15 psi. Add 2 ml of ampicillin (50 mg/ml) into warm medium (50 °C). The medium was poured into glass plate.

LB (Luria-Bertani) broth (supplement with 30 µg/ml kanamycin)

Tryptone 10 g

Yeast extract 5 g

NaCl 5 g

Adjust the volume of the solution to 1000 ml with distilled water and sterilize by autoclaving for 20 min at 15 psi. Add 1.5 ml of kanamycin (20 mg/ml) into warm medium (50 °C).

LB agar (supplement with 30 µg/ml kanamycin)

Tryptone	10 g
Yeast extract	5 g
NaCl	5 g
Agar	15 g

Adjust the volume of the solution to 1000 ml with distilled water and sterilize by autoclaving for 20 min at 15 psi. Add 1.5 ml of kanamycin (20 mg/ml) into warm medium (50 °C). The medium was poured into glass plate.

7. Solution for protein purification**Lysis buffer**

NaH ₂ PO ₄ ·2H ₂ O	7.8 g
NaCl	17.54 g
Imidazole	0.68 g

Dissolve the ingredients in 800 ml of distilled water. Adjust the pH to 8.0 by adding 1 M NaOH. Adjust the volume of the solution to 1000 ml with distilled water and sterilize by autoclaving.

Washing buffer

NaH ₂ PO ₄ ·2H ₂ O	7.8 g
NaCl	17.54 g
Imidazole	1.36 g

Dissolve the ingredients in 800 ml of distilled water. Adjust the pH to 8.0 by adding 1 M NaOH. Adjust the volume of the solution to 1000 ml with distilled water and sterilize by autoclaving.

Elution buffer

NaH ₂ PO ₄ ·2H ₂ O	7.8 g
NaCl	17.54 g
Imidazole	34 g

Dissolve the ingredients in 800 ml of distilled water. Adjust the pH to 8.0 by adding 1 M NaOH. Adjust the volume of the solution to 1000 ml with distilled water and sterilize by autoclaving.

Dialysis buffer

NaH ₂ PO ₄ ·2H ₂ O	7.8 g
NaCl	17.54 g

Dissolve the ingredients in 800 ml of distilled water. Adjust the pH to 7.4 by adding 1 M NaOH. Adjust the volume of solution to 1000 ml and store at room temperature.

8. Solutions for protein measurement (Lowry's Method)**Copper tartrate carbonate solution (CTC solution)**

NaCO ₃	10 g
CuSO ₄ ·5H ₂ O	0.5 g
Na-tartrate	2 g

Dissolve the ingredients in 400 ml of distilled water. Adjust the volume of the solution to 500 ml with distilled water. Sterilization is not necessary.

Reagent A (CTC solution: 10% SDS: 1 N NaOH = 1: 2: 1)

CTC solution	15 ml
10% SDS	15 ml
1 N NaOH	12 ml

Mix the solutions and adjust the volume of the solution to 60 ml with distilled water and store at 4 °C. Sterilization is not necessary.

Reagent B (2 N Folin-Ciocalteu phenol: H₂O = 1:5)

2 N Folin-Ciocalteu phenol	10 ml
H ₂ O	50 ml

Mix the solutions and store at 4 °C. Sterilization is not necessary.

9. Solution for explants culture**2X Leibovitz's L-15 Medium**

Leibovitz's L-15 powder	27.4 g
D-glucose	10 g
Fetal calf serum	100 ml
100x antibiotic-antimycotic	10 ml

Dissolve Leibovitz's L-15 powder and D-glucose in 800 ml of sterilized distilled water and adjust the pH to 7.4 with 1 M HCl. Then, fetal calf serum and antibiotic-antimycotic were added to the solution. Sterilization by filtration and then store at 4 °C.

Dulbecco's Modified Eagle's Medium (DMEM)

Dulbecco's Modified Eagle's Medium powder for 1 L

Sodium Bicarbonate	3.7 g
Fetal calf serum	100 ml
100x antibiotic-antimycotic	10 ml

Dissolve Dulbecco's Modified Eagle's Medium powder and Sodium Bicarbonate in 800 ml of sterilized distilled water and adjust the pH to 7.4 with 1 M HCl. Then, fetal calf serum and antibiotic-antimycotic were added to the solution. Sterilization by filtration and then store at 4 °C.

10. Zebrafish water preparation

Zebrafish Embryos (E3 Medium)

NaCl	172 g
KCl	7.6 g
CaCl ₂ ·2H ₂ O	29 g
MgSO ₄ ·7H ₂ O	49 g

Dissolve these component together and prepare into 60x stock solution,
Store stock in a fridge.

Working E3 Medium

60x stock solution	160 ml
0.01% Methylene Blue	30 ml

Dissolve in distilled water to make up 10 L of E3, and add 30 ml of 0.01%
Methylene Blue as a fungicide. Control the temperature at 28.5 °C.

Zebrafish water

Marine salt	8 g
Tetra AquaSafe	8 ml
KCl	25 ml

Dissolve in distilled water to make up 30 L, and control the temperature
at 28.5 °C.

VITAE

Name Miss Kunwadee Palasin

Student ID 5410230002

Educational Attainment

Degree	Name of Institution	Year of Graduation
Bachelor of Science (Biotechnology)	Prince of Songkla University	2010

Scholarship Awards during Enrolment

2011 - Present The Royal Golden Jubilee Ph.D. Program (RGJ-Ph.D. Program)

List of Publication and Proceeding

Palasin K, Makkapan W, Thongnoi T, Chotigeat W. 2014. Stimulation of ovarian development in white shrimp, *Fenneropenaeus merguensis* De Man, with a recombinant ribosomal protein L10a. *Aquaculture*. 432: 38-45.

Palasin K, Makkapan W, Wonglapsuwan M, Chotigeat W. 2019. Effect of recombinant ribosomal L10a (RpL10a) on mouse spermatogenesis. *Songklanakarin Journal of Science and Technology (SJST)*. 41(4).